Triggering Discoveries in High Energy Physics III
9–13 December 2024, Vysoké Tatry, Slovakia

Searching for saturation with large-|t| incoherent J/ψ production at the LHC

J. Cepila, Guillermo Contreras, M. Matas, A. Ridzikova

Czech Technical University in Prague

Cepila, JGC, Matas, Ridzikova, PLB 852 (2024) 138613

Co-funded by
the European Union

MINISTRY OF EDUCATION,
YOUTH AND SPORTS

Saturation in QCD

The gluons in the proton

Deep-inelastic scattering

The structure function of the proton grows rapidly at small Bjorken x

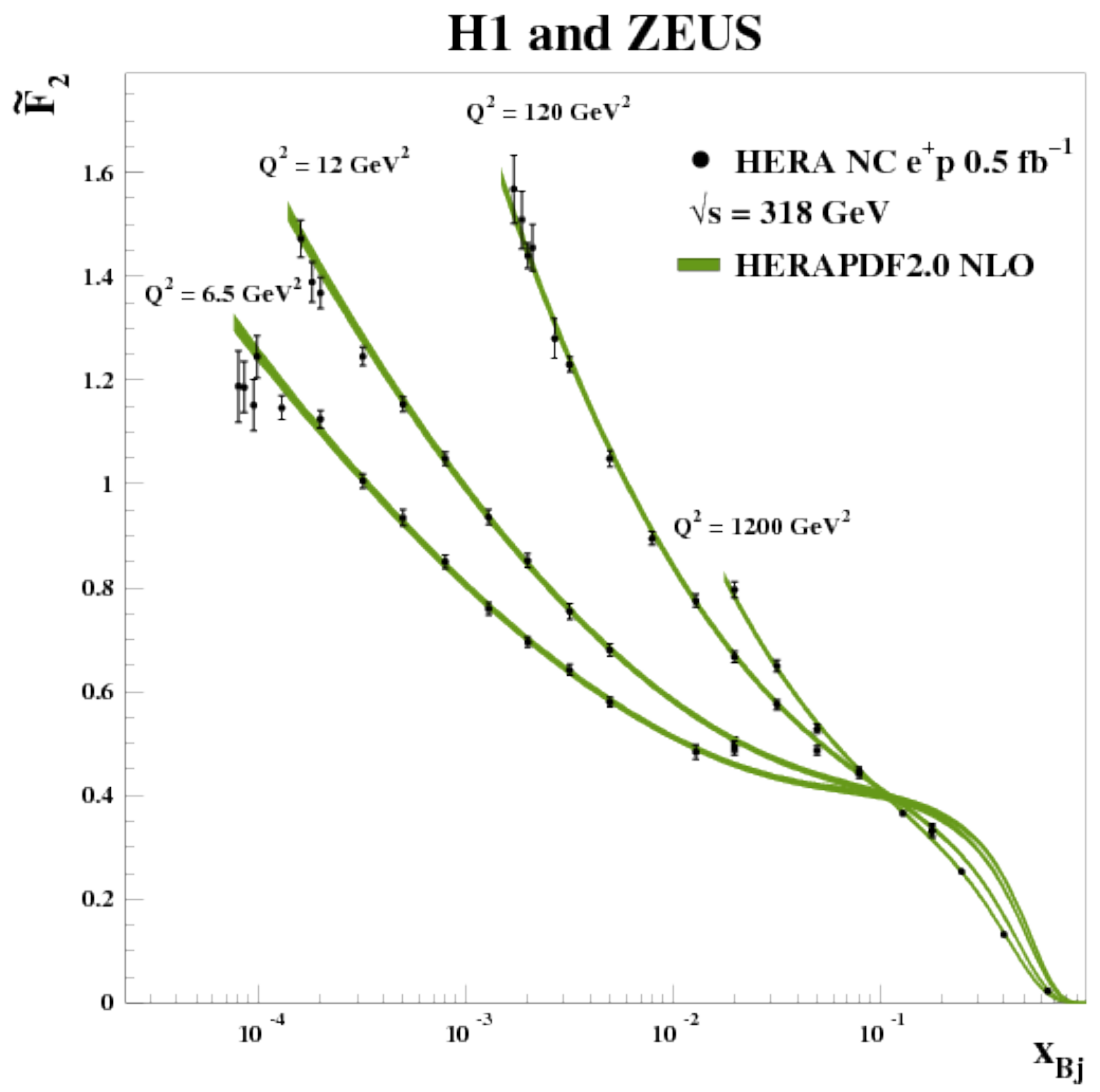

H1 and Zeus, EPJC 75 (2015) 12, 580

The gluons in the proton

Deep-inelastic scattering

The structure function of the proton grows rapidly at small Bjorken x

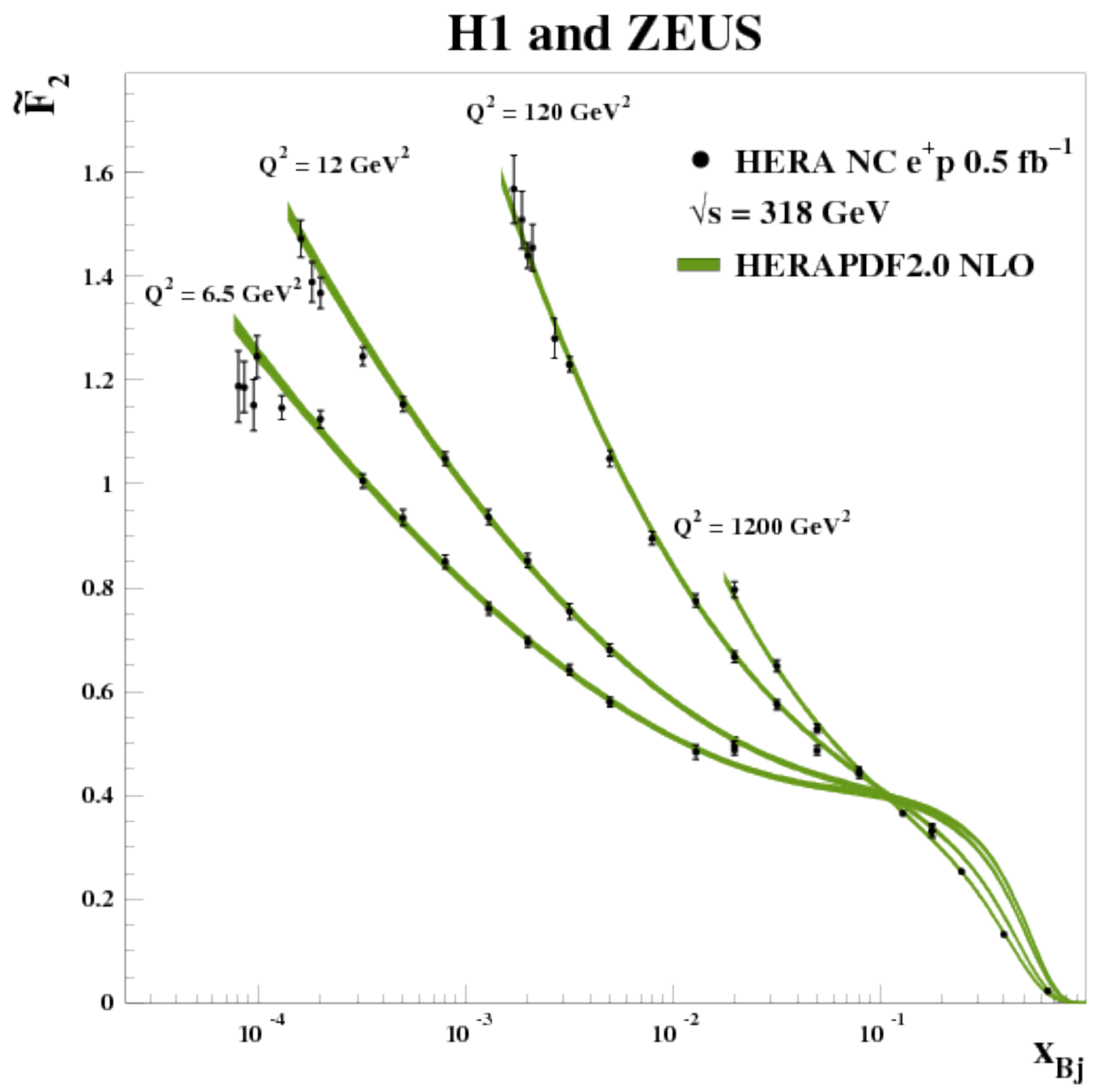

Quantum chromodynamics

The proton can be seen as formed by **quasi-free** partons: quarks and gluons

The gluons in the proton

Deep-inelastic scattering

The structure function of the proton grows rapidly at small Bjorken x

Quantum chromodynamics

The proton can be seen as formed by **quasi-free** partons: quarks and gluons

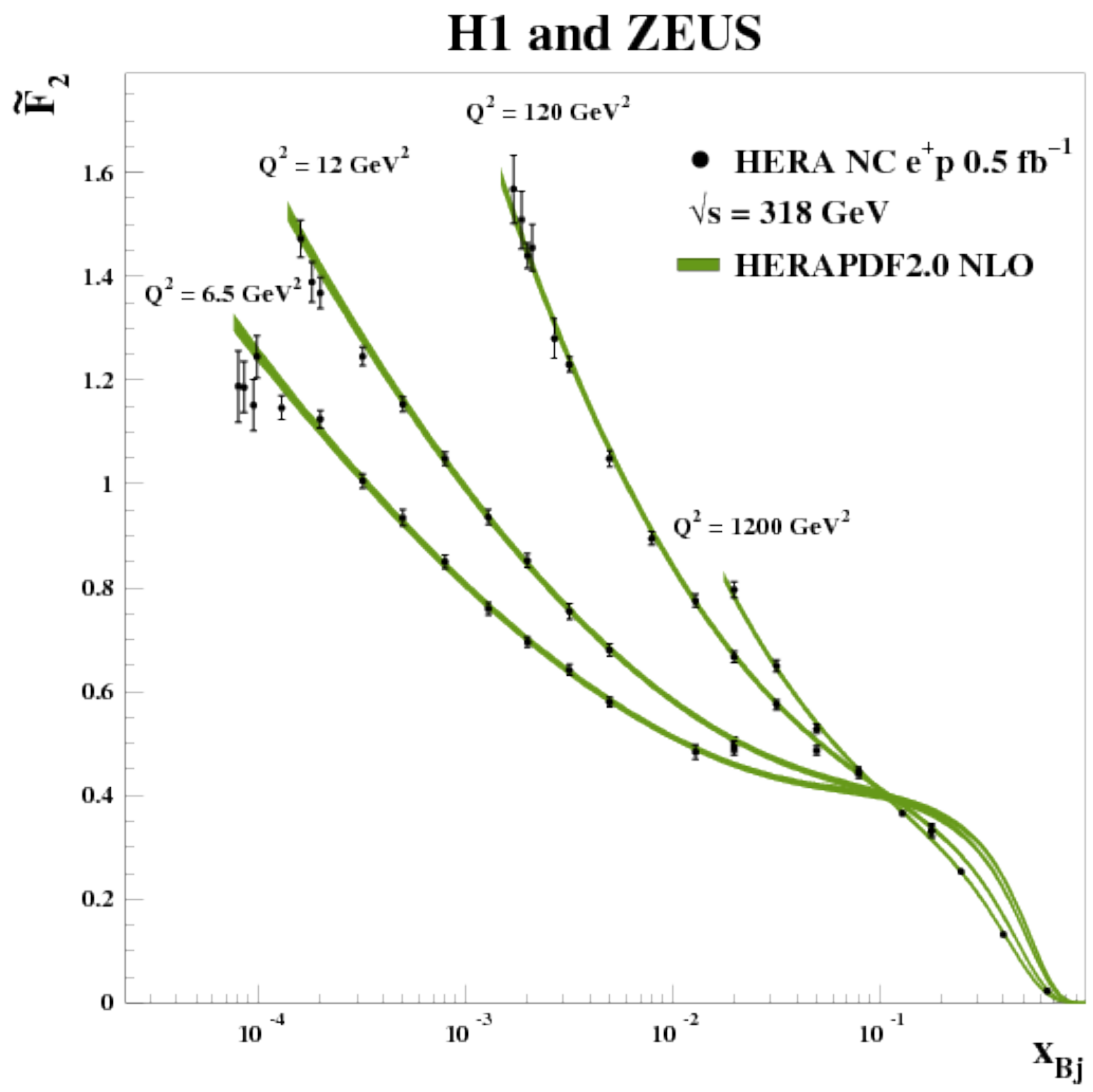

At small Bjorken-x the proton is mainly made of gluons

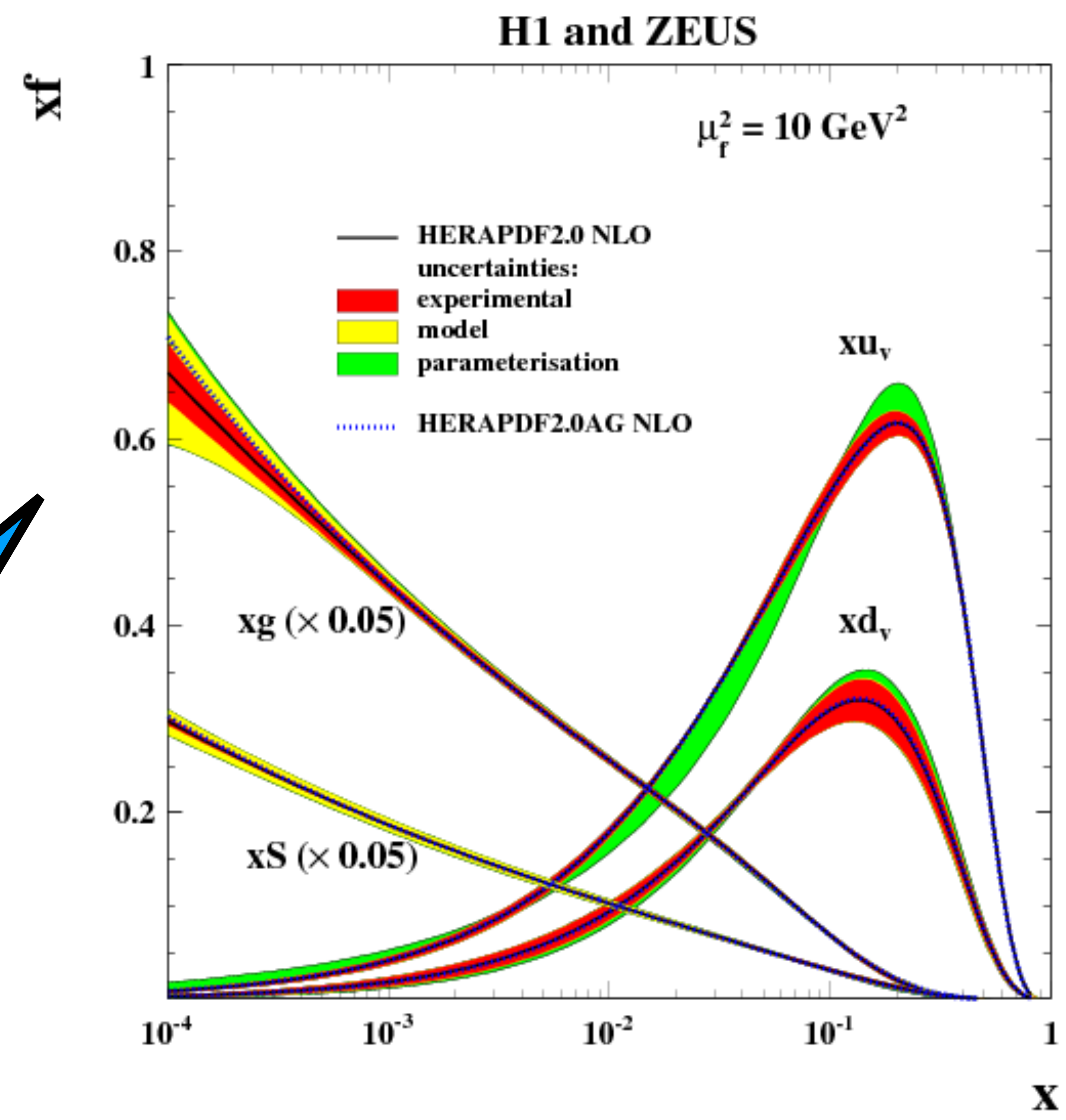

Gluon saturation in QCD

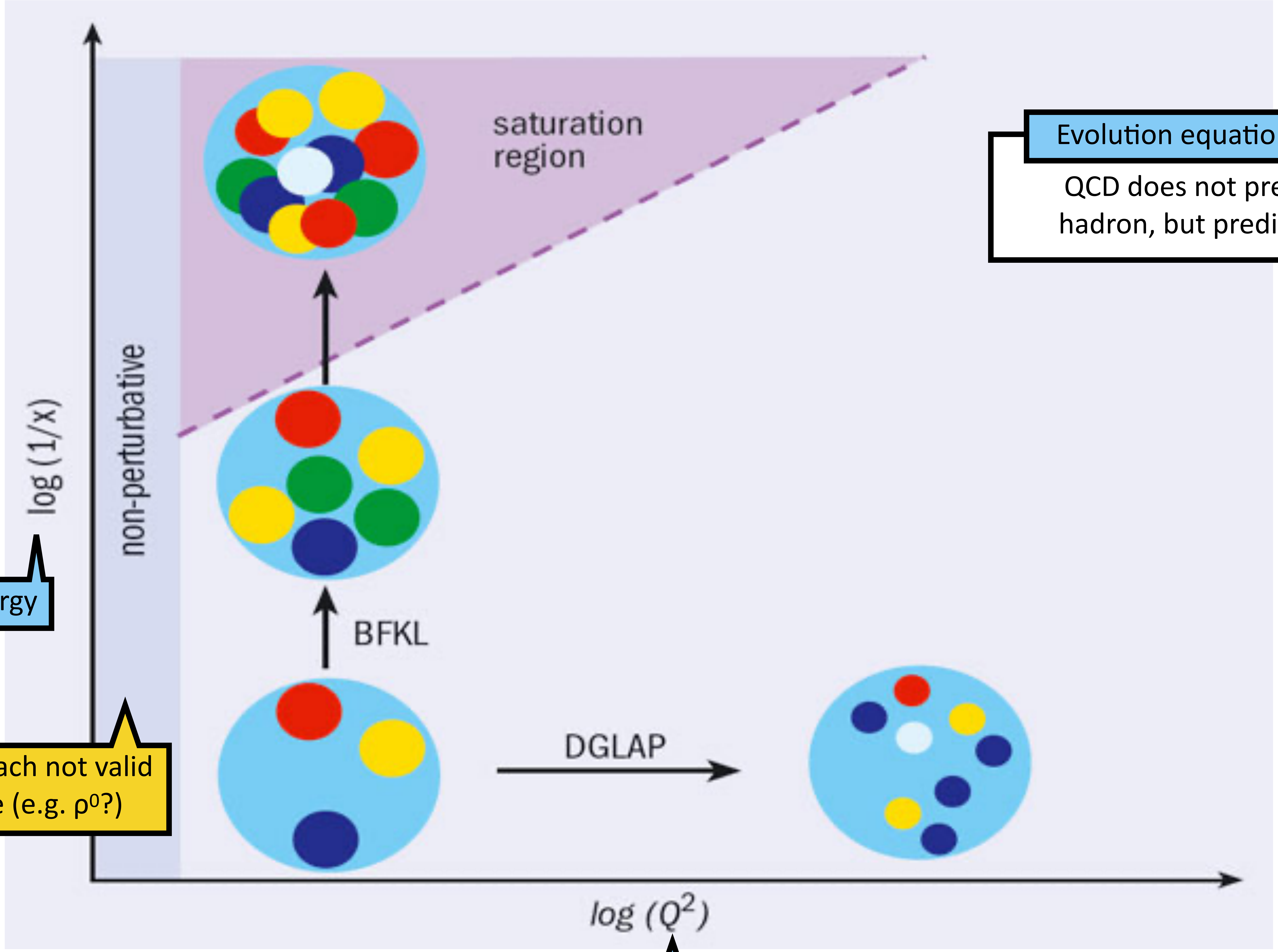

Evolution equations

QCD does not predict the parton structure of a hadron, but predicts how the structure changes

Interaction energy

Approach not valid here (e.g. ρ^0?)

Interaction scale

D. Diakonov, CERN Courier, July 2010

Gluon saturation in QCD

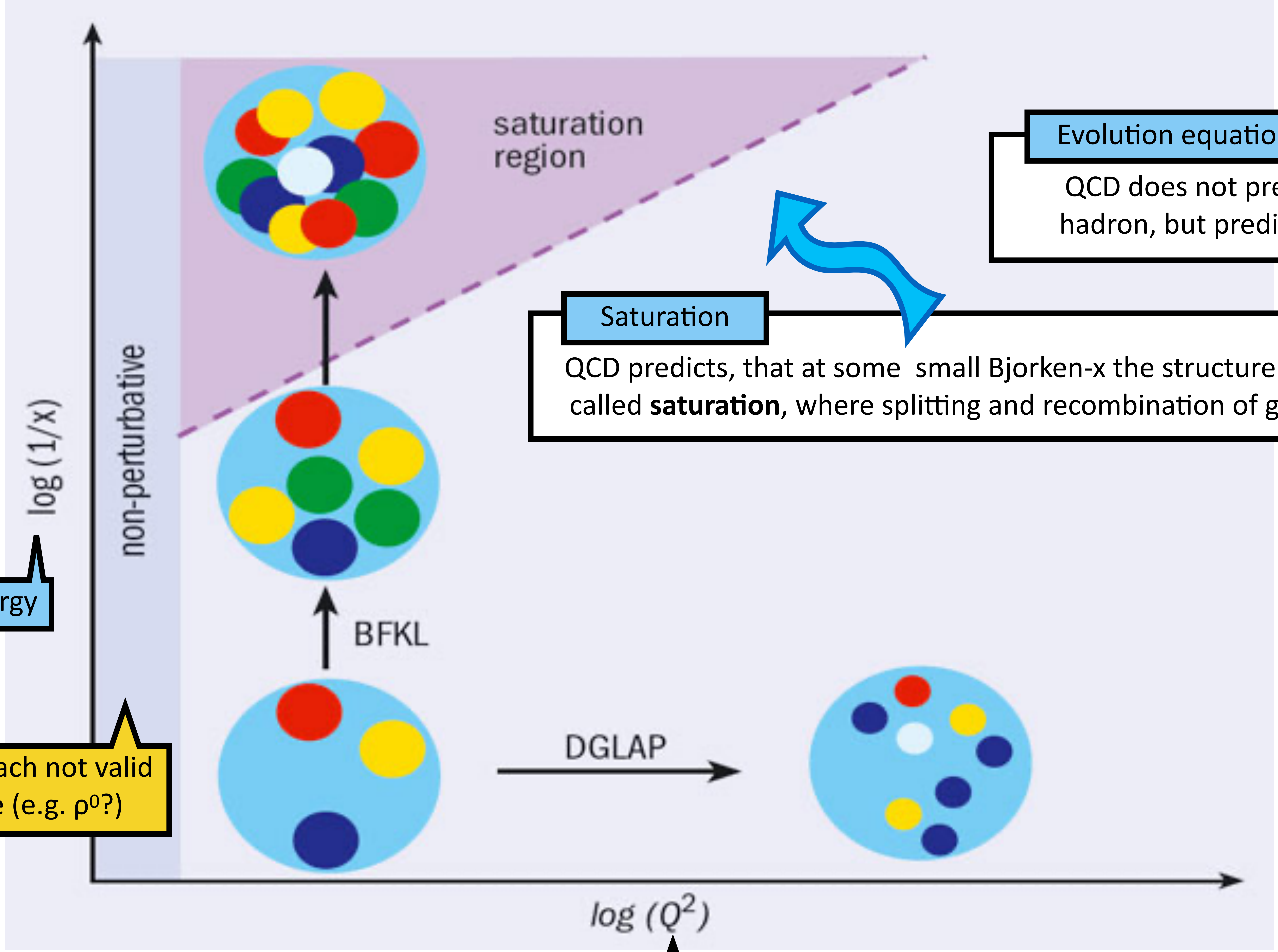

Evolution equations

QCD does not predict the parton structure of a hadron, but predicts how the structure changes

Saturation

QCD predicts, that at some small Bjorken-x the structure of a hadron reaches a new regime, called **saturation**, where splitting and recombination of gluons are in a dynamic equilibrium

Interaction energy

Approach not valid here (e.g. ρ^0?)

Interaction scale

D. Diakonov, CERN Courier, July 2010

Gluon saturation in QCD

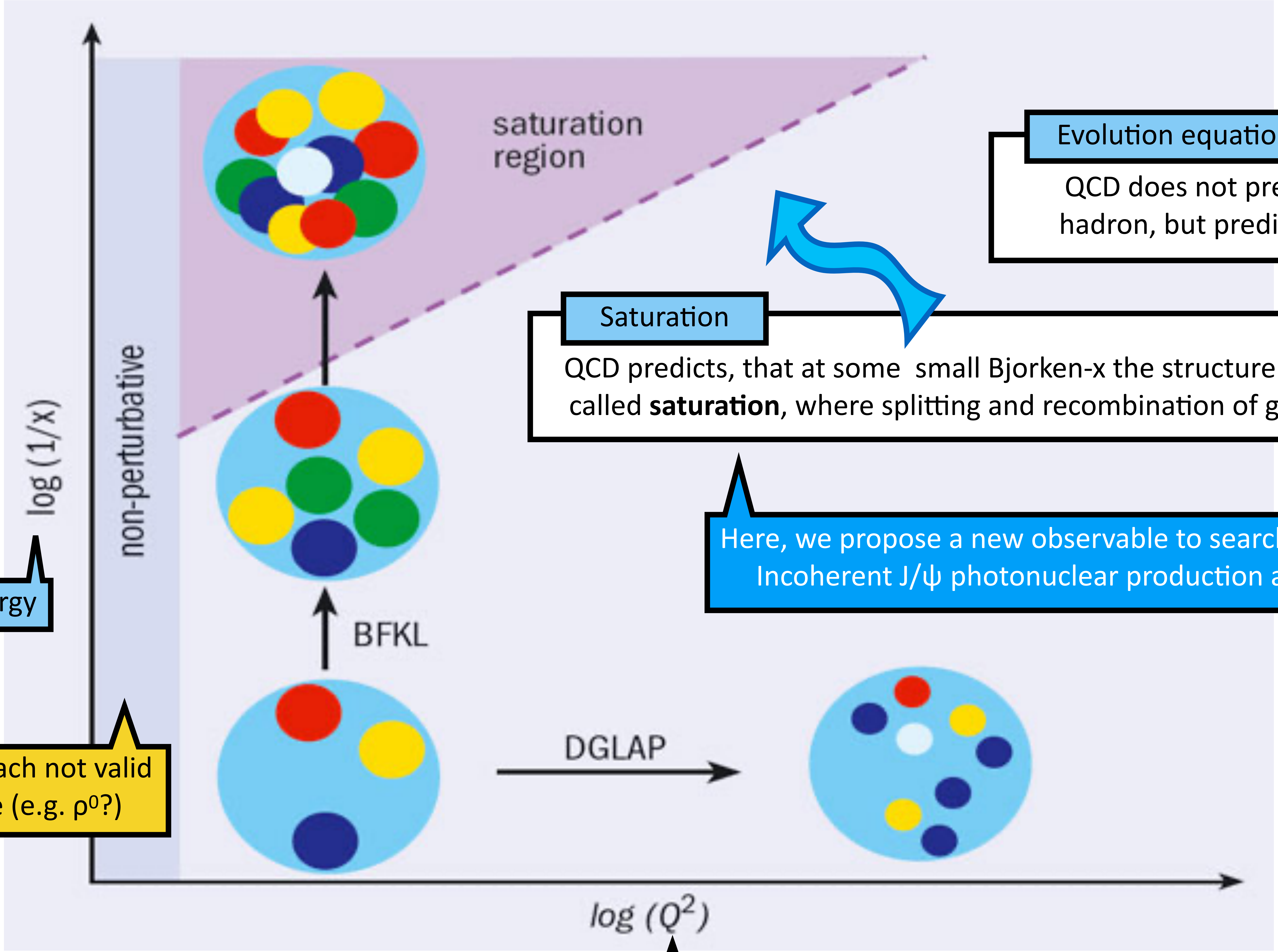

Evolution equations

QCD does not predict the parton structure of a hadron, but predicts how the structure changes

Saturation

QCD predicts, that at some small Bjorken-x the structure of a hadron reaches a new regime, called **saturation**, where splitting and recombination of gluons are in a dynamic equilibrium

Here, we propose a new observable to search for saturation at the LHC:
Incoherent J/ψ photonuclear production at large Mandelstam-|t|

Interaction energy

Approach not valid here (e.g. ρ^0?)

Interaction scale

D. Diakonov, CERN Courier, July 2010

The formalism

Diffractive vector meson photoproduction

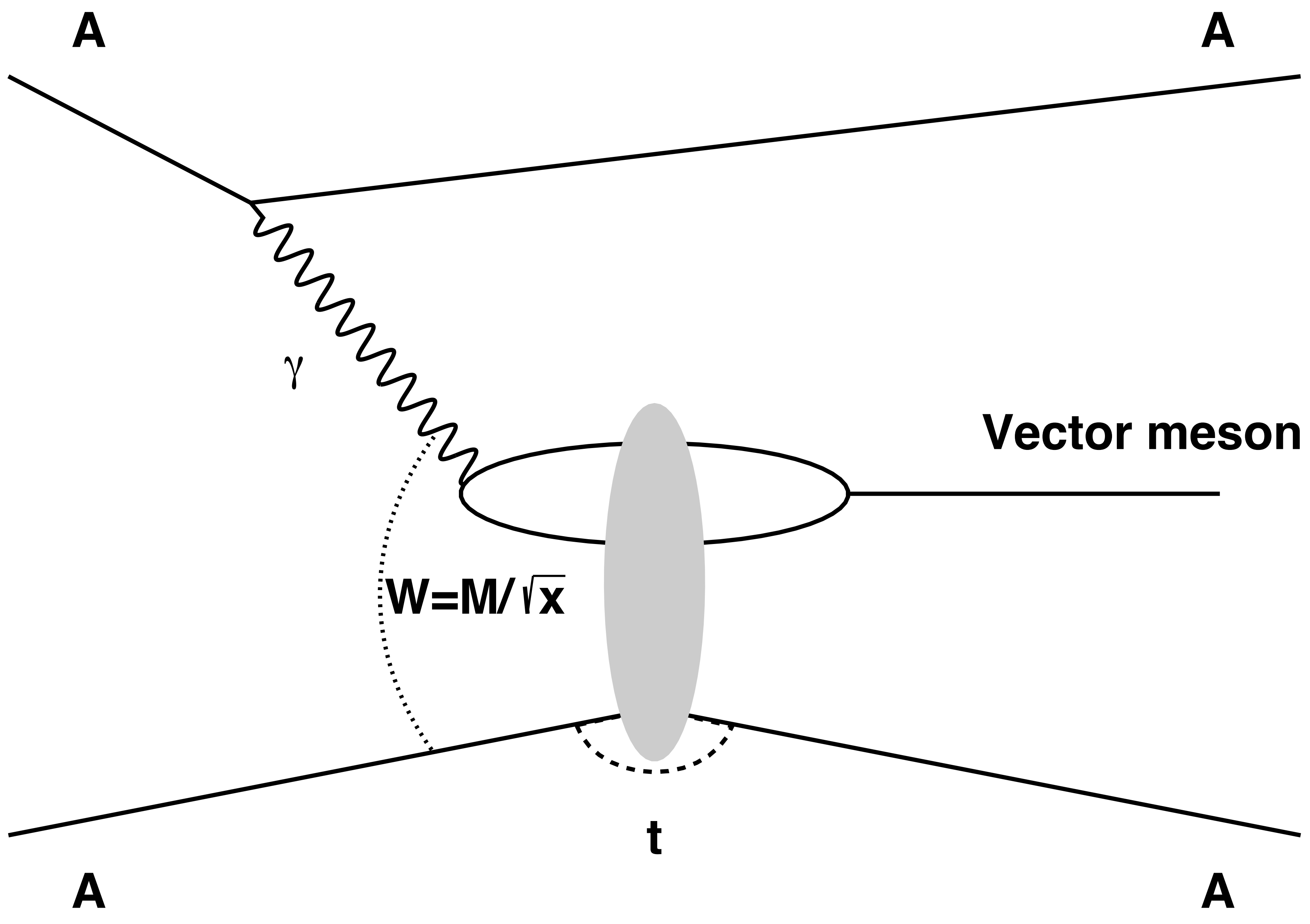

Diffractive vector meson photoproduction

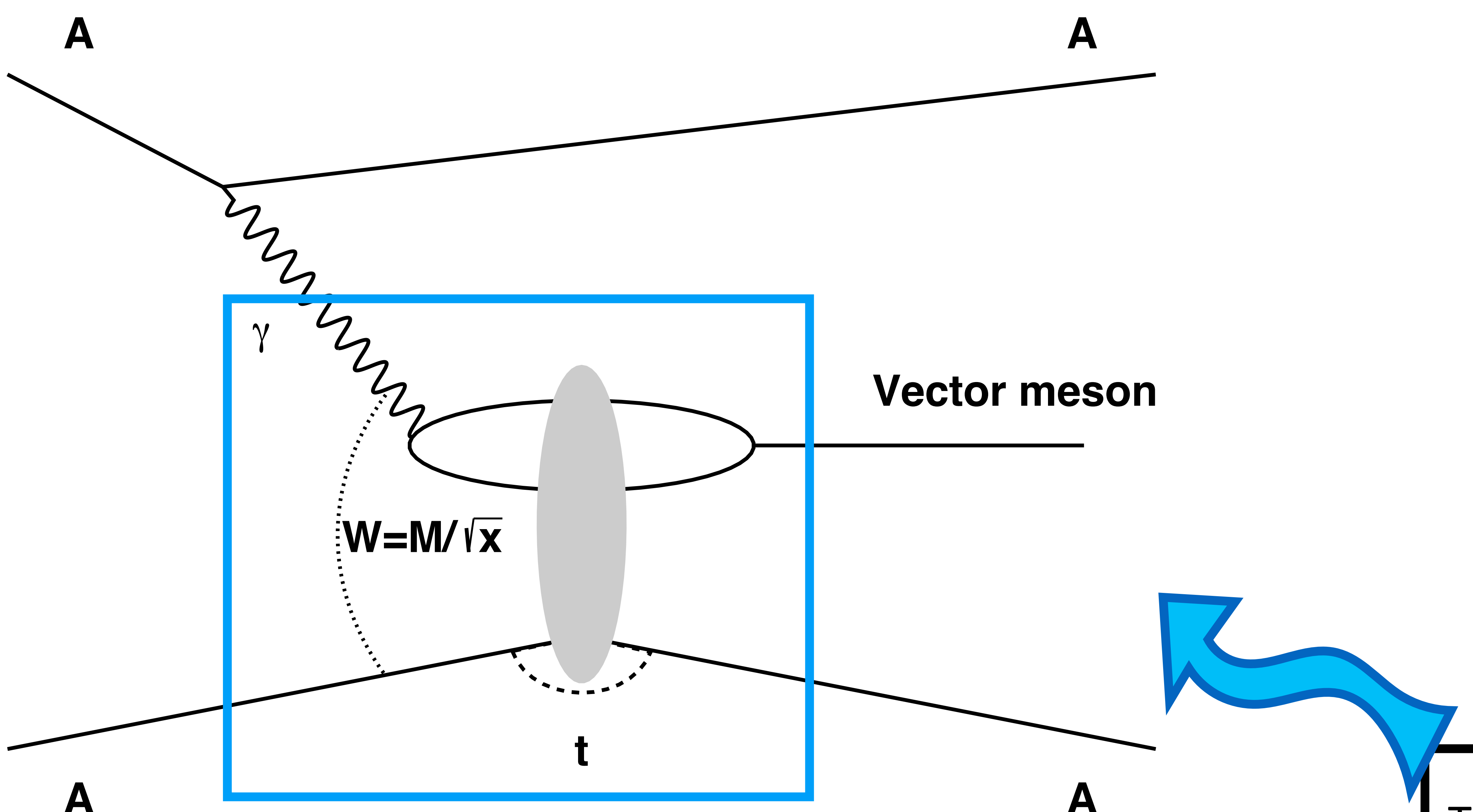

Dipole picture

The photon fluctuates into a long-lived quark-antiquark colour dipole which interacts with the hadronic target and then creates a vector meson

Diffractive vector meson photoproduction

$$\mathscr{A}_{\mathrm{T,L}}(x, Q^2, \vec{\Delta}) = i \int \mathrm{d}\vec{r} \int_0^1 \frac{\mathrm{d}z}{4\pi} \int \mathrm{d}\vec{b}\, |\Psi_\gamma^* \Psi_\mathrm{V}|_{\mathrm{T,L}} \exp\left[-i\left(\vec{b} - (\frac{1}{2} - z)\vec{r}\right)\vec{\Delta}\right] \frac{\mathrm{d}\sigma_\mathrm{H}^{\mathrm{dip}}}{\mathrm{d}\vec{b}}$$

Amplitude

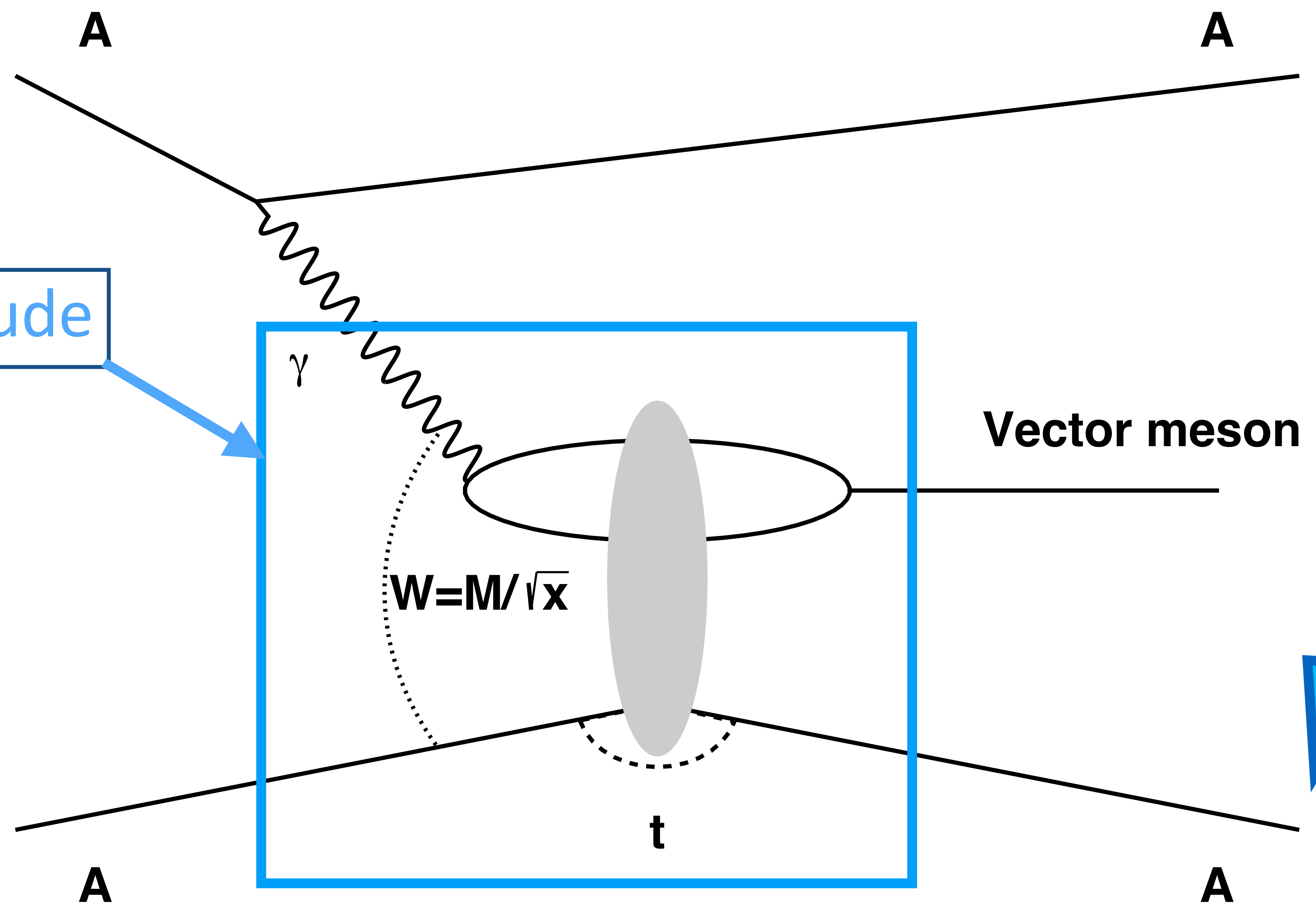

Dipole picture

The photon fluctuates into a long-lived quark-antiquark colour dipole which interacts with the hadronic target and then creates a vector meson

Diffractive vector meson photoproduction

Δ^2=-t

$$\mathscr{A}_{\mathrm{T,L}}(x, Q^2, \vec{\Delta}) = i \int \mathrm{d}\vec{r} \int_0^1 \frac{\mathrm{d}z}{4\pi} \int \mathrm{d}\vec{b}\, |\Psi_\gamma^* \Psi_{\mathrm{V}}|_{\mathrm{T,L}} \exp\left[-i\left(\vec{b} - (\frac{1}{2} - z)\vec{r}\right)\vec{\Delta}\right] \frac{\mathrm{d}\sigma_{\mathrm{H}}^{\mathrm{dip}}}{\mathrm{d}\vec{b}}$$

Amplitude

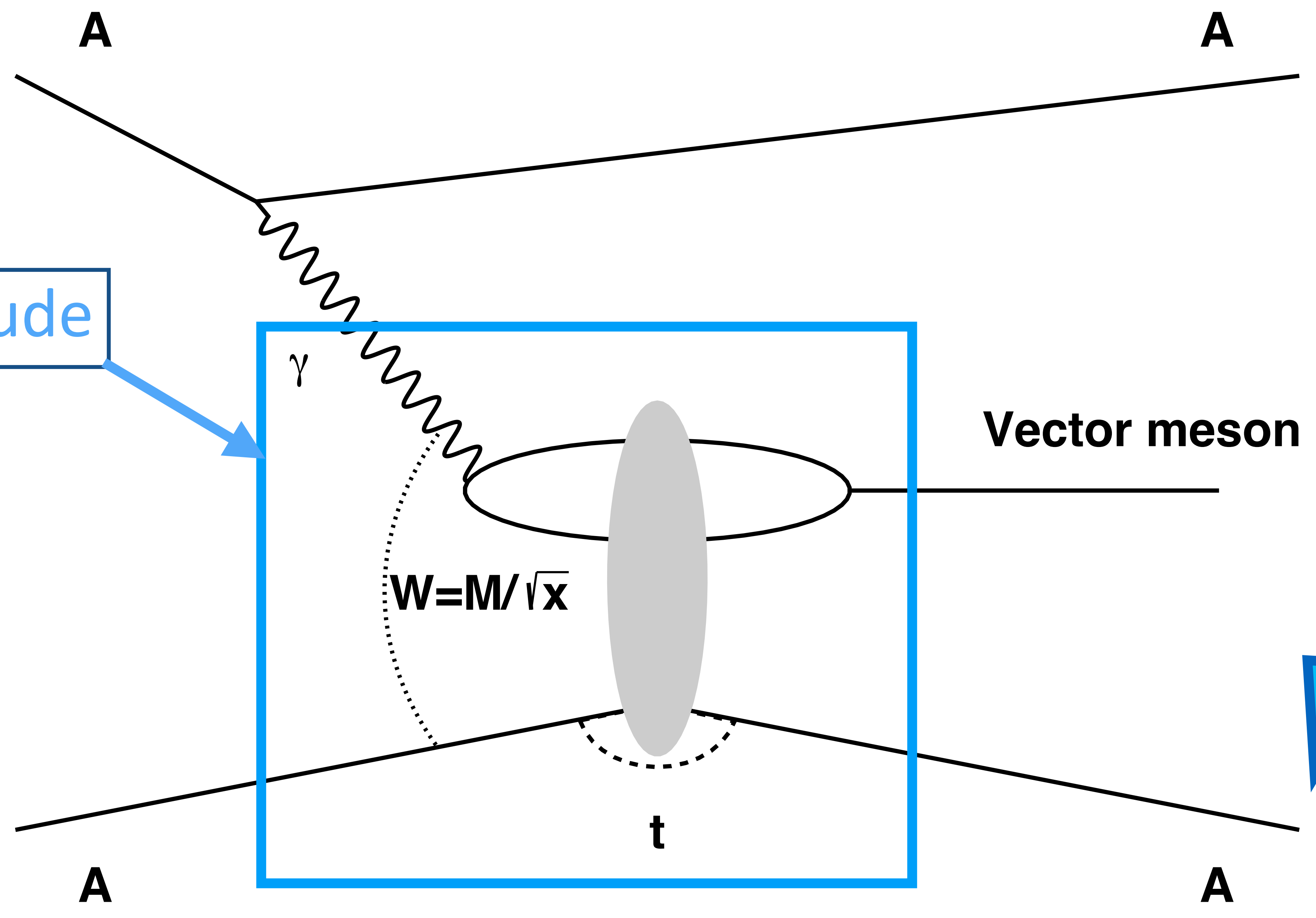

Dipole picture

The photon fluctuates into a long-lived quark-antiquark colour dipole which interacts with the hadronic target and then creates a vector meson

Guillermo Contreras, CTU in Prague

Diffractive vector meson photoproduction

Δ^2=-t

Dipole size

Quark energy fraction

$$\mathcal{A}_{\mathrm{T,L}}(x, Q^2, \vec{\Delta}) = i \int \mathrm{d}\vec{r} \int_0^1 \frac{\mathrm{d}z}{4\pi} \int \mathrm{d}\vec{b}\, |\Psi_\gamma^* \Psi_{\mathrm{V}}|_{\mathrm{T,L}} \exp\left[-i\left(\vec{b} - (\frac{1}{2} - z)\vec{r}\right)\vec{\Delta}\right] \frac{\mathrm{d}\sigma_{\mathrm{H}}^{\mathrm{dip}}}{\mathrm{d}\vec{b}}$$

Amplitude

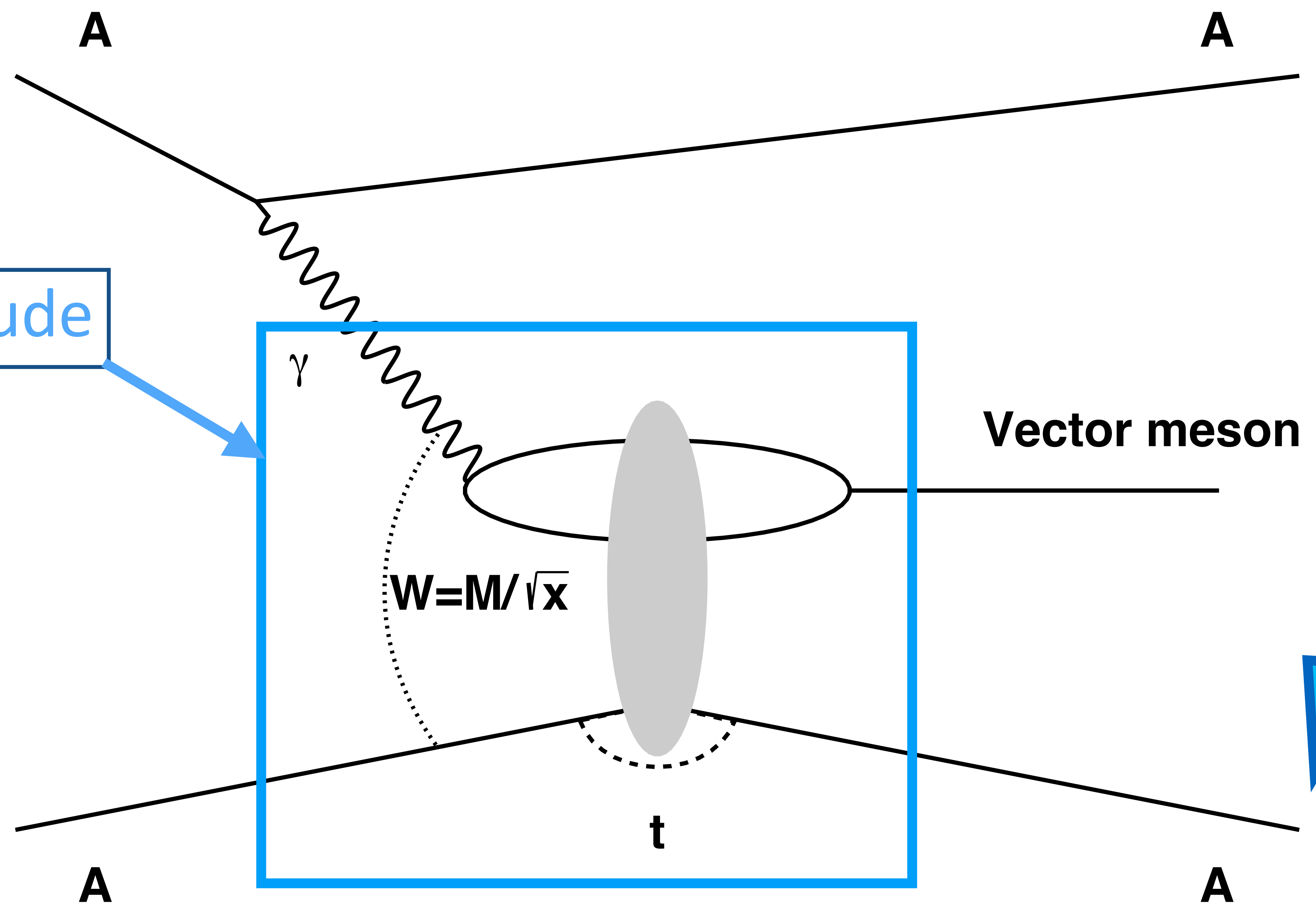

Dipole picture

The photon fluctuates into a long-lived quark-antiquark colour dipole which interacts with the hadronic target and then creates a vector meson

Diffractive vector meson photoproduction

$\Delta^2=-t$ — Dipole size — Quark energy fraction — Impact parameter

$$\mathcal{A}_{T,L}(x,Q^2,\vec{\Delta}) = i\int d\vec{r}\int_0^1 \frac{dz}{4\pi}\int d\vec{b}\,|\Psi_\gamma^*\Psi_V|_{T,L}\exp\left[-i\left(\vec{b}-(\frac{1}{2}-z)\vec{r}\right)\vec{\Delta}\right]\frac{d\sigma_H^{dip}}{d\vec{b}}$$

Amplitude

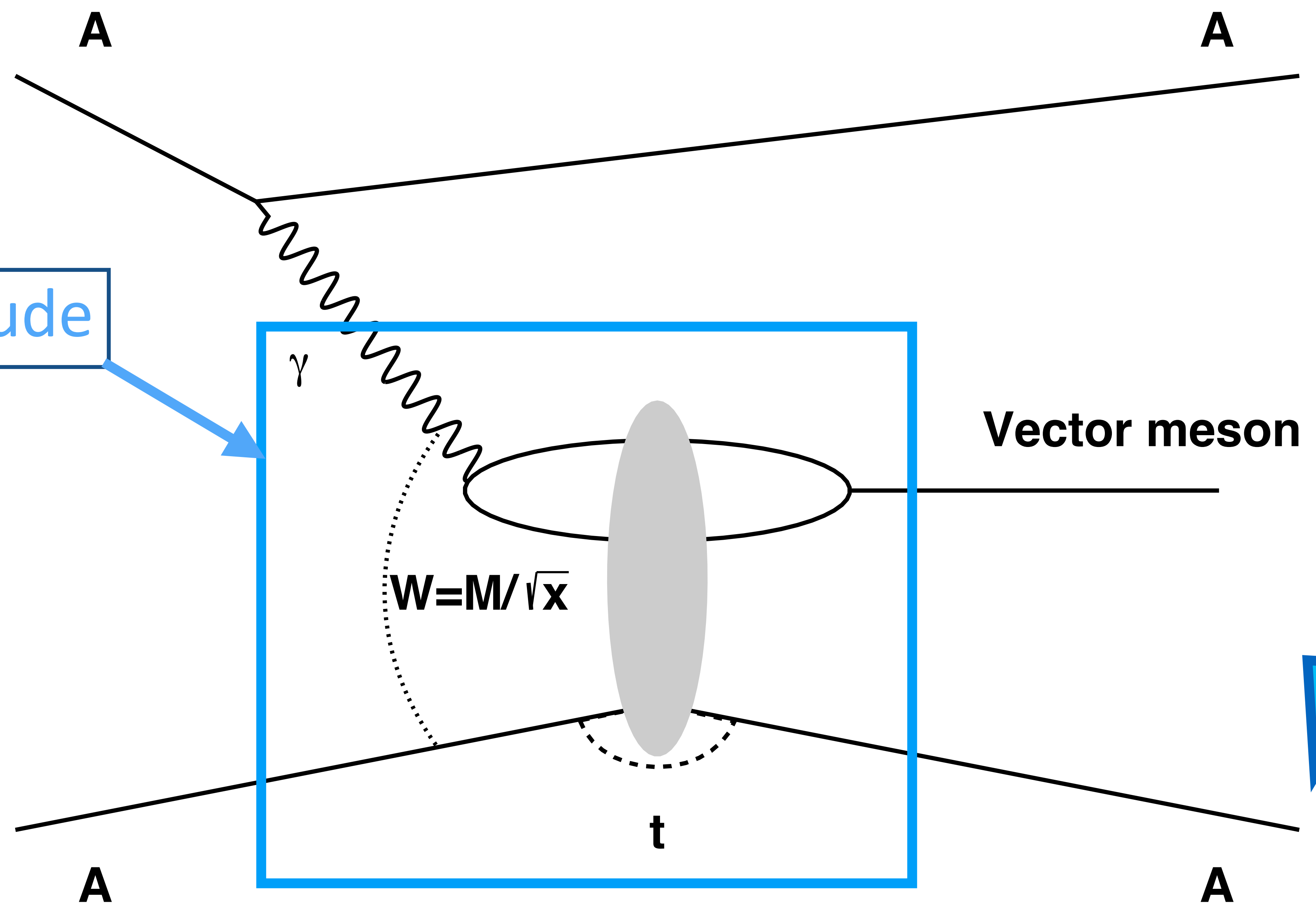

Dipole picture

The photon fluctuates into a long-lived quark-antiquark colour dipole which interacts with the hadronic target and then creates a vector meson

Diffractive vector meson photoproduction

Δ^2=-t | Dipole size | Quark energy fraction | Impact parameter | conjugate variable

$$\mathscr{A}_{\mathrm{T,L}}(x, Q^2, \vec{\Delta}) = i \int \mathrm{d}\vec{r} \int_0^1 \frac{\mathrm{d}z}{4\pi} \int \mathrm{d}\vec{b}\, |\Psi_\gamma^* \Psi_{\mathrm{V}}|_{\mathrm{T,L}} \exp\left[-i\left(\vec{b} - (\frac{1}{2} - z)\vec{r}\right)\vec{\Delta}\right] \frac{\mathrm{d}\sigma_{\mathrm{H}}^{\mathrm{dip}}}{\mathrm{d}\vec{b}}$$

Amplitude

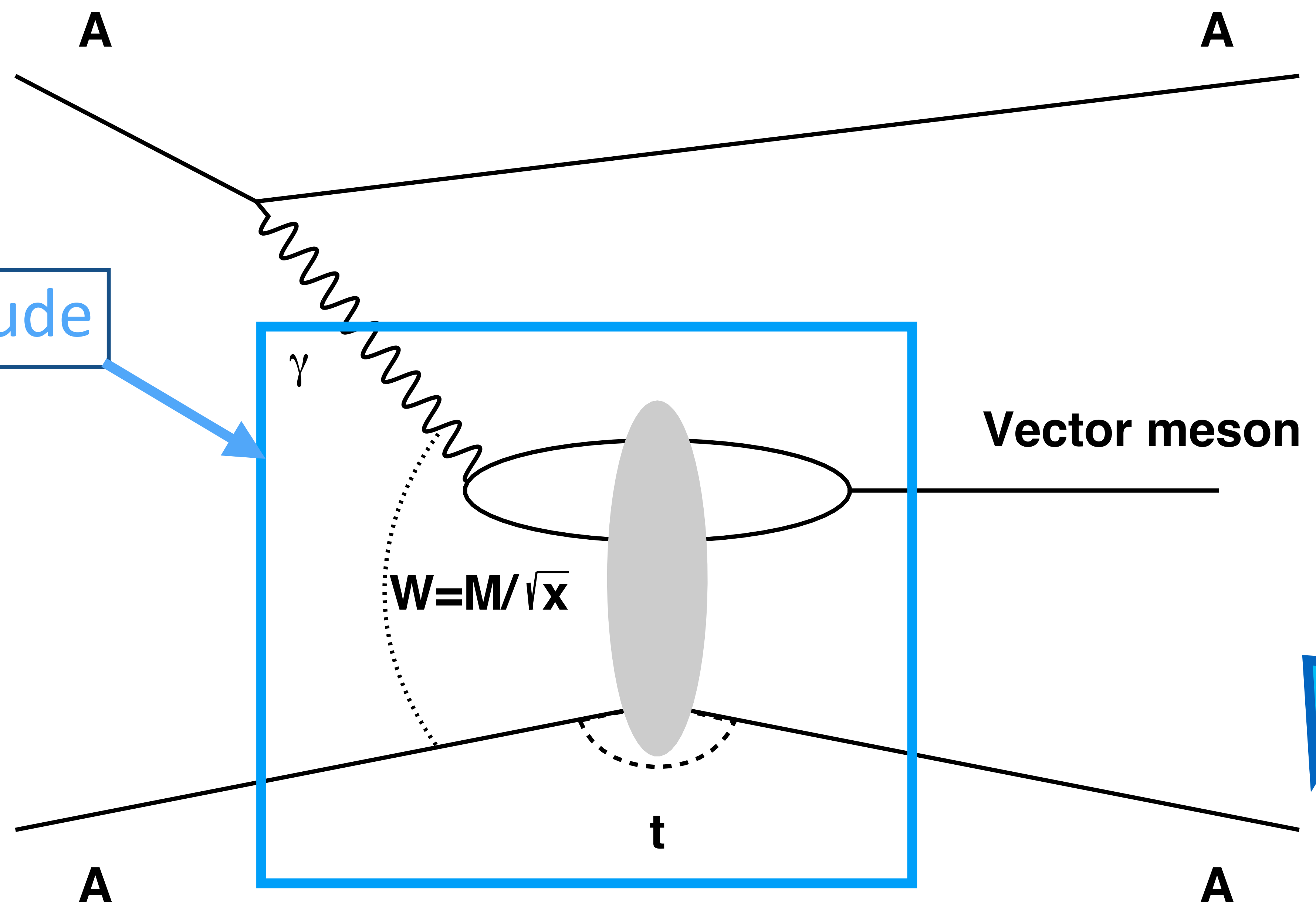

Dipole picture

The photon fluctuates into a long-lived quark-antiquark colour dipole which interacts with the hadronic target and then creates a vector meson

Diffractive vector meson photoproduction

Δ^2=-t

Dipole size

Quark energy fraction

Impact parameter

conjugate variable

$$\mathscr{A}_{\mathrm{T,L}}(x, Q^2, \vec{\Delta}) = i\int \mathrm{d}\vec{r}\int_0^1 \frac{\mathrm{d}z}{4\pi}\int \mathrm{d}\vec{b}\,|\Psi_\gamma^*\Psi_{\mathrm{V}}|_{\mathrm{T,L}}\exp\left[-i\left(\vec{b}-(\frac{1}{2}-z)\vec{r}\right)\vec{\Delta}\right]\frac{\mathrm{d}\sigma_{\mathrm{H}}^{\mathrm{dip}}}{\mathrm{d}\vec{b}}$$

Amplitude

Photon-dipole wave function

Vector meson wave function

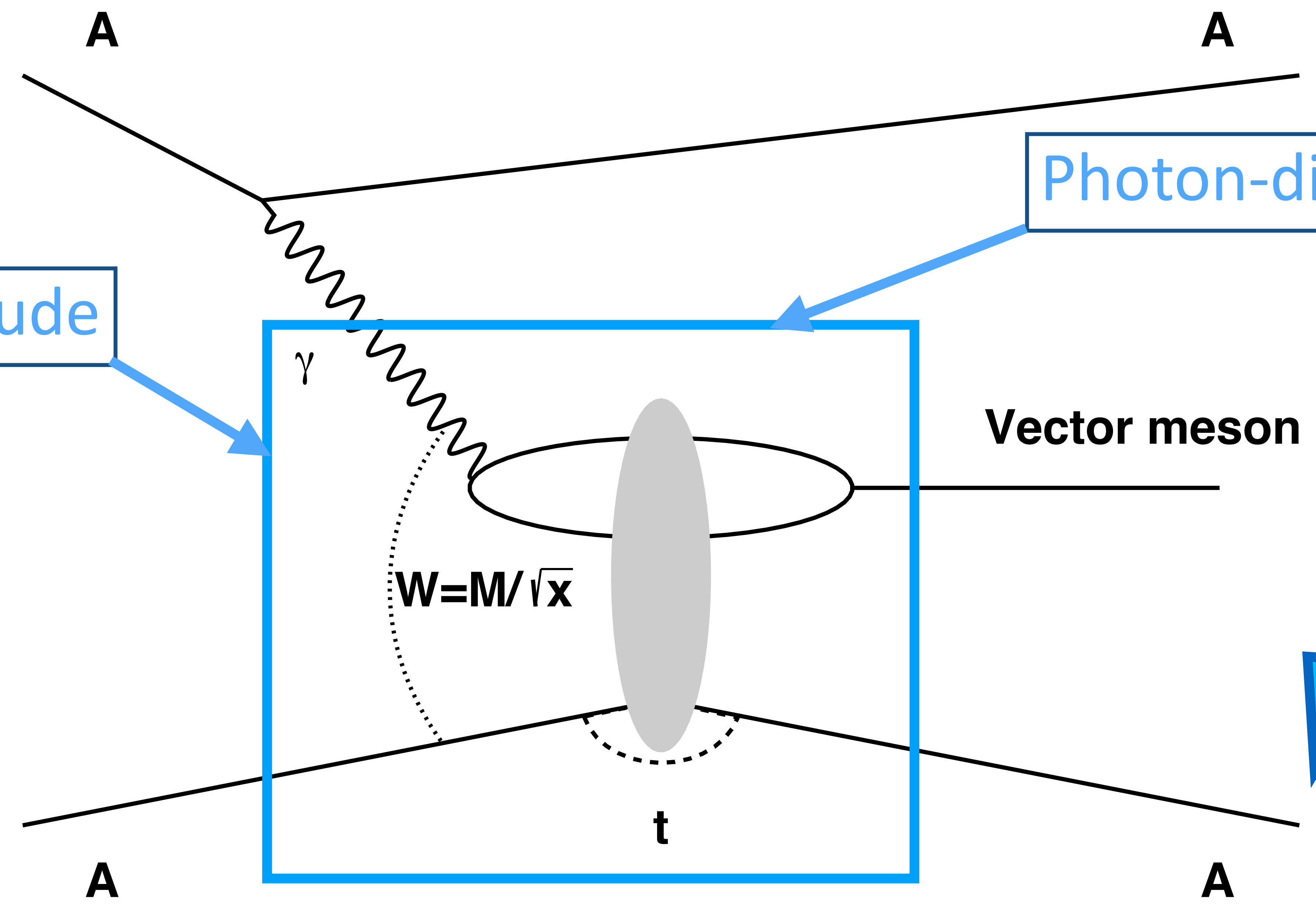

Dipole picture

The photon fluctuates into a long-lived quark-antiquark colour dipole which interacts with the hadronic target and then creates a vector meson

Diffractive vector meson photoproduction

Δ^2=-t

Dipole size

Quark energy fraction

Impact parameter

conjugate variable

$$\mathcal{A}_{\mathrm{T,L}}(x, Q^2, \vec{\Delta}) = i \int \mathrm{d}\vec{r} \int_0^1 \frac{\mathrm{d}z}{4\pi} \int \mathrm{d}\vec{b}\, |\Psi^*_\gamma \Psi_{\mathrm{V}}|_{\mathrm{T,L}} \exp\left[-i\left(\vec{b} - (\frac{1}{2} - z)\vec{r}\right)\vec{\Delta}\right] \frac{\mathrm{d}\sigma_{\mathrm{H}}^{\mathrm{dip}}}{\mathrm{d}\vec{b}}$$

Amplitude

Photon-dipole wave function

Vector meson wave function

Dipole-hadron cross section, our knowledge of pQCD is encoded here

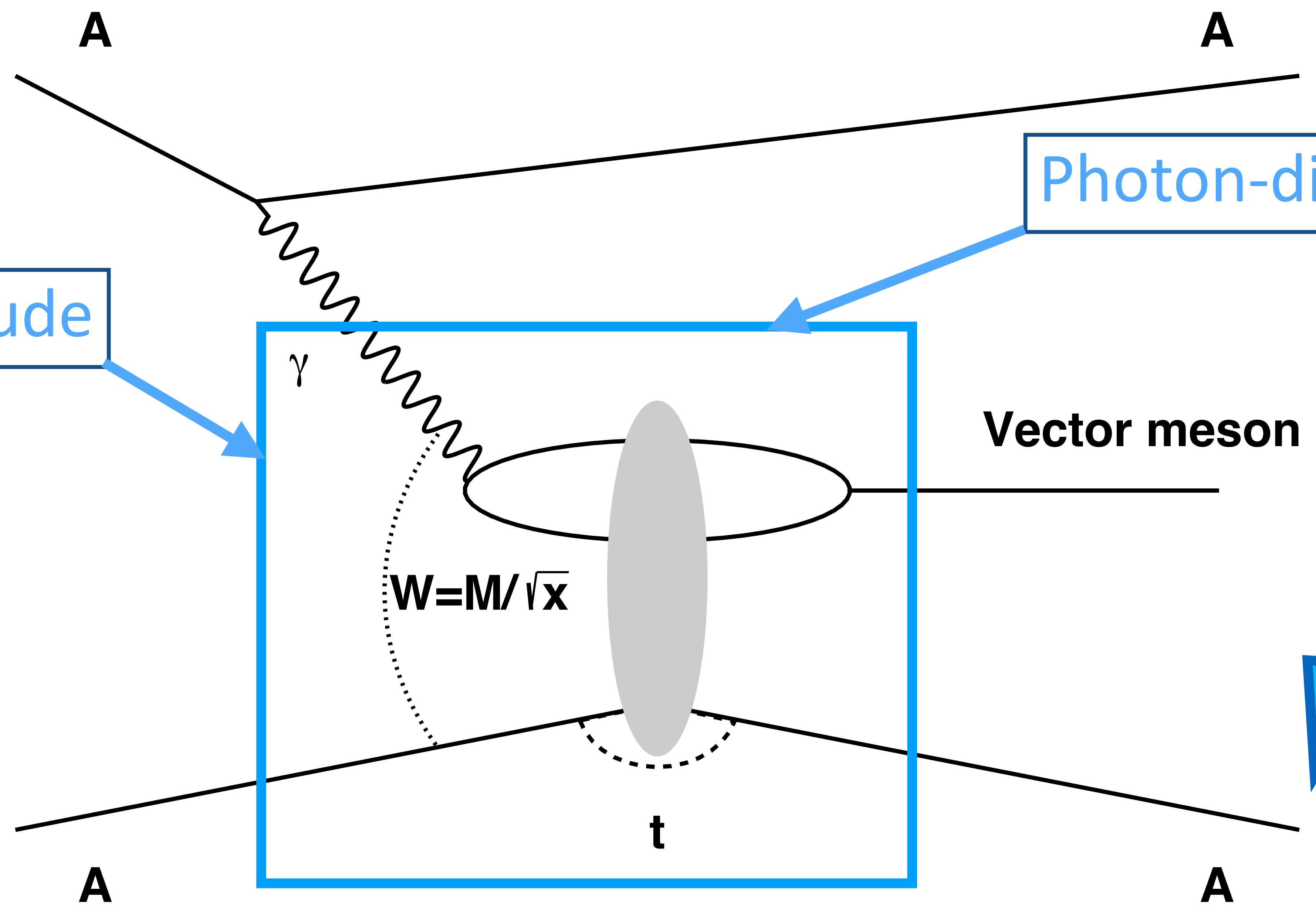

Dipole picture

The photon fluctuates into a long-lived quark-antiquark colour dipole which interacts with the hadronic target and then creates a vector meson

The Good-Walker picture of vector meson photoproduction

Coherent (Exclusive)

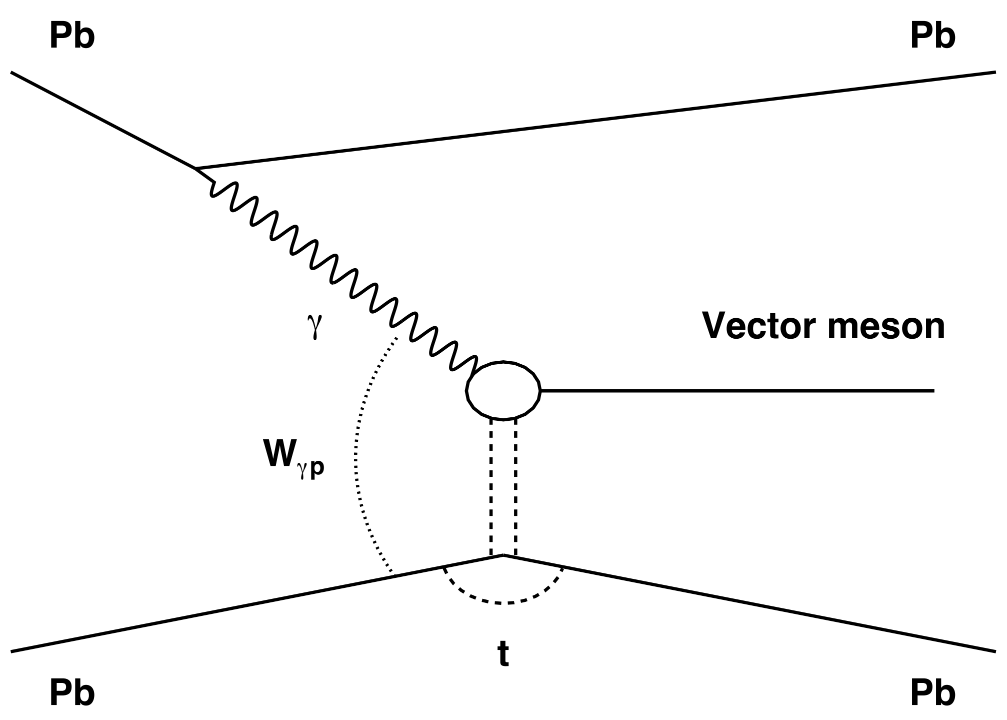

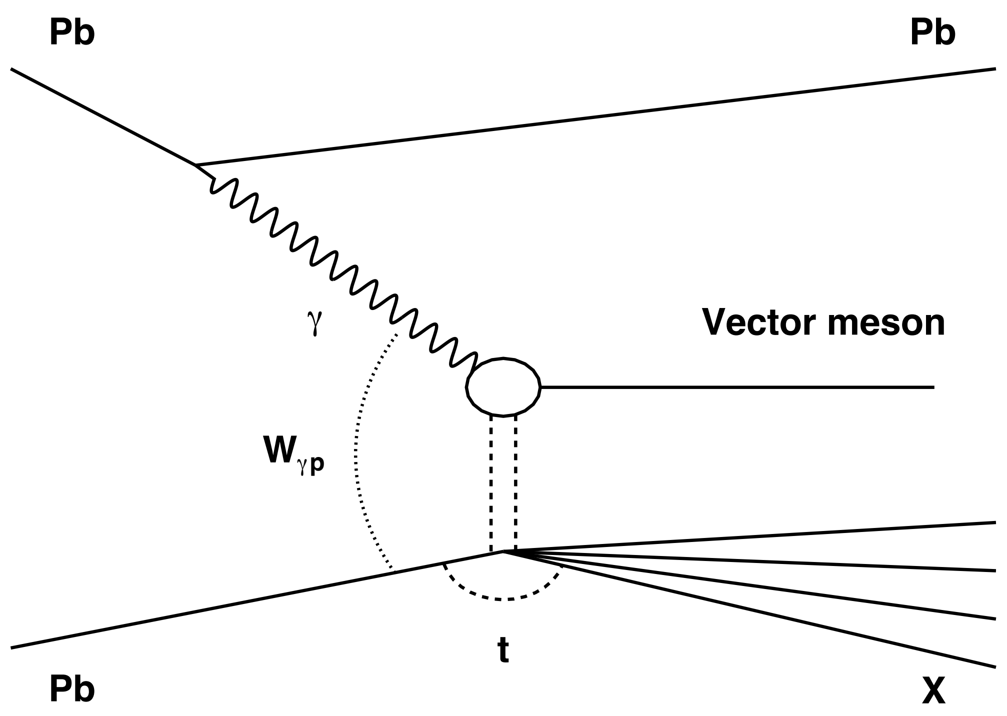

Incoherent (Dissociative)

Guillermo Contreras, CTU in Prague

The Good-Walker picture of vector meson photoproduction

Average over colour configurations

$$\left.\frac{d\sigma^{\gamma^* H \to VH}}{d|t|}\right|_{T,L} = \frac{\left(R_g^{T,L}\right)^2}{16\pi} |\langle \mathcal{A}_{T,L} \rangle|^2$$

Coherent (Exclusive)

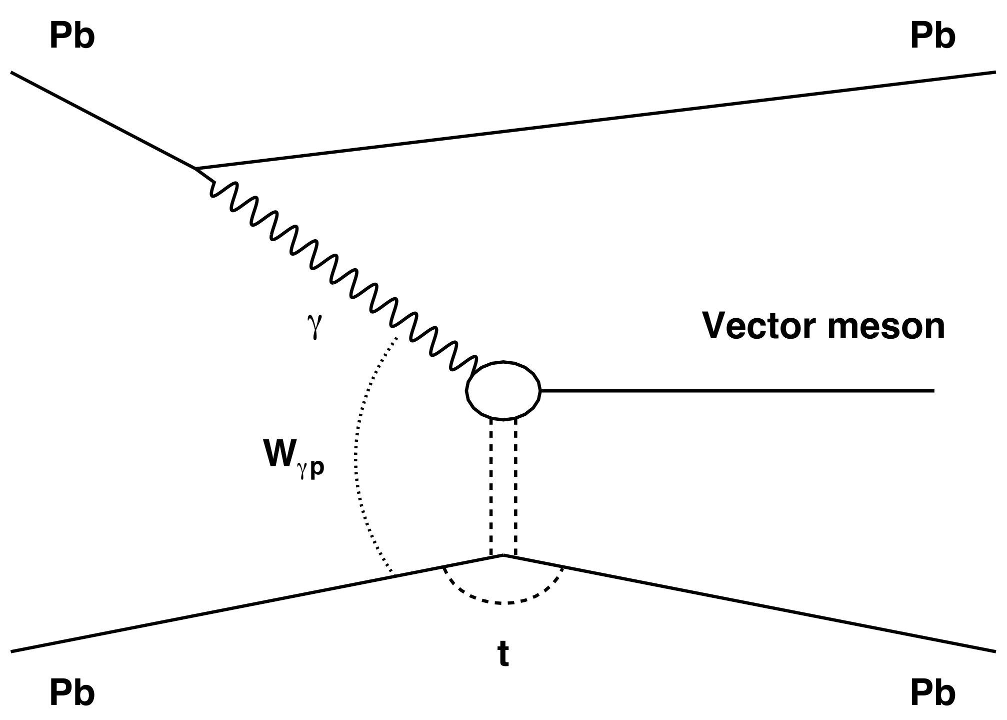

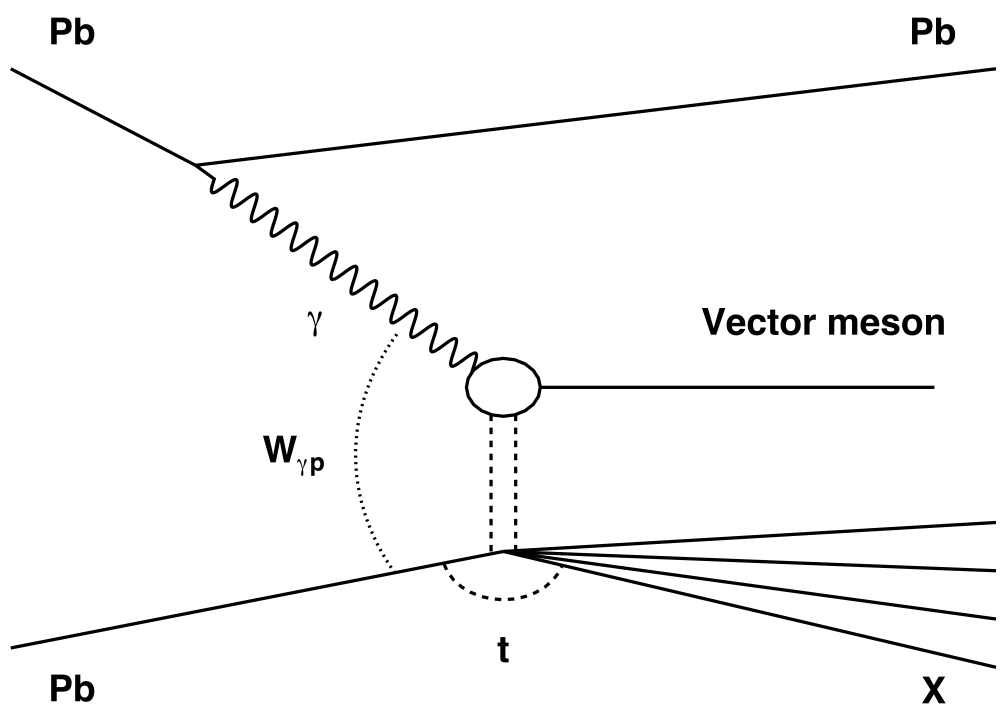

Incoherent (Dissociative)

The Good-Walker picture of vector meson photoproduction

Average over colour configurations

$$\left.\frac{d\sigma^{\gamma^* H \to VH}}{d|t|}\right|_{T,L} = \frac{\left(R_g^{T,L}\right)^2}{16\pi} \left|\langle \mathcal{A}_{T,L} \rangle\right|^2$$

Variance over colour configurations

$$\left.\frac{d\sigma^{\gamma^* p \to VY}}{d|t|}\right|_{T,L} = \frac{\left(R_g^{T,L}\right)^2}{16\pi} \left(\langle |\mathcal{A}_{T,L}|^2 \rangle - |\langle \mathcal{A}_{T,L} \rangle|^2 \right)$$

Coherent (Exclusive)

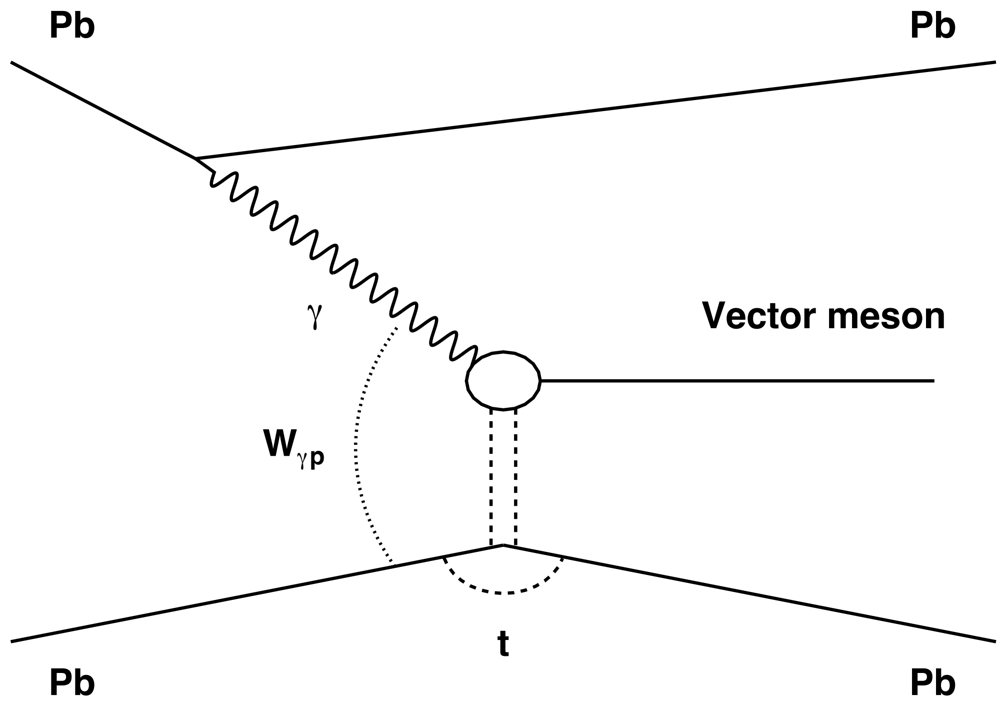

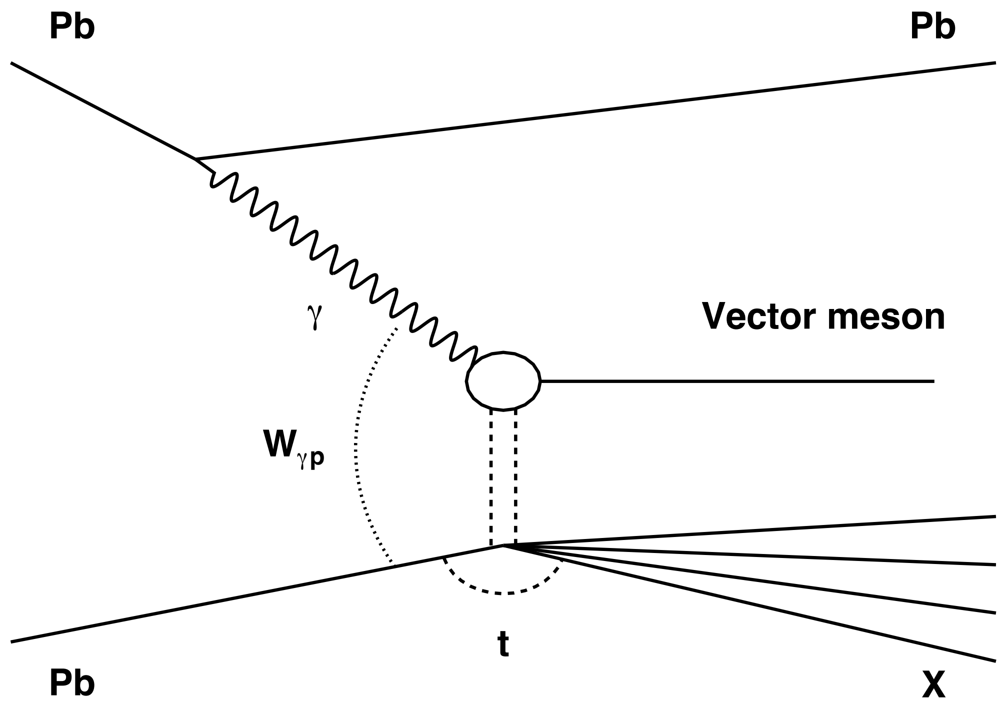

Incoherent (Dissociative)

The Good-Walker picture of vector meson photoproduction

Coherent (Exclusive)

Average over colour configurations

$$\left.\frac{d\sigma^{\gamma^* H \to VH}}{d|t|}\right|_{T,L} = \frac{\left(R_g^{T,L}\right)^2}{16\pi} |\langle \mathcal{A}_{T,L} \rangle|^2$$

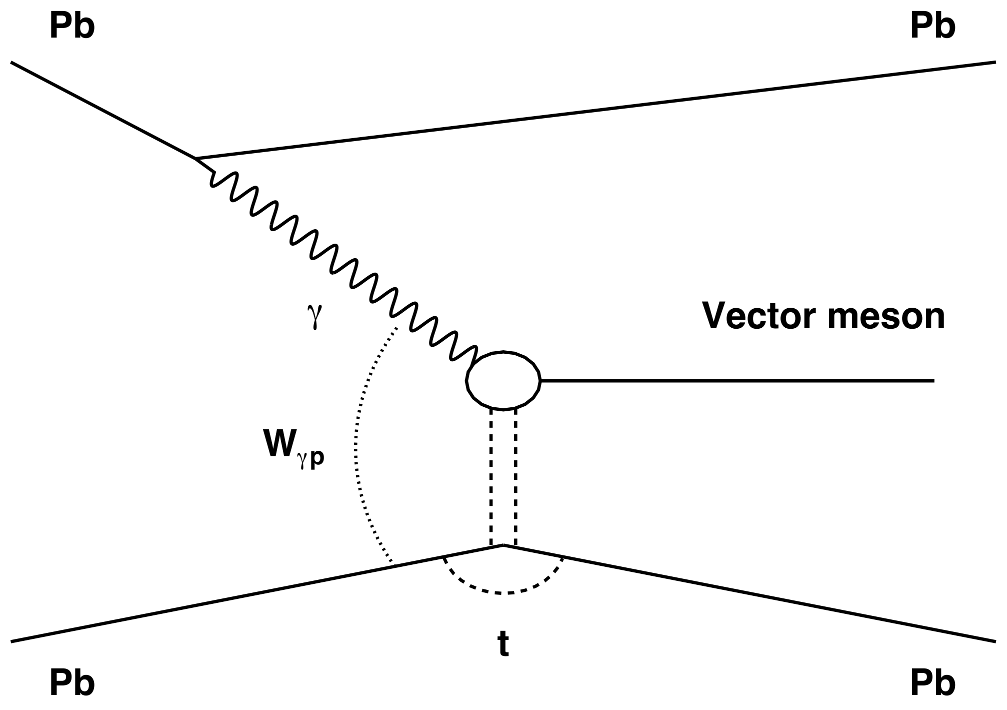

Variance over colour configurations

$$\left.\frac{d\sigma^{\gamma^* p \to VY}}{d|t|}\right|_{T,L} = \frac{\left(R_g^{T,L}\right)^2}{16\pi} \left(\langle |\mathcal{A}_{T,L}|^2 \rangle - |\langle \mathcal{A}_{T,L} \rangle|^2 \right)$$

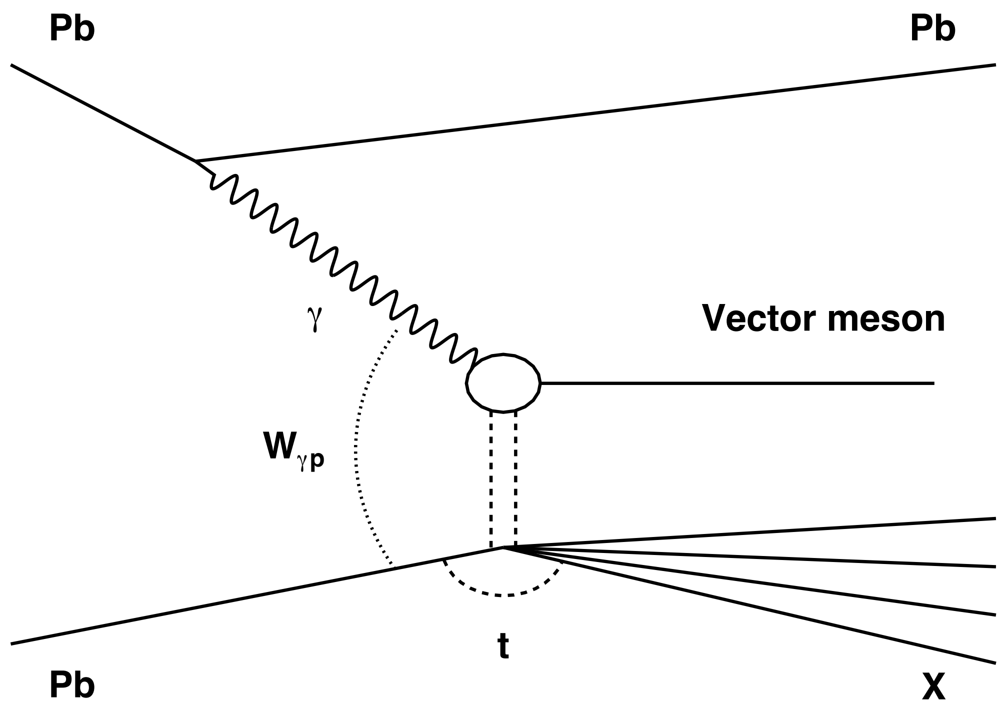

How to include different configurations in the dipole-hadron cross section?

Incoherent (Dissociative)

The energy-dependent hot-spot model

The dipole cross section in the energy-dependent hot-spot model

Ansatz

The Bjorken-x and impact-parameter dependence of the γp cross section are factorised

The dipole cross section in the energy-dependent hot-spot model

Ansatz

The Bjorken-x and impact-parameter dependence of the γp cross section are factorised

$$\frac{d\sigma_p^{dip}}{d\vec{b}} = \sigma_0 N(x, r) T_p(\vec{b})$$

Target profile

The dipole-target amplitude

Cepila, JGC, Tapia Takaki, PLB766 (2017) 186-191

The dipole cross section in the energy-dependent hot-spot model

Ansatz

The Bjorken-x and impact-parameter dependence of the γp cross section are factorised

Target profile

$$\frac{d\sigma_p^{dip}}{d\vec{b}} = \sigma_0 N(x, r) T_p(\vec{b})$$

The dipole-target amplitude

Different configurations are taken into account in the profile distribution

The dipole amplitude in the energy-dependent hot-spot model

GBW model

$$N(x,r) = \left[1 - \exp\left(-\frac{r^2 Q_s^2(x)}{4}\right)\right]$$

Golec-Biernat,Wusthoff, PRD59 (1998) 014017

The dipole amplitude in the energy-dependent hot-spot model

GBW model

Saturation scale

$$N(x,r) = \left[1 - \exp\left(-\frac{r^2 Q_s^2(x)}{4}\right)\right]$$

Golec-Biernat,Wusthoff, PRD59 (1998) 014017

The dipole amplitude in the energy-dependent hot-spot model

GBW model

Saturation scale

$$N(x,r) = \left[1 - \exp\left(-\frac{r^2 Q_s^2(x)}{4}\right)\right]$$

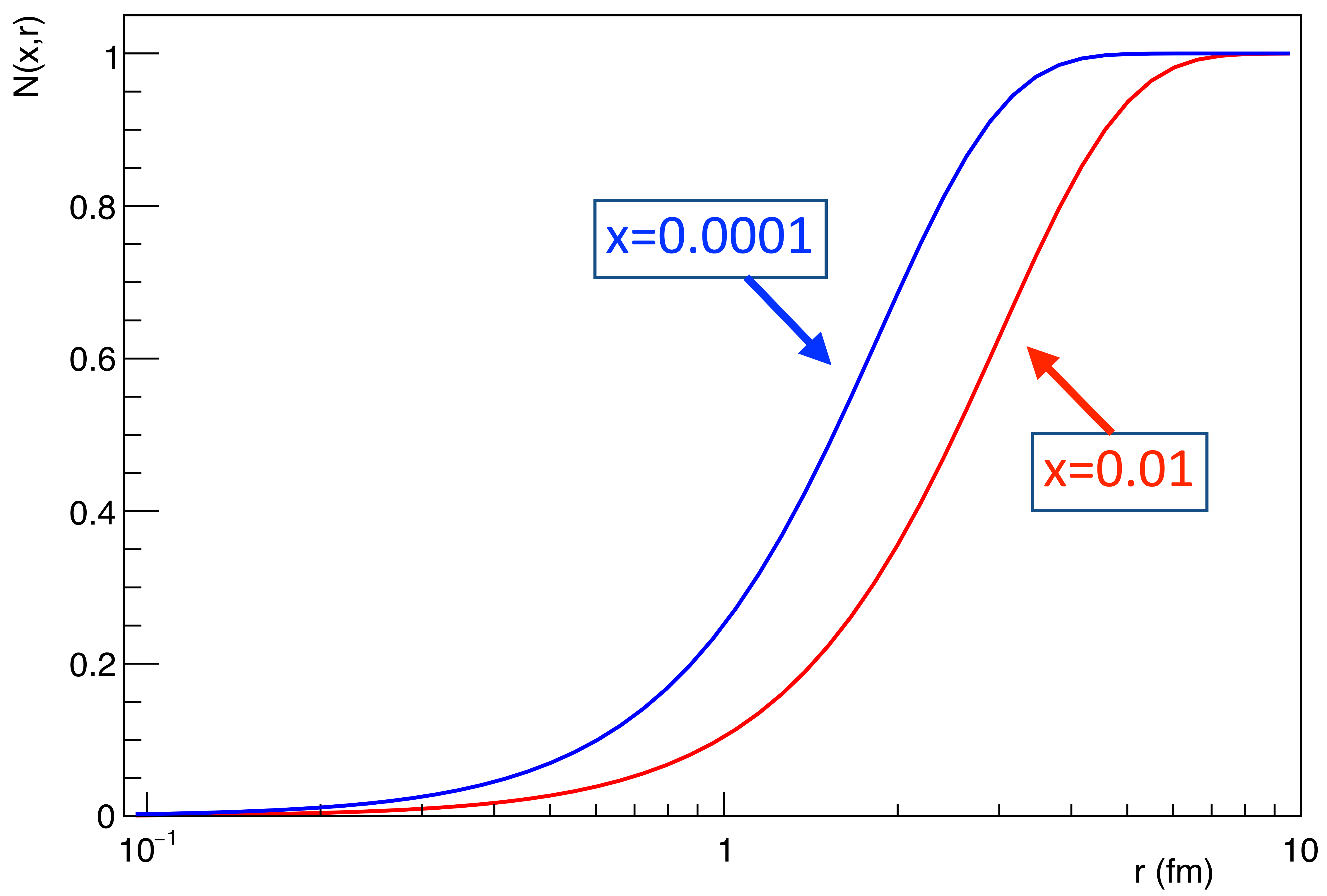

Golec-Biernat,Wusthoff, PRD59 (1998) 014017

The dipole amplitude in the energy-dependent hot-spot model

GBW model

Saturation scale

$$N(x,r) = \left[1 - \exp\left(-\frac{r^2 Q_s^2(x)}{4}\right)\right]$$

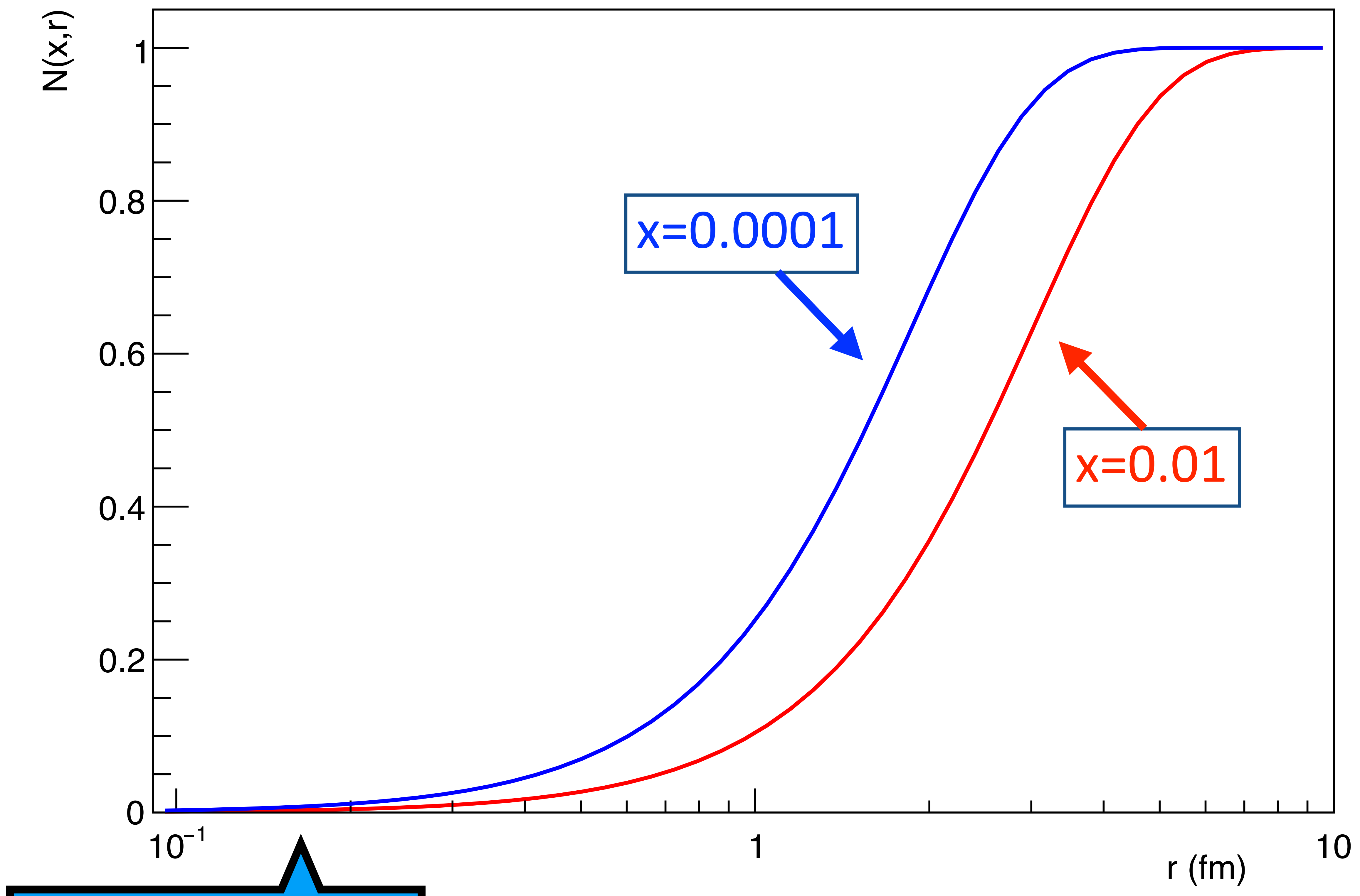

For small values of r, N goes to zero

Golec-Biernat,Wusthoff, PRD59 (1998) 014017

The dipole amplitude in the energy-dependent hot-spot model

GBW model

Saturation scale

$$N(x,r) = \left[1 - \exp\left(-\frac{r^2 Q_s^2(x)}{4}\right)\right]$$

For large values of r, N saturates

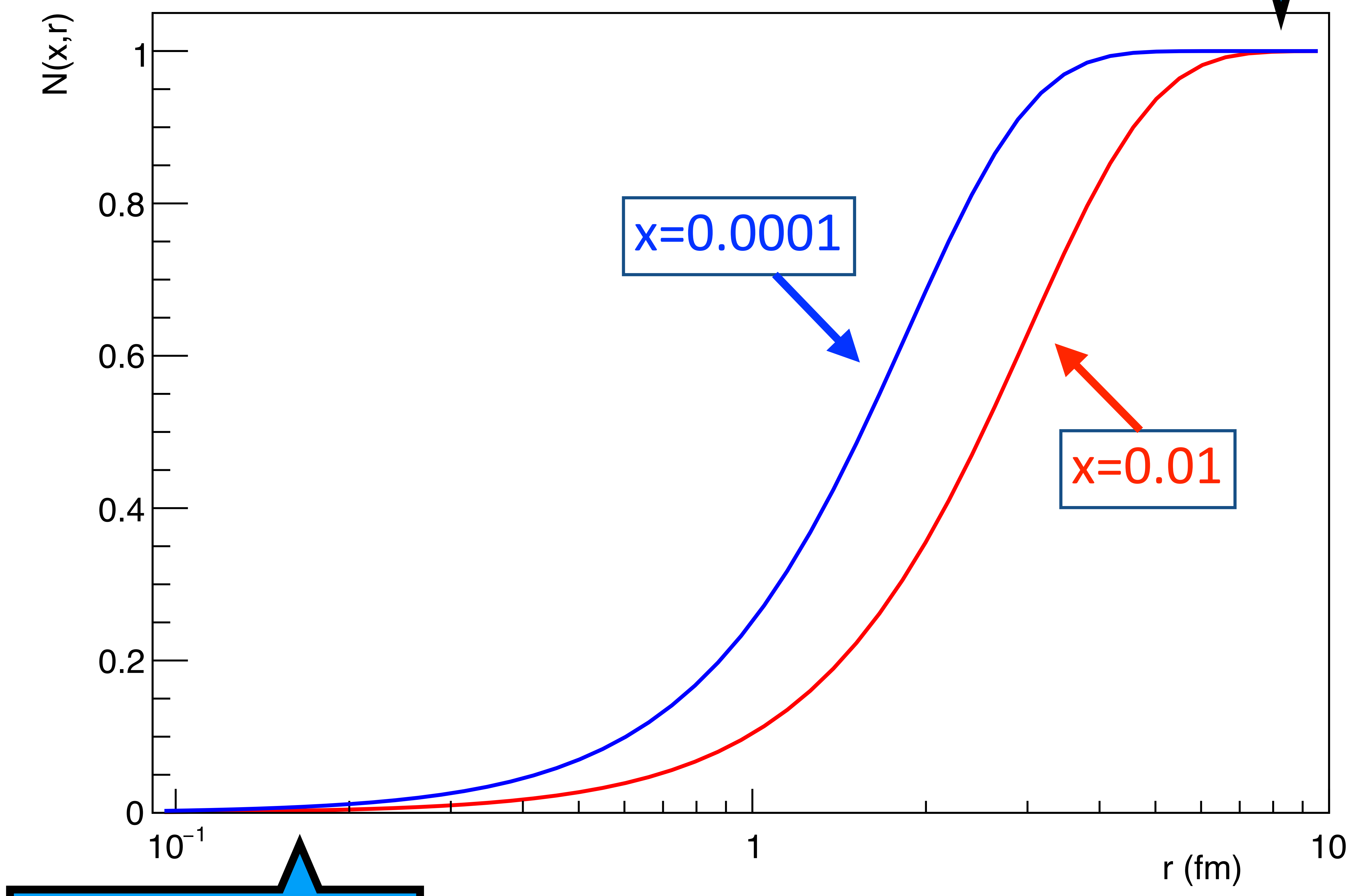

For small values of r, N goes to zero

Golec-Biernat,Wusthoff, PRD59 (1998) 014017

The dipole amplitude in the energy-dependent hot-spot model

GBW model

Saturation scale

$$N(x,r) = \left[1 - \exp\left(-\frac{r^2 Q_s^2(x)}{4}\right)\right]$$

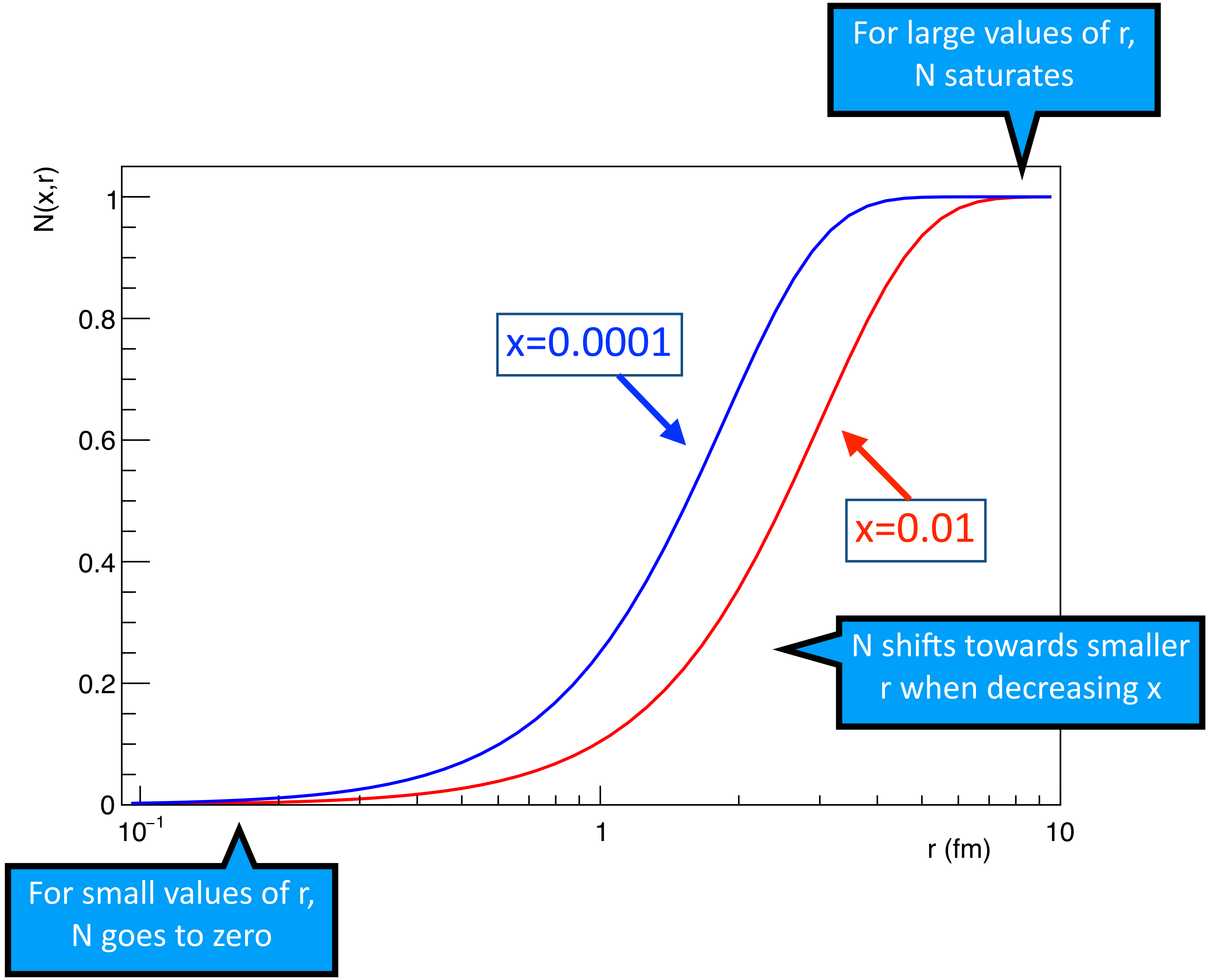

Golec-Biernat,Wusthoff, PRD59 (1998) 014017

The dipole amplitude in the energy-dependent hot-spot model

GBW model

Saturation scale

$$N(x, r) = \left[1 - \exp\left(-\frac{r^2 Q_s^2(x)}{4}\right)\right]$$

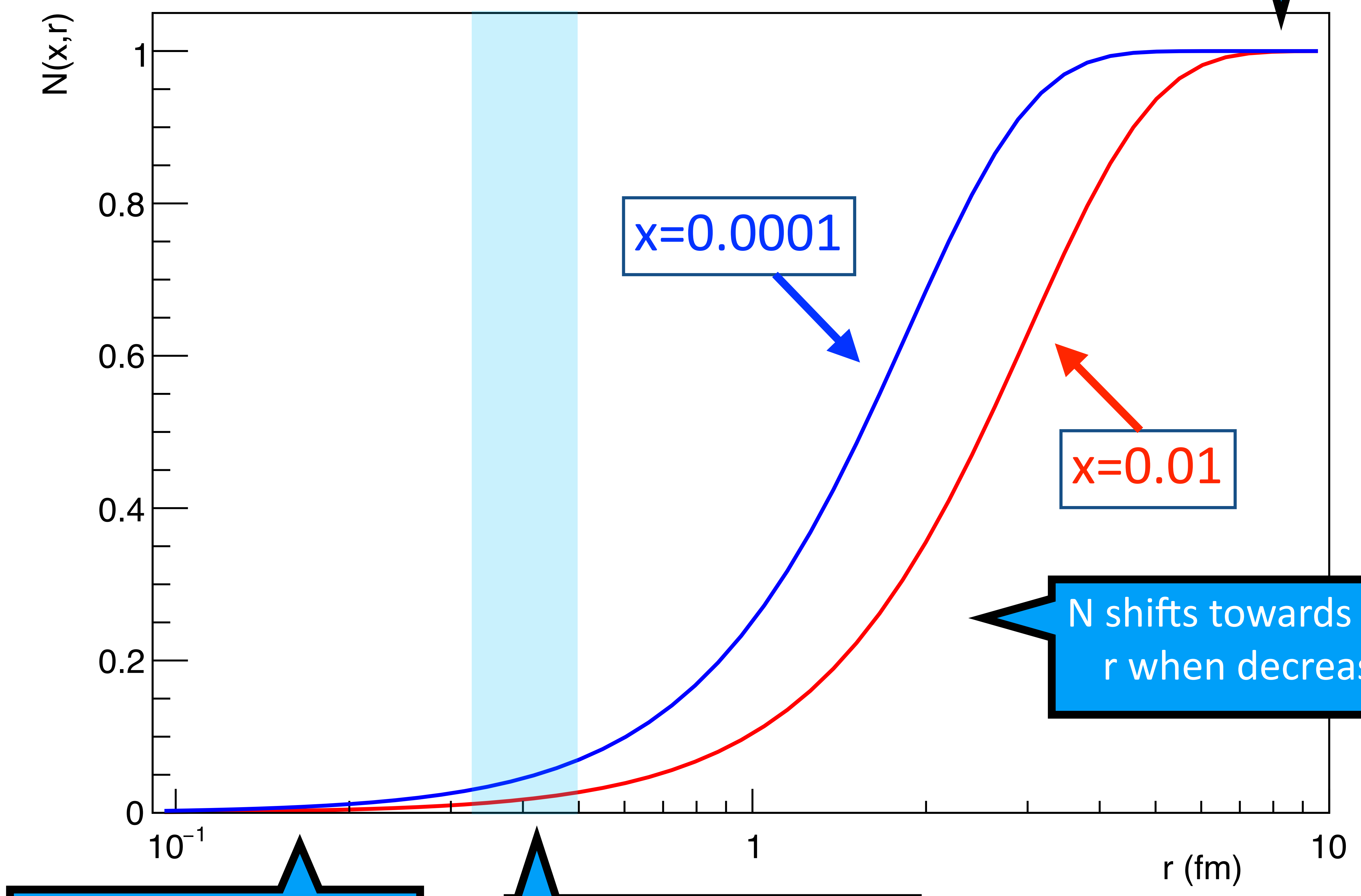

For large values of r, N saturates

N shifts towards smaller r when decreasing x

For small values of r, N goes to zero

The wave functions "select" a range in r

The proton profile in the energy-dependent hot-spot model

The proton is made off a certain number of hot spots

$$T_{\rm p}(\vec{b}) = \frac{1}{N_{\rm hs}} \sum_{i=1}^{N_{\rm hs}} T_{\rm hs}\left(\vec{b} - \vec{b}_i\right)$$

The proton profile in the energy-dependent hot-spot model

The proton is made off a certain number of hot spots

The number of hot spots at a given Bjorken x varies e-b-e and grows with decreasing x

$$T_{\mathrm{p}}(\vec{b}) = \frac{1}{N_{\mathrm{hs}}} \sum_{i=1}^{N_{\mathrm{hs}}} T_{\mathrm{hs}}\left(\vec{b} - \vec{b}_i\right)$$

The proton profile in the energy-dependent hot-spot model

The proton is made off a certain number of hot spots

The number of hot spots at a given Bjorken x varies e-b-e and grows with decreasing x

$$T_{\rm p}(\vec{b}) = \frac{1}{N_{\rm hs}} \sum_{i=1}^{N_{\rm hs}} T_{\rm hs}\left(\vec{b} - \vec{b}_i\right)$$

The positions of the hot spots are obtained e-b-e from a Gaussian distribution representing the proton

The proton profile in the energy-dependent hot-spot model

The proton is made off a certain number of hot spots

The number of hot spots at a given Bjorken x varies e-b-e and grows with decreasing x

$$T_{\rm p}(\vec{b}) = \frac{1}{N_{\rm hs}} \sum_{i=1}^{N_{\rm hs}} T_{\rm hs}\left(\vec{b} - \vec{b}_i\right)$$

The positions of the hot spots are obtained e-b-e from a Gaussian distribution representing the proton

$$T_{\rm hs}(\vec{b} - \vec{b}_i) = \frac{1}{2\pi B_{\rm hs}} \exp\left(-\frac{\left(\vec{b} - \vec{b}_i\right)^2}{2B_{\rm hs}} \right)$$

The hot spots have a Gaussian shape in impact parameter

The number of hot spots in the proton in the energy-dependent hot-spot model

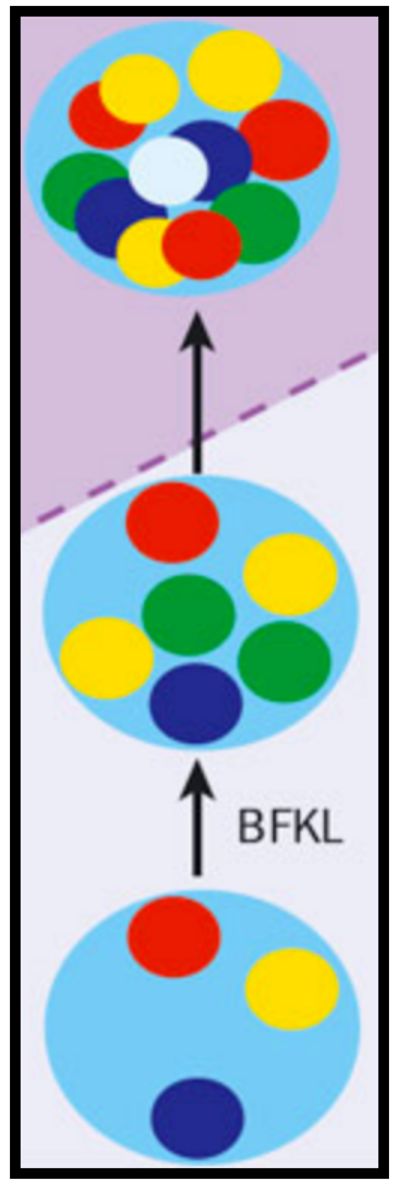

Cepila, JGC, Tapia Takaki, PLB766 (2017) 186-191

The number of hot spots in the proton in the energy-dependent hot-spot model

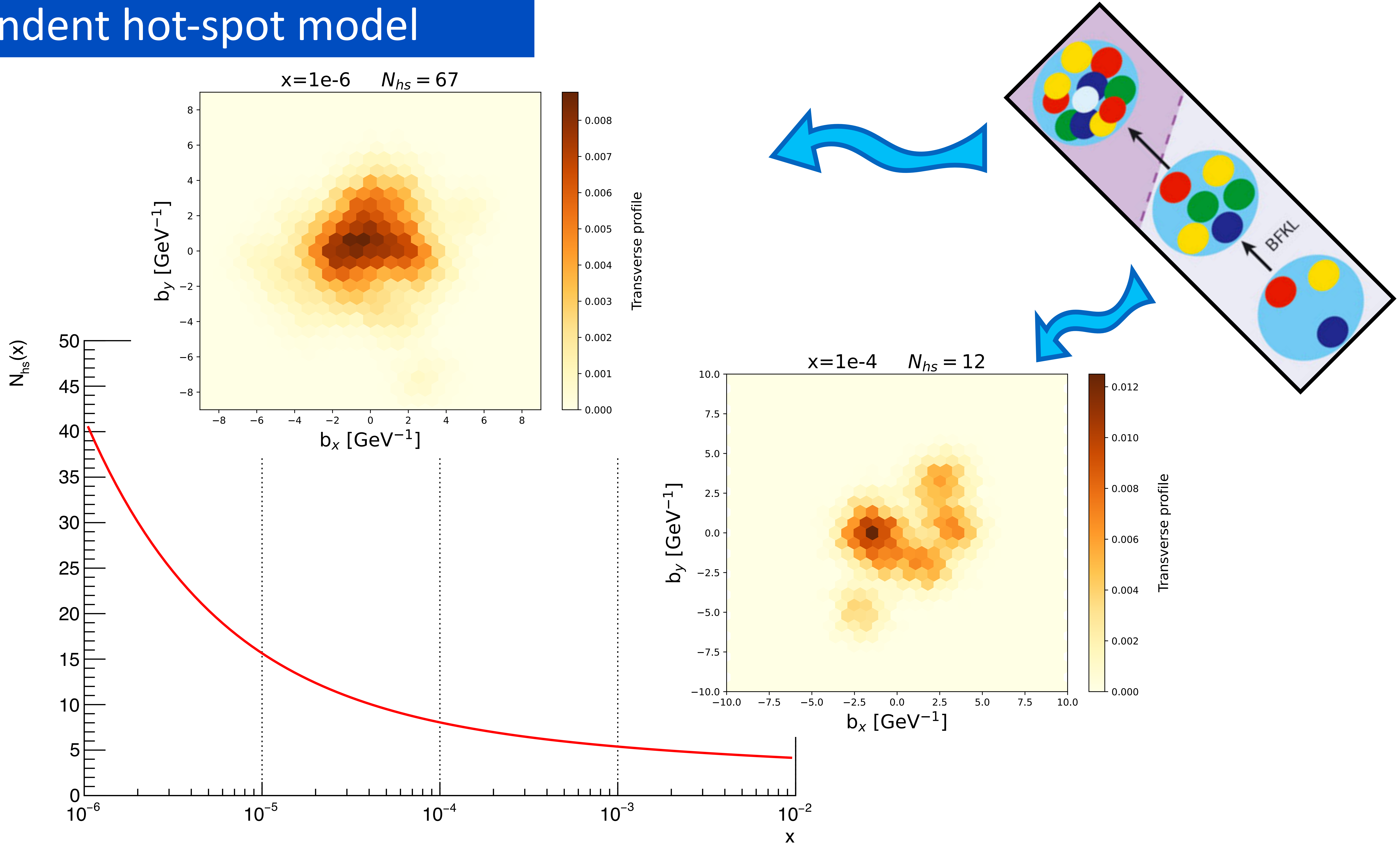

Cepila, JGC, Tapia Takaki, PLB766 (2017) 186-191

The number of hot spots in the proton in the energy-dependent hot-spot model

At small Bjorken-x the hot spots overlap and all configurations resemble each other

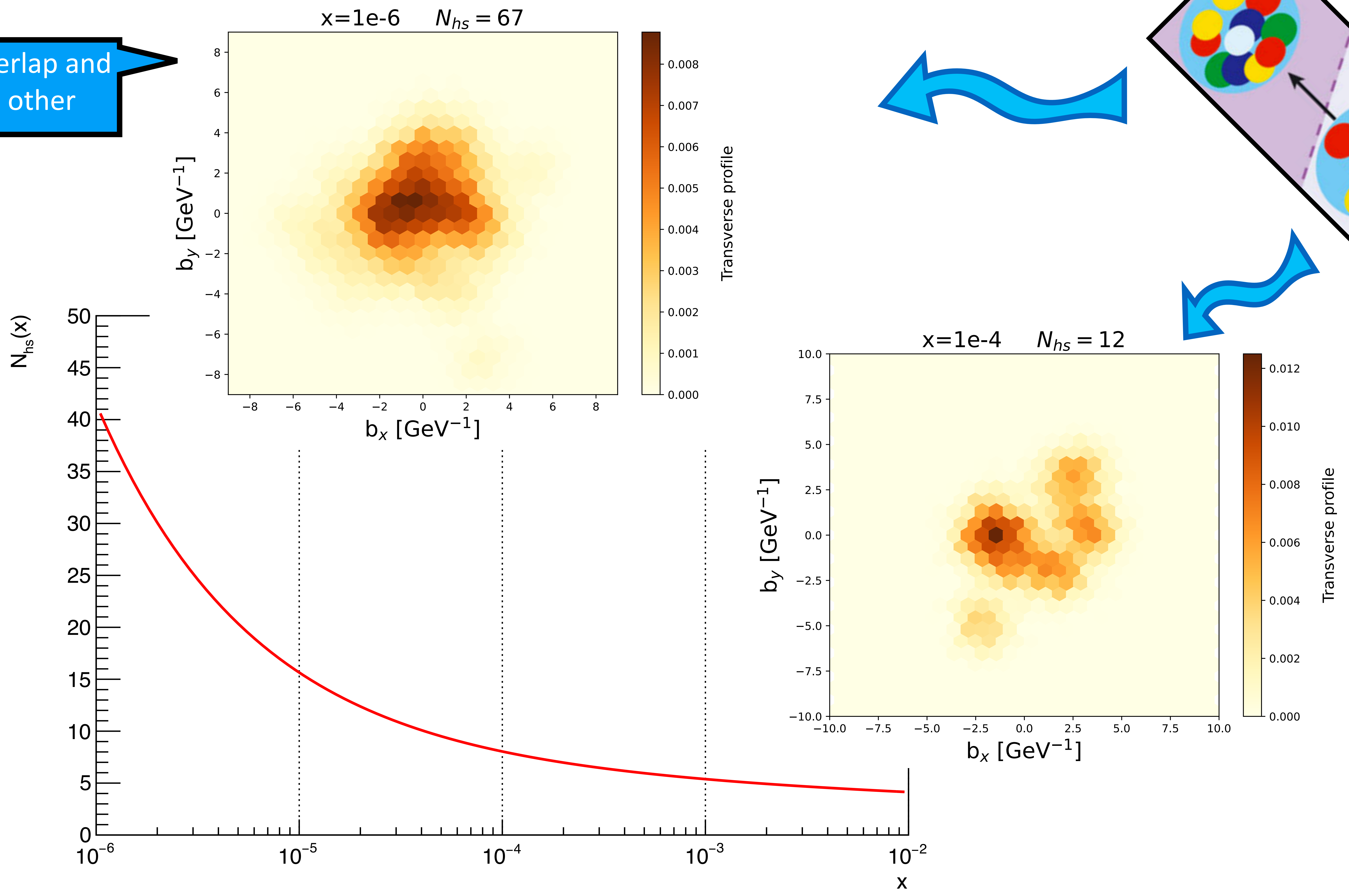

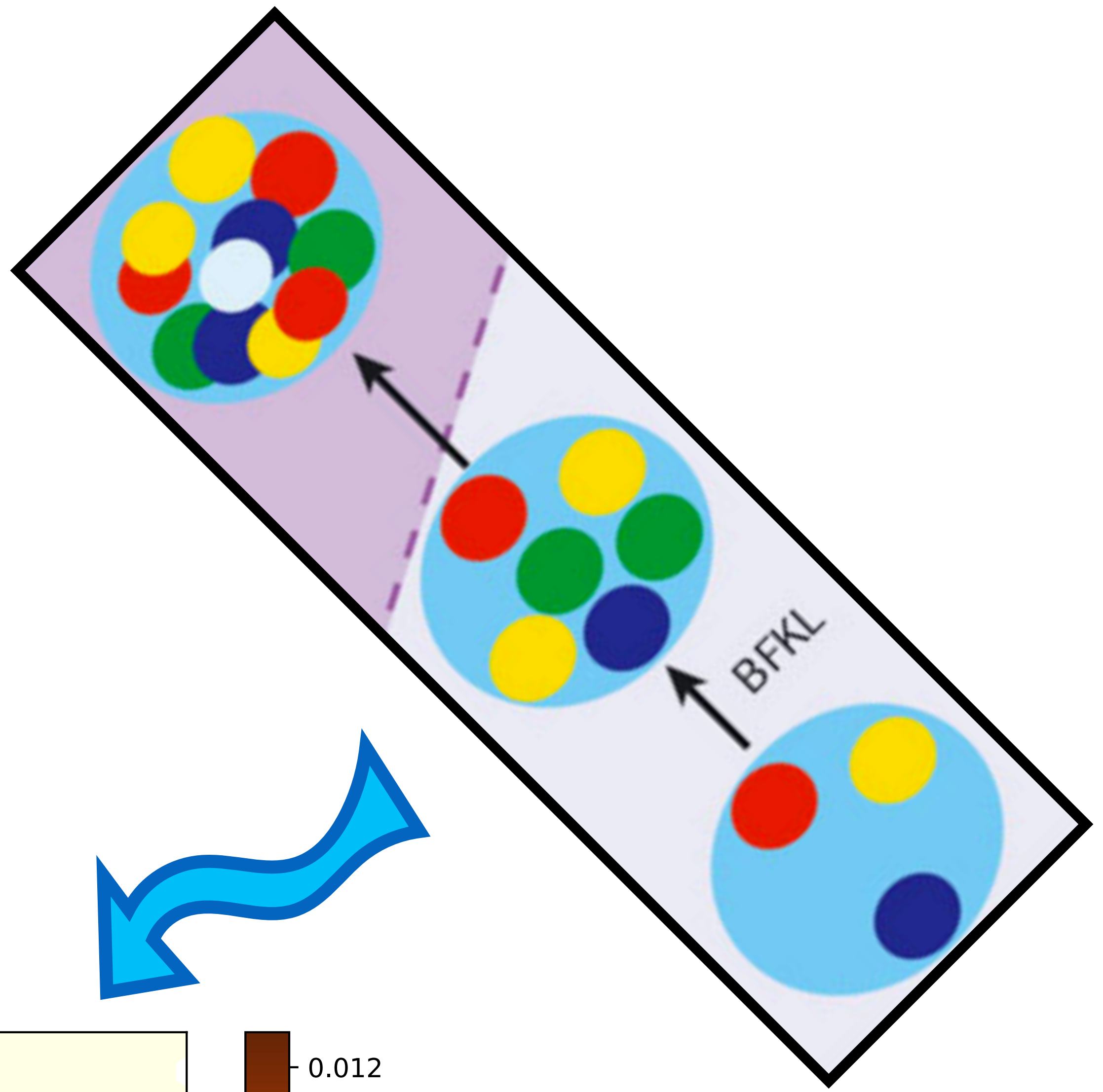

Cepila, JGC, Tapia Takaki, PLB766 (2017) 186-191

The number of hot spots in the proton in the energy-dependent hot-spot model

At small Bjorken-x the hot spots overlap and all configurations resemble each other

In the limit where all configurations look the same, the variance goes to zero

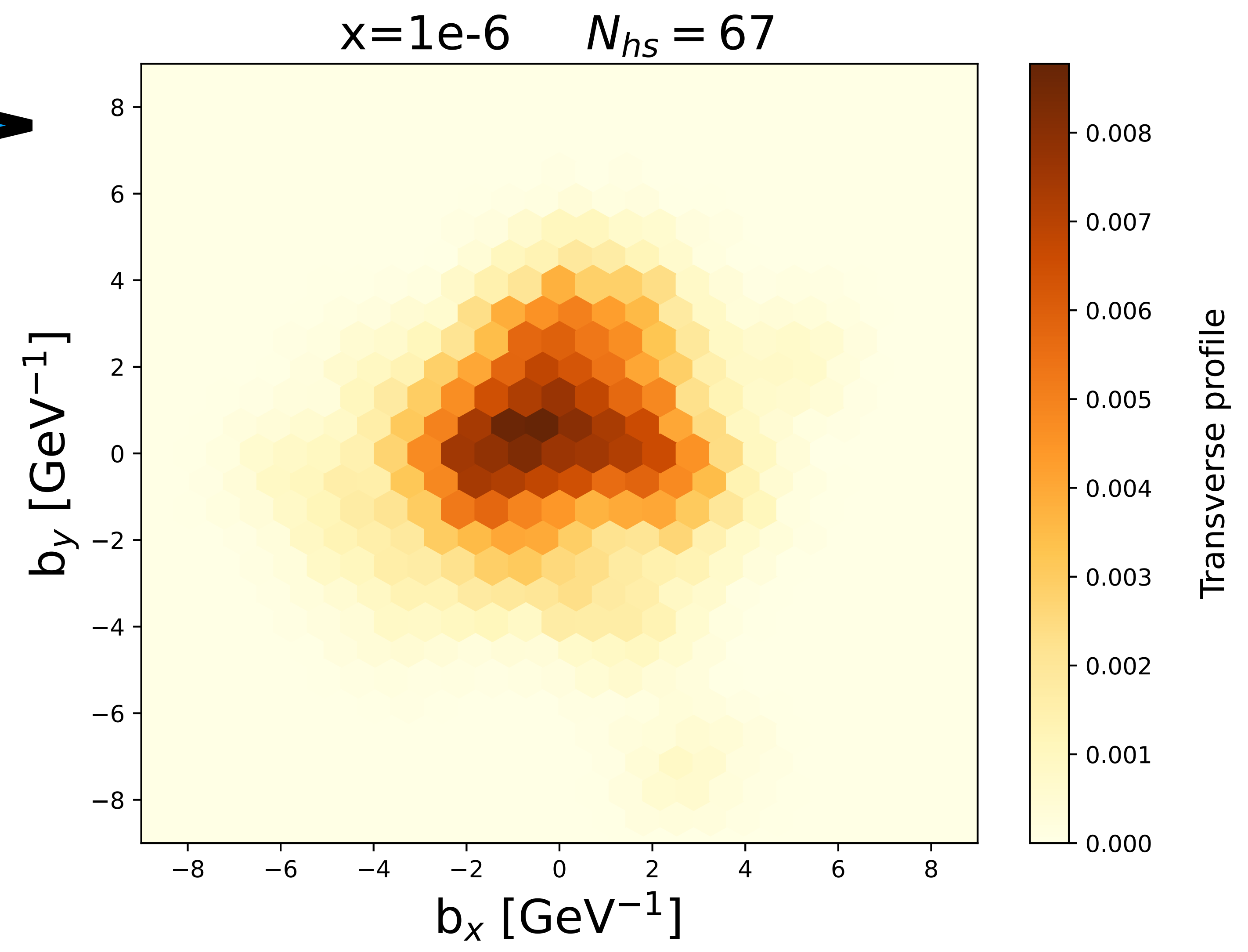

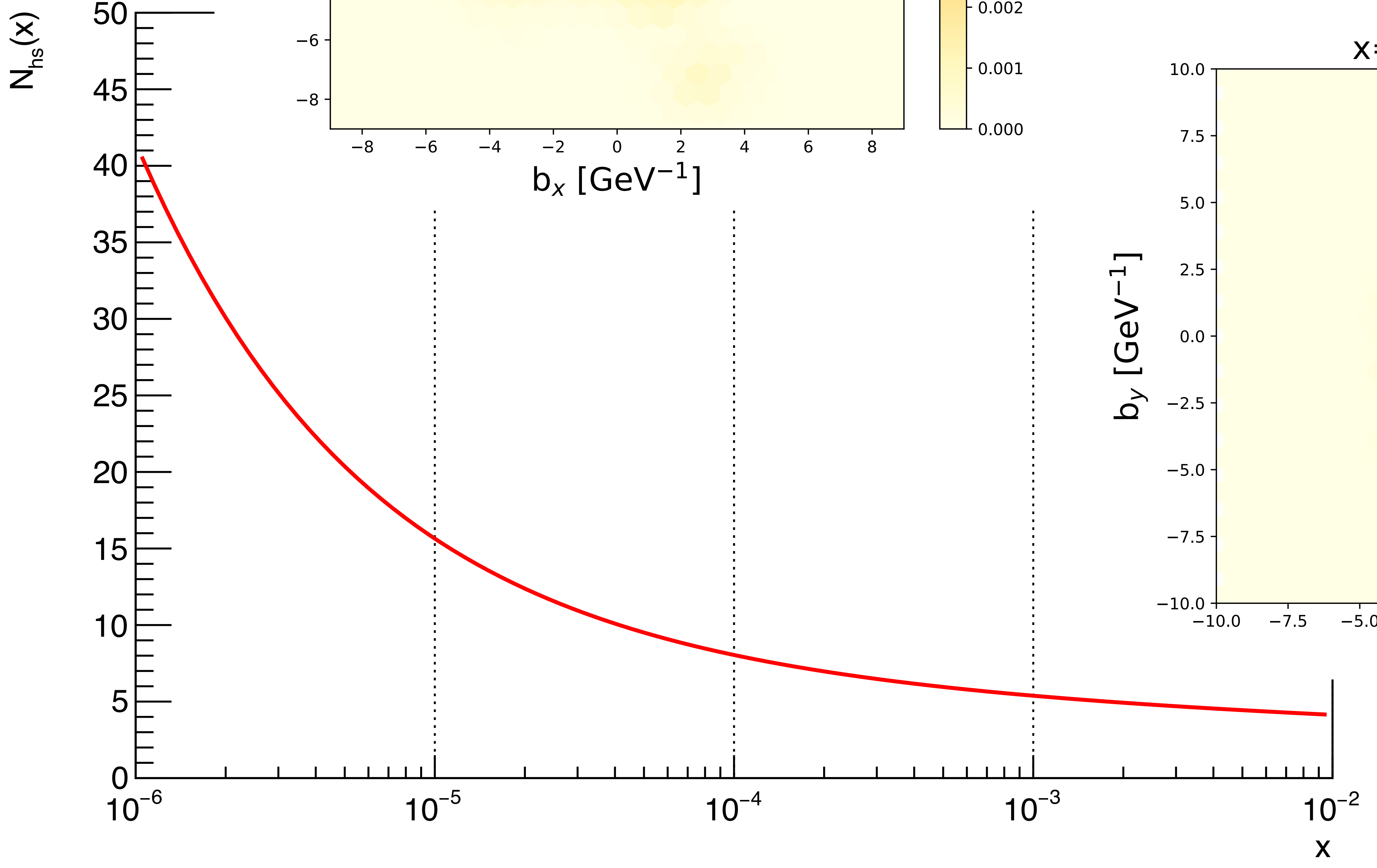

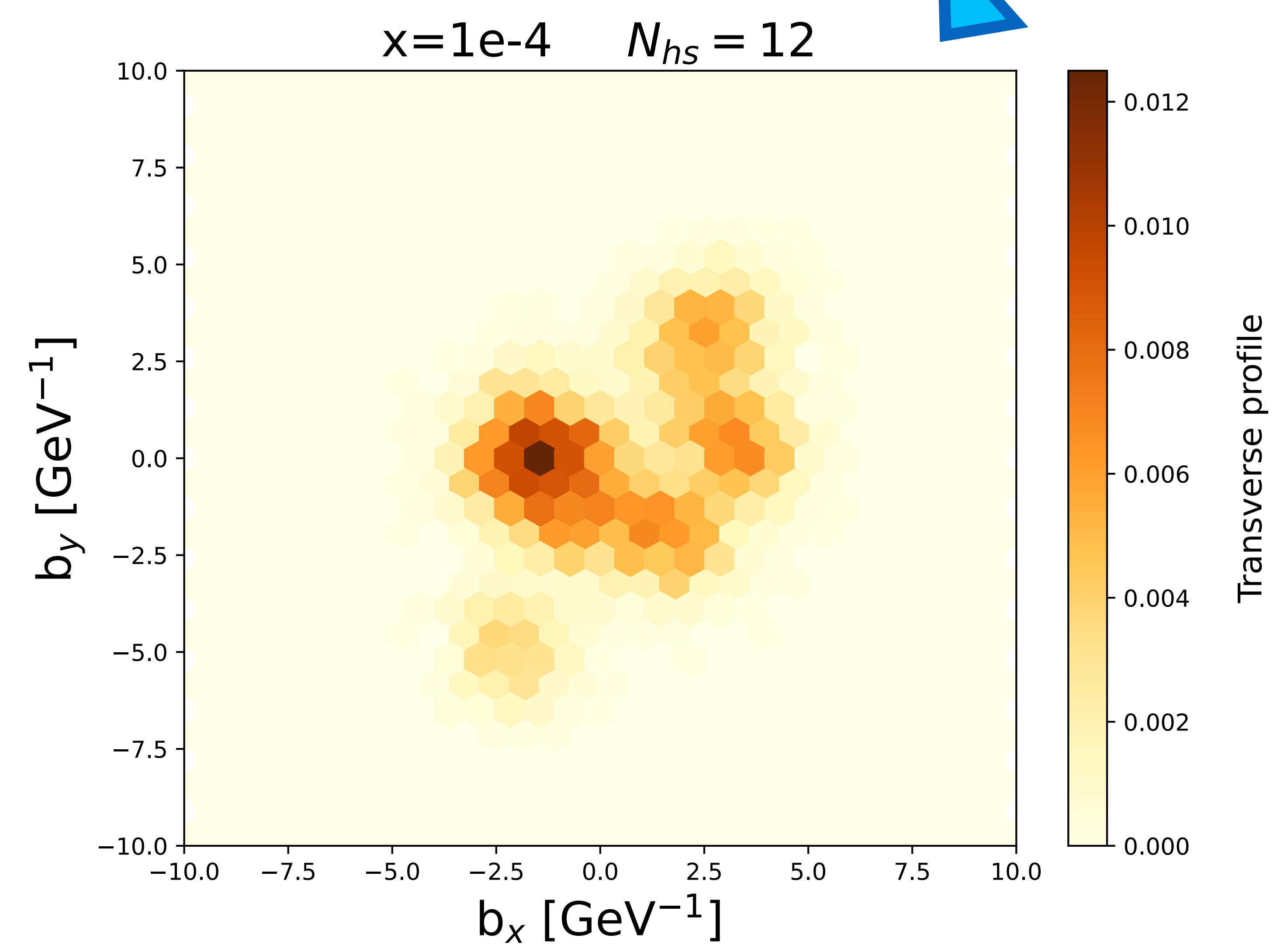

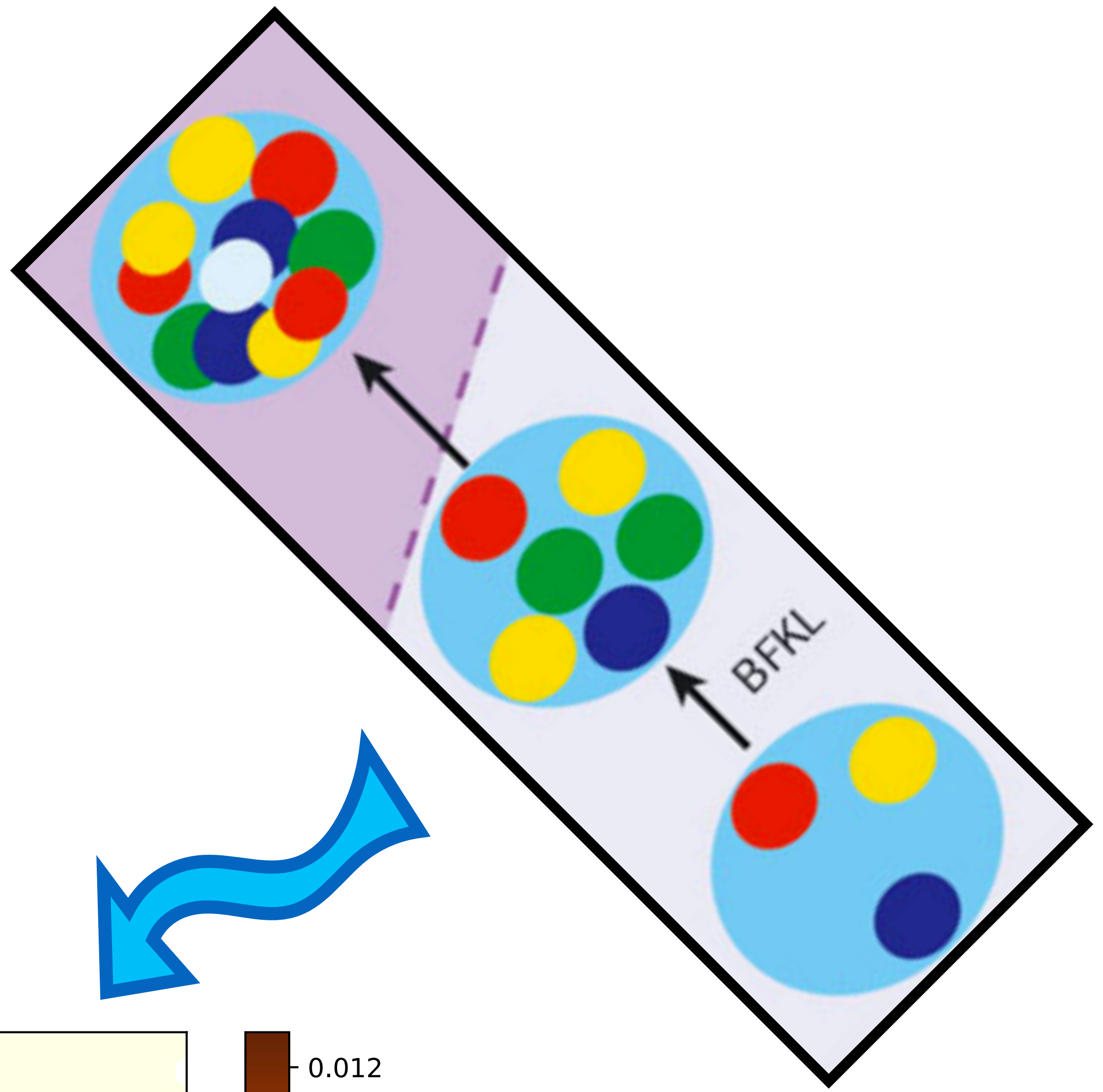

Cepila, JGC, Tapia Takaki, PLB766 (2017) 186-191

The nucleus profile in the energy-dependent hot-spot model

Nuclei are made of nucleons, which are made of hot spots

Position of nucleons sampled from a Woods-Saxon profile

$$T_{\mathrm{Pb}}(\vec{b}) = \frac{1}{2\pi B_{\mathrm{p}}} \sum_{j=1}^{A=208} \exp\left(-\frac{\left(\vec{b} - \vec{b}_j\right)^2}{2B_{\mathrm{p}}} \right)$$

The nucleus profile in the energy-dependent hot-spot model

Nuclei are made of nucleons, which are made of hot spots

Position of nucleons sampled from a Woods-Saxon profile

$$T_{\mathrm{Pb}}(\vec{b}) = \frac{1}{2\pi B_{\mathrm{p}}} \sum_{j=1}^{A=208} \exp\left(-\frac{\left(\vec{b} - \vec{b}_j\right)^2}{2B_{\mathrm{p}}} \right)$$

$$T_{\mathrm{hs}}(\vec{b} - \vec{b}_i) = \frac{1}{2\pi B_{\mathrm{hs}}} \sum_{i=1}^{A=208} \frac{1}{N_{\mathrm{hs}}} \sum_{j=1}^{N_{\mathrm{hs}}} \exp\left(-\frac{\left(\vec{b} - \vec{b}_i - \vec{b}_j\right)^2}{2B_{\mathrm{hs}}} \right)$$

Cepila, JGC, Matas, Ridzikova, PLB 852 (2024) 138613

The nucleus profile in the energy-dependent hot-spot model

Nuclei are made of nucleons, which are made of hot spots

Position of nucleons sampled from a Woods-Saxon profile

$$T_{\rm Pb}(\vec{b}) = \frac{1}{2\pi B_{\rm p}} \sum_{j=1}^{A=208} \exp\left(-\frac{\left(\vec{b} - \vec{b}_j\right)^2}{2B_{\rm p}} \right)$$

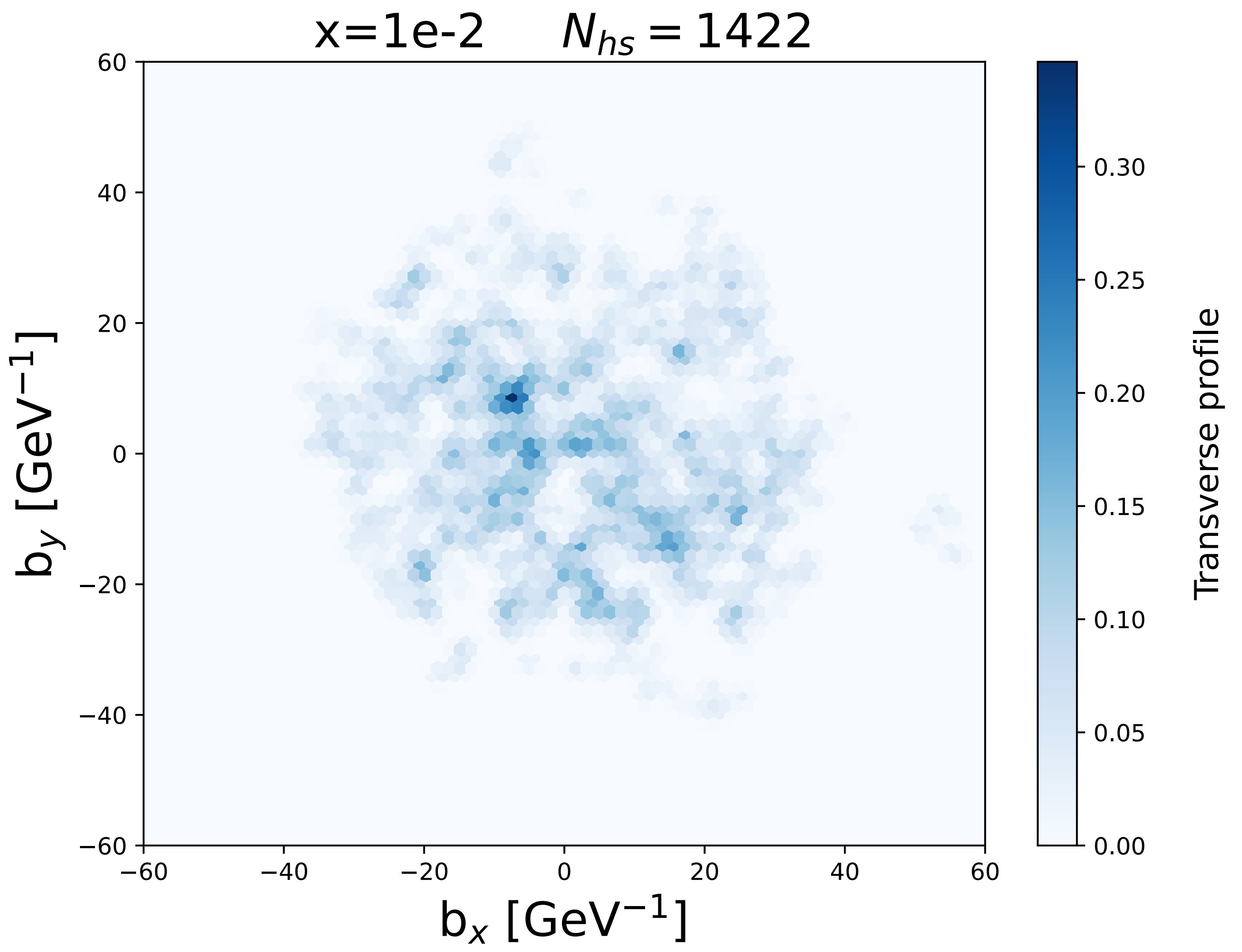

$$T_{\rm hs}(\vec{b} - \vec{b}_i) = \frac{1}{2\pi B_{\rm hs}} \sum_{i=1}^{A=208} \frac{1}{N_{\rm hs}} \sum_{j=1}^{N_{\rm hs}} \exp\left(-\frac{\left(\vec{b} - \vec{b}_i - \vec{b}_j\right)^2}{2B_{\rm hs}} \right)$$

Cepila, JGC, Matas, Ridzikova, PLB 852 (2024) 138613

The nucleus profile in the energy-dependent hot-spot model

Nuclei are made of nucleons, which are made of hot spots

Position of nucleons sampled from a Woods-Saxon profile

$$T_{\mathrm{Pb}}(\vec{b}) = \frac{1}{2\pi B_{\mathrm{p}}} \sum_{j=1}^{A=208} \exp\left(-\frac{\left(\vec{b}-\vec{b}_j\right)^2}{2B_{\mathrm{p}}} \right)$$

$$T_{\mathrm{hs}}(\vec{b}-\vec{b}_i) = \frac{1}{2\pi B_{\mathrm{hs}}} \sum_{i=1}^{A=208} \frac{1}{N_{\mathrm{hs}}} \sum_{j=1}^{N_{\mathrm{hs}}} \exp\left(-\frac{\left(\vec{b}-\vec{b}_i-\vec{b}_j\right)^2}{2B_{\mathrm{hs}}} \right)$$

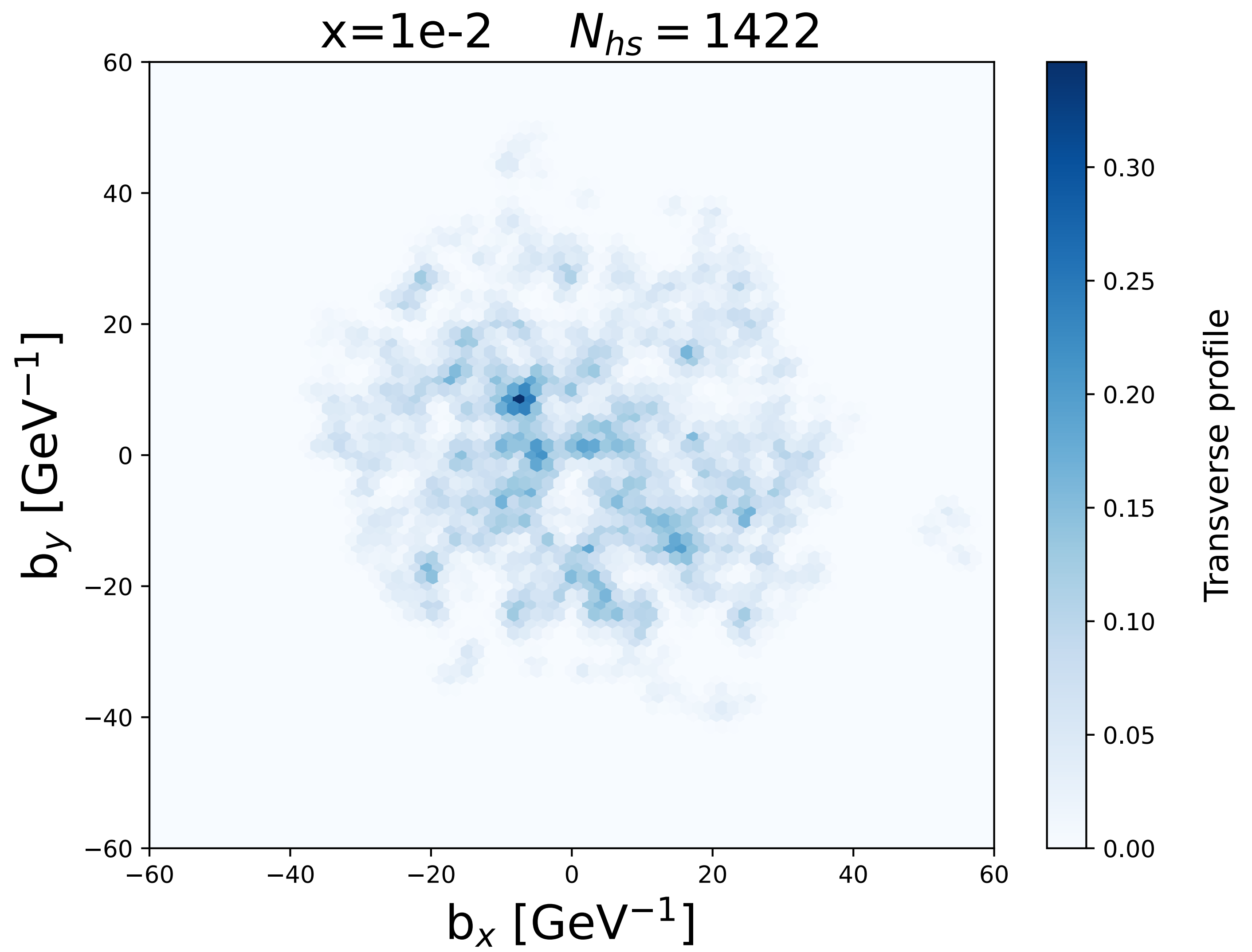

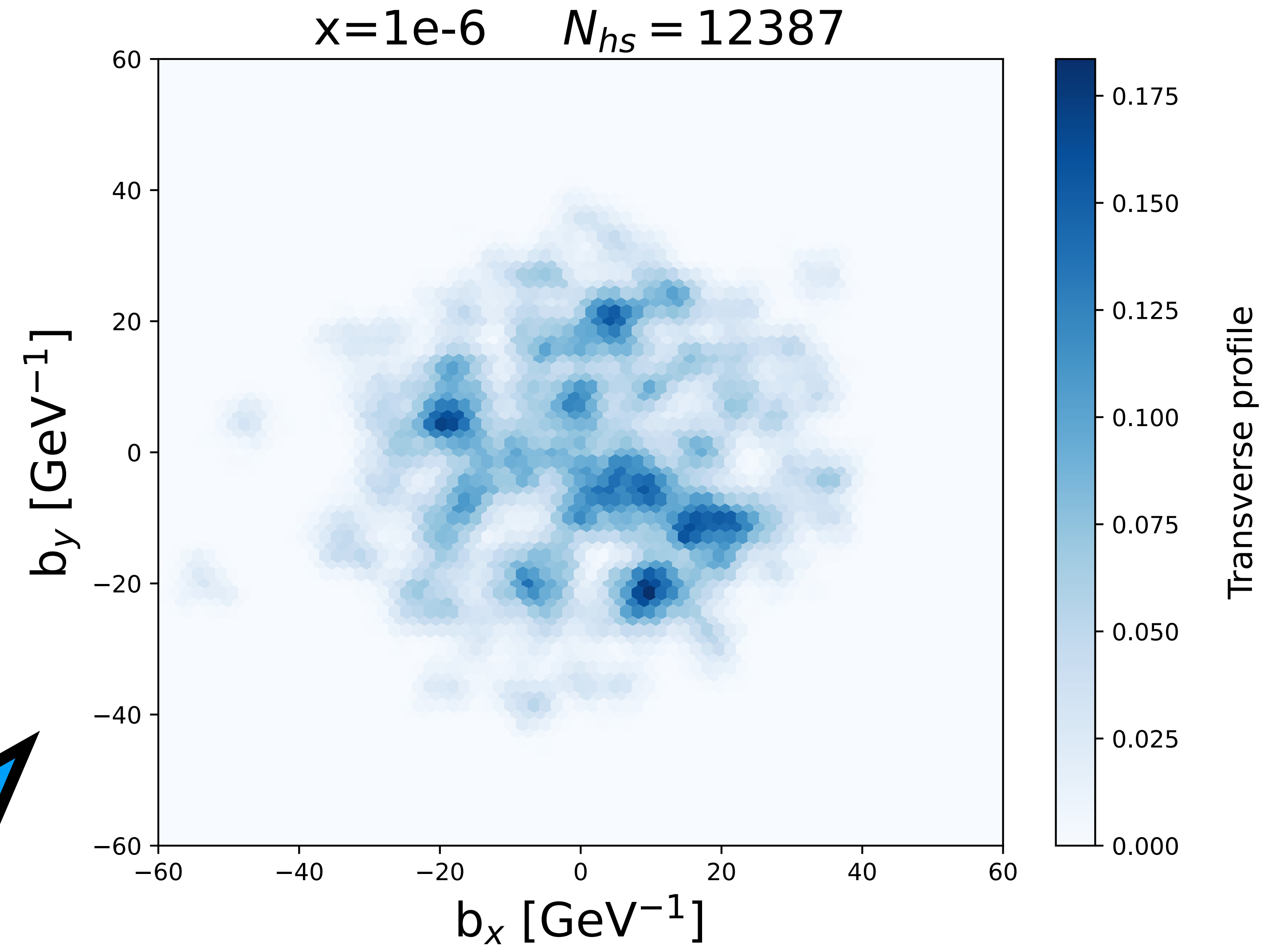

For nuclear targets, in our model the hot spots start to overlap locally

Cepila, JGC, Matas, Ridzikova, PLB 852 (2024) 138613

Predictions: energy dependence

Energy dependence for γp collisions

J/ψ

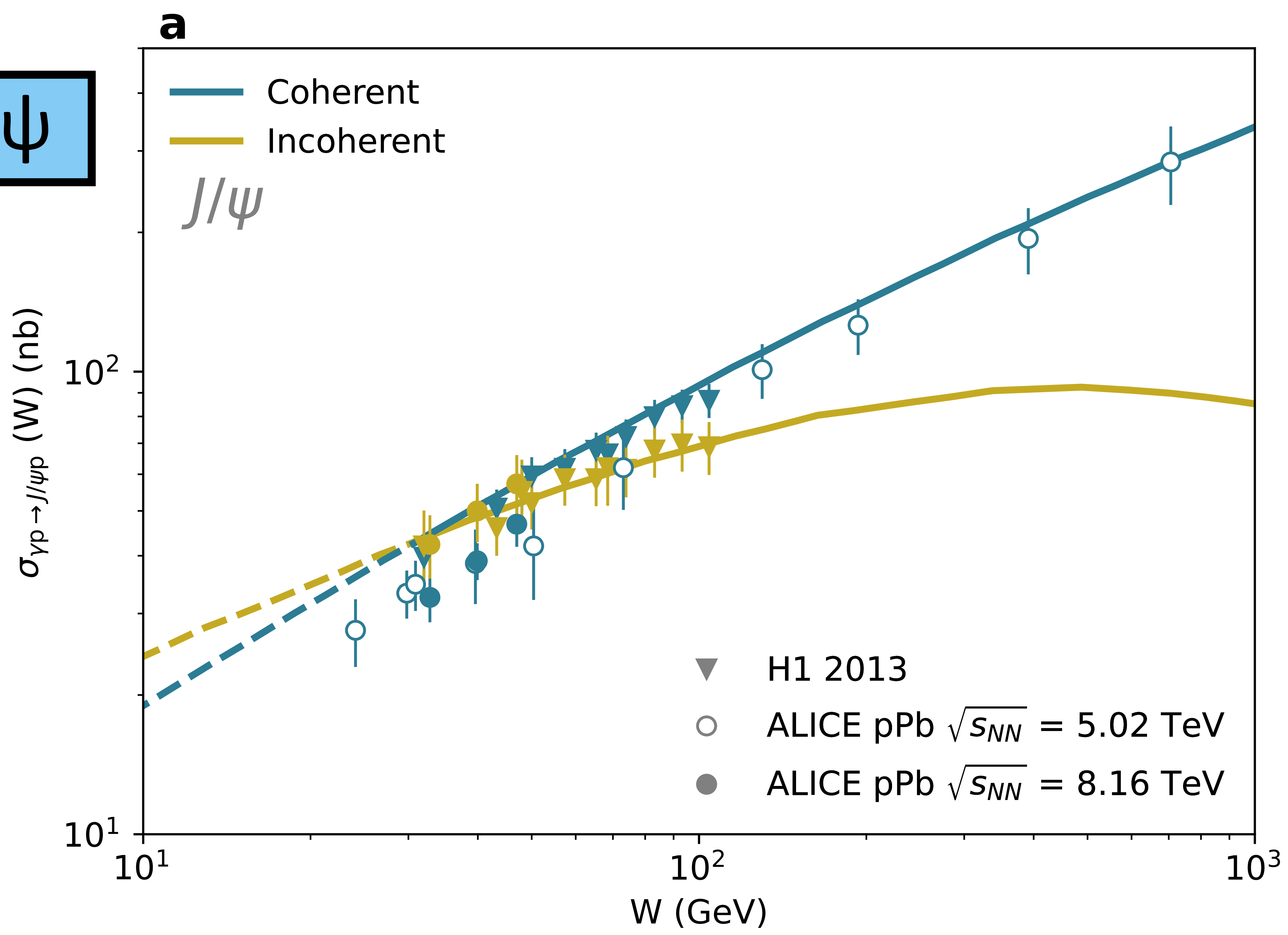

Cepila, JGC, Matas, Ridzikova, PLB 852 (2024) 138613

Energy dependence for γp collisions

The coherent (exclusive) cross section rises with energy showing no obvious saturation behaviour

J/ψ

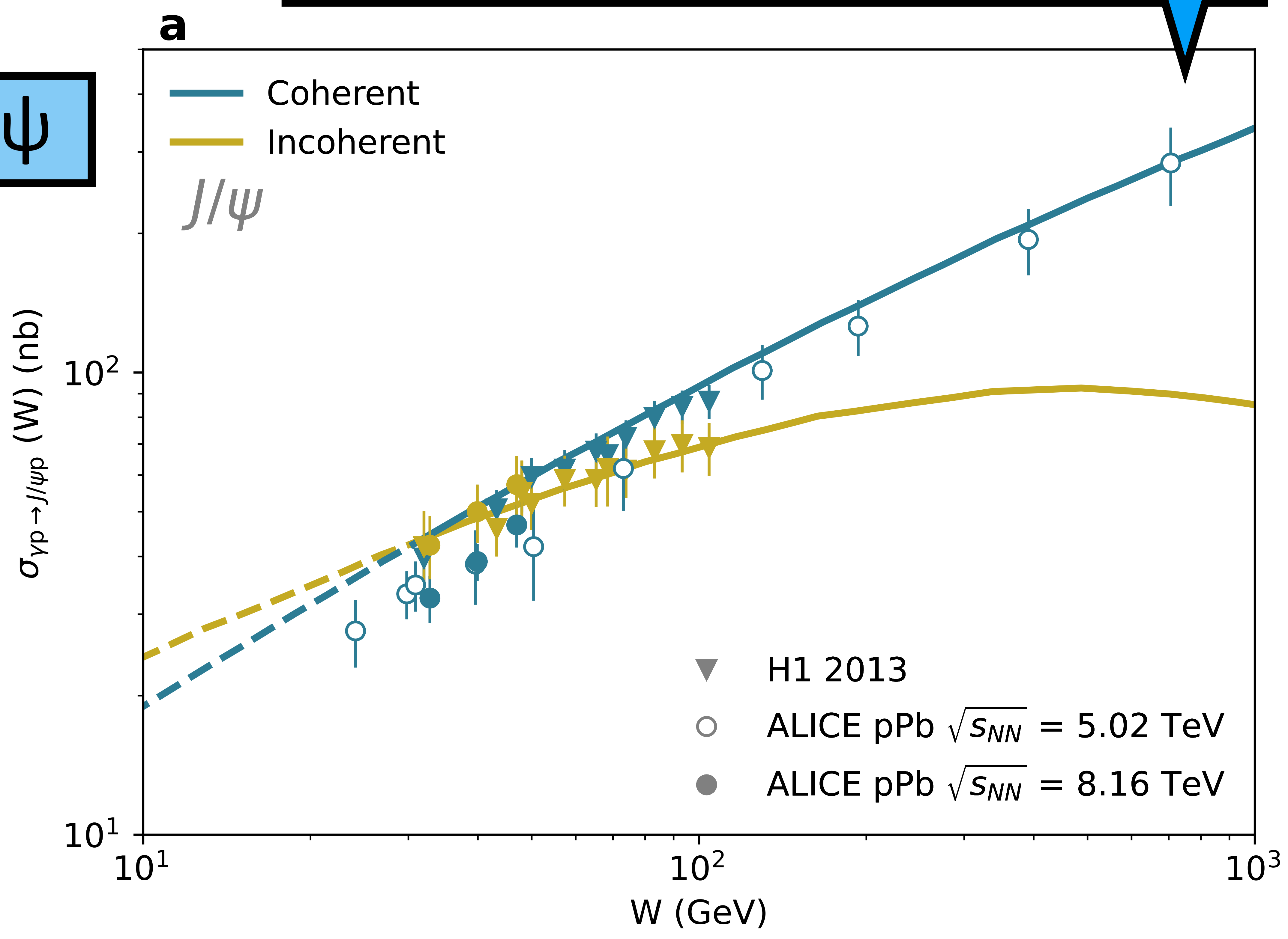

Cepila, JGC, Matas, Ridzikova, PLB 852 (2024) 138613

Energy dependence for γp collisions

The coherent (exclusive) cross section rises with energy showing no obvious saturation behaviour

J/ψ

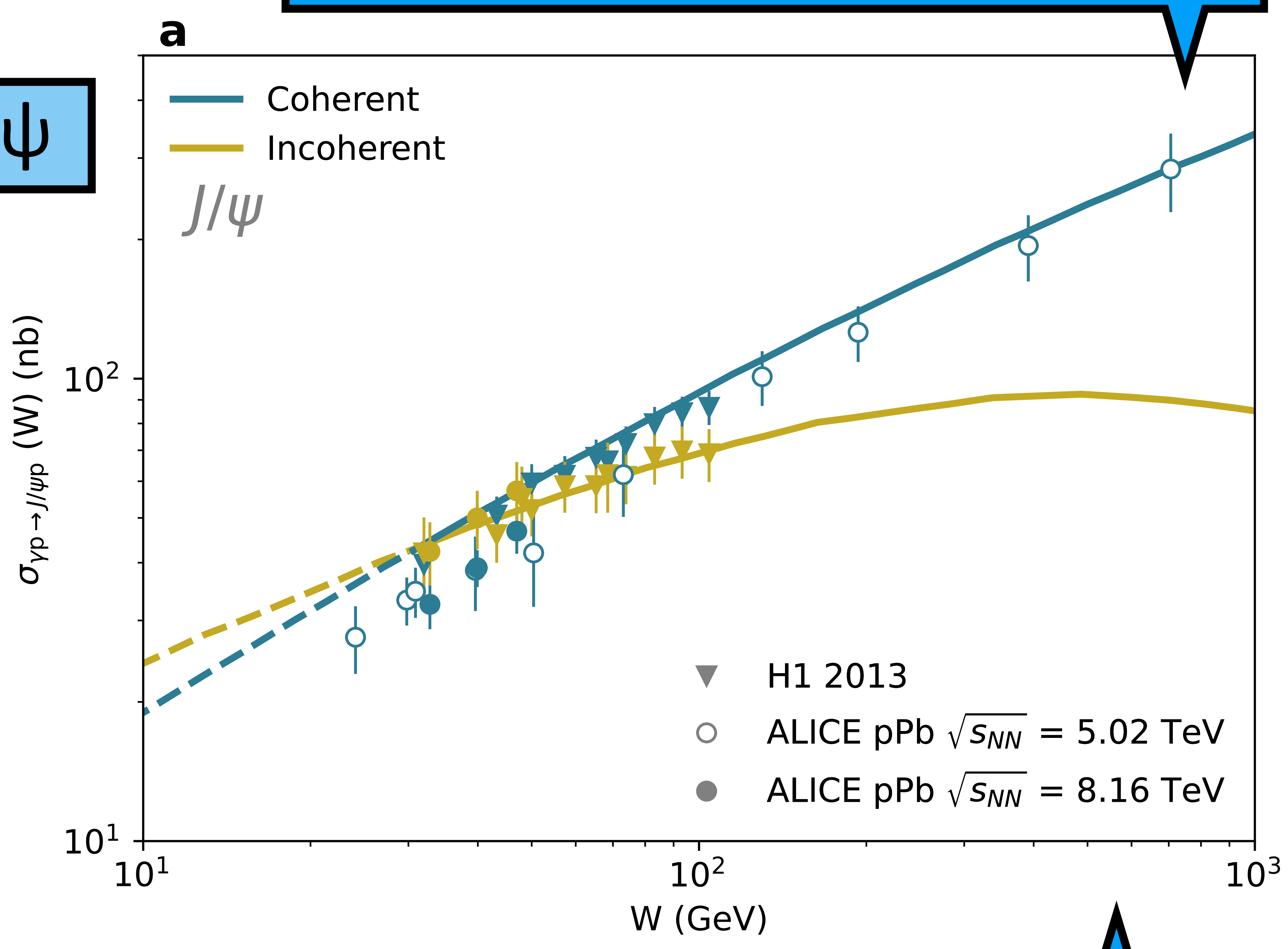

The incoherent (dissociative) cross section is predicted to reach a maximum and then decrease with increasing energy

Cepila, JGC, Matas, Ridzikova, PLB 852 (2024) 138613

Energy dependence for γp collisions

J/ψ

The coherent (exclusive) cross section rises with energy showing no obvious saturation behaviour

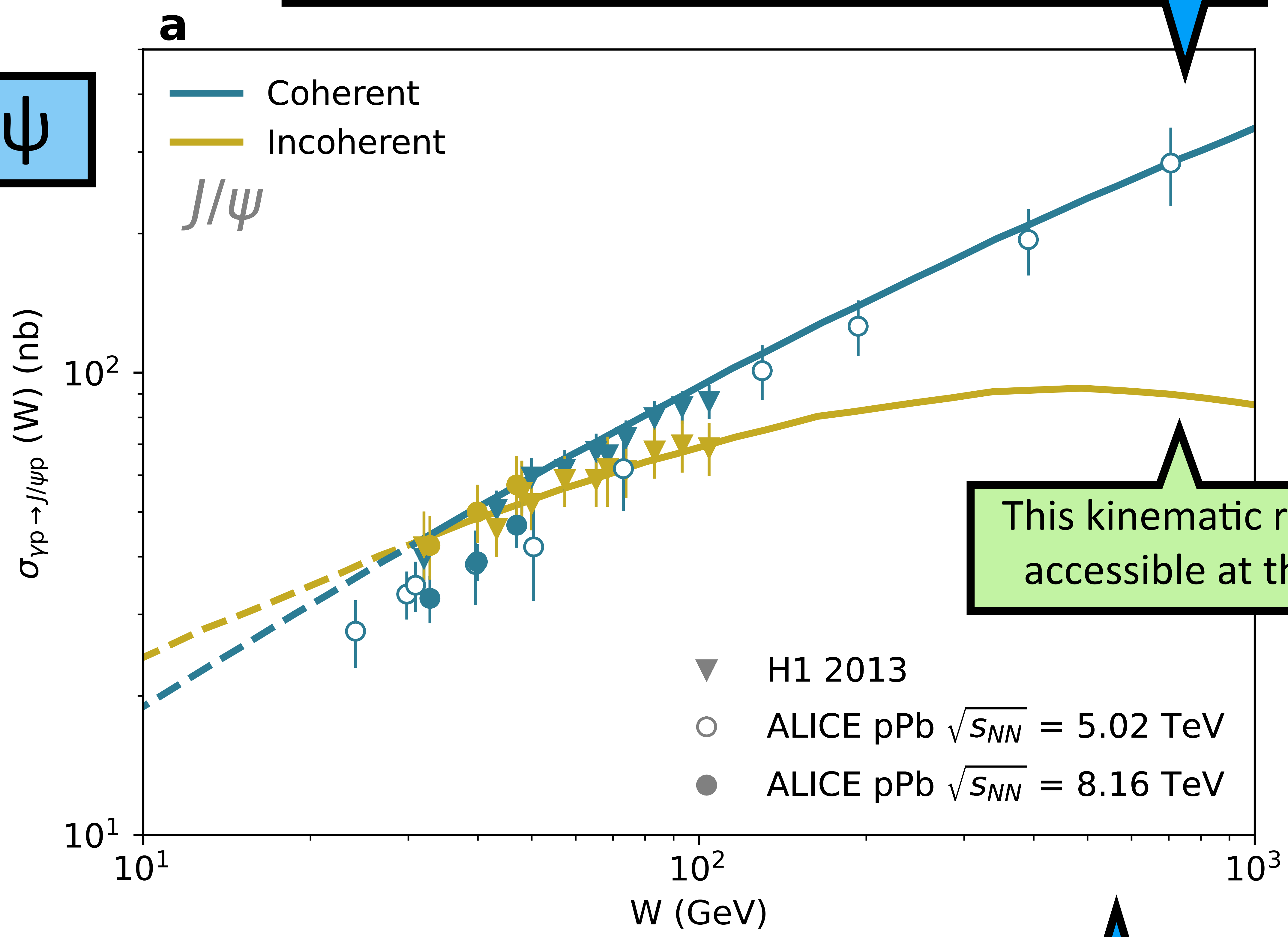

This kinematic region is accessible at the LHC

The incoherent (dissociative) cross section is predicted to reach a maximum and then decrease with increasing energy

Cepila, JGC, Matas, Ridzikova, PLB 852 (2024) 138613

Energy dependence for γp collisions

The coherent (exclusive) cross section rises with energy showing no obvious saturation behaviour

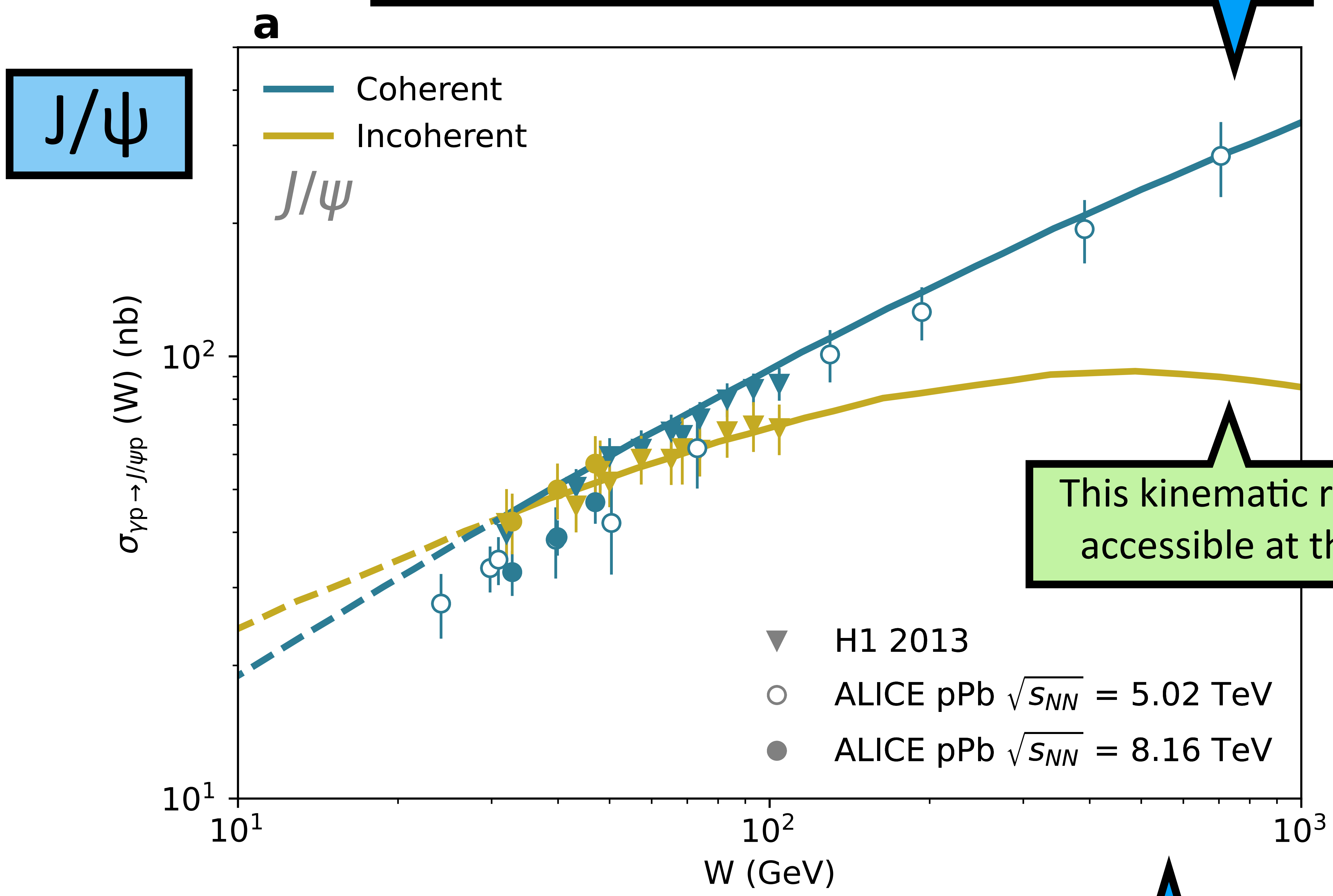

This kinematic region is accessible at the LHC

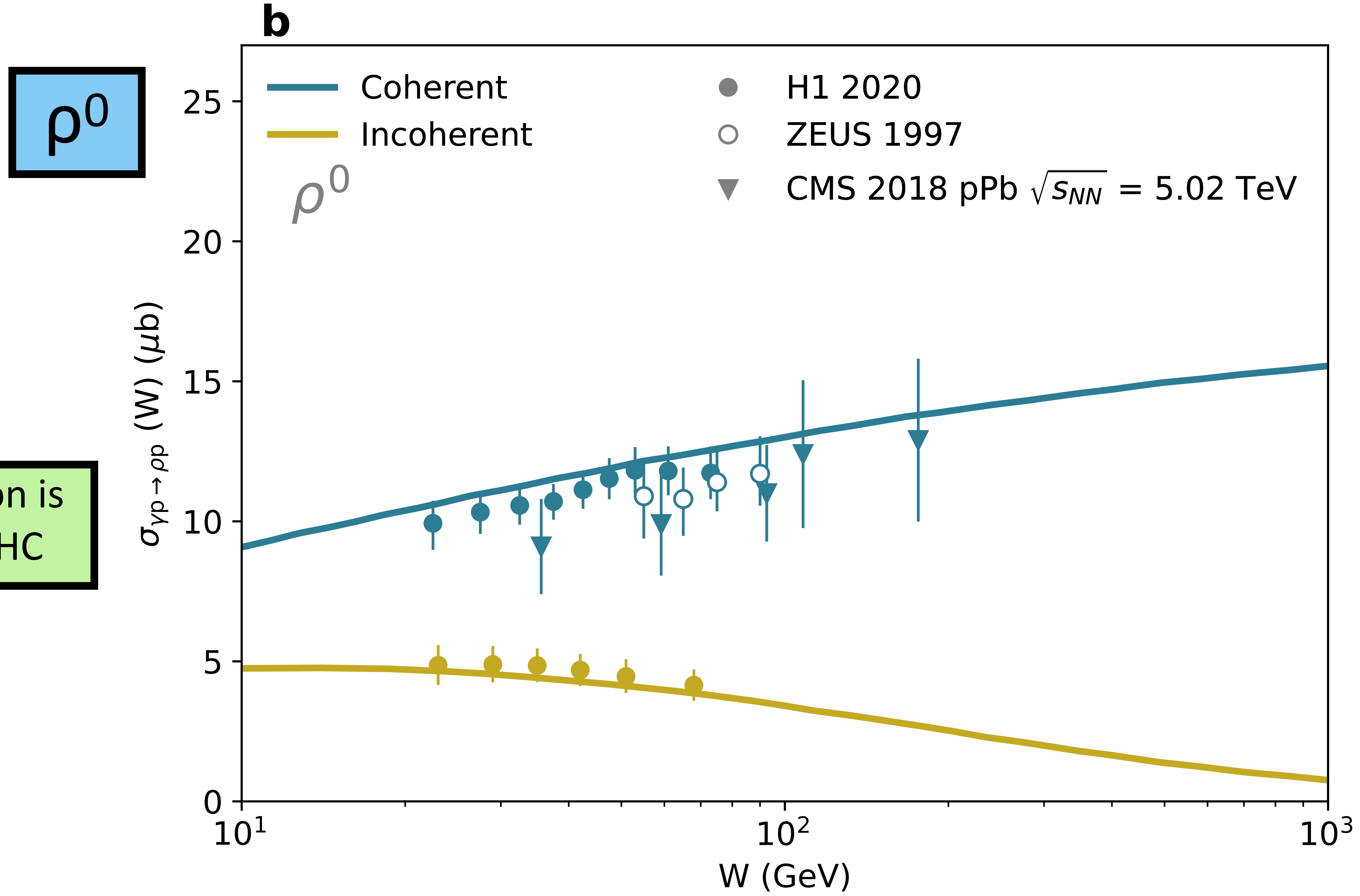

The incoherent (dissociative) cross section is predicted to reach a maximum and then decrease with increasing energy

Cepila, JGC, Matas, Ridzikova, PLB 852 (2024) 138613

Energy dependence for γp collisions

The coherent (exclusive) cross section rises with energy showing no obvious saturation behaviour

Is this mass scale in the perturbative region?

J/ψ

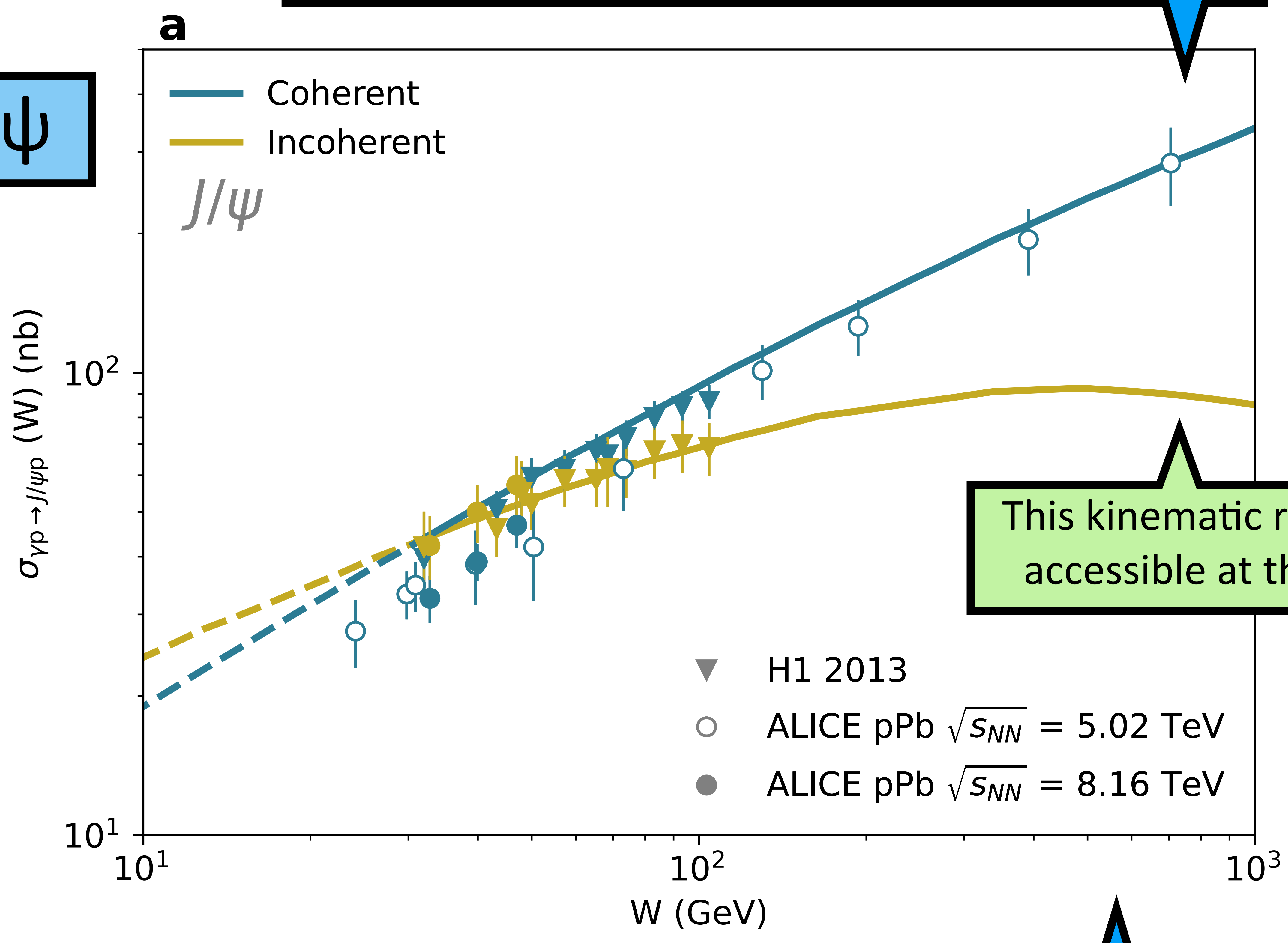

This kinematic region is accessible at the LHC

ρ^0

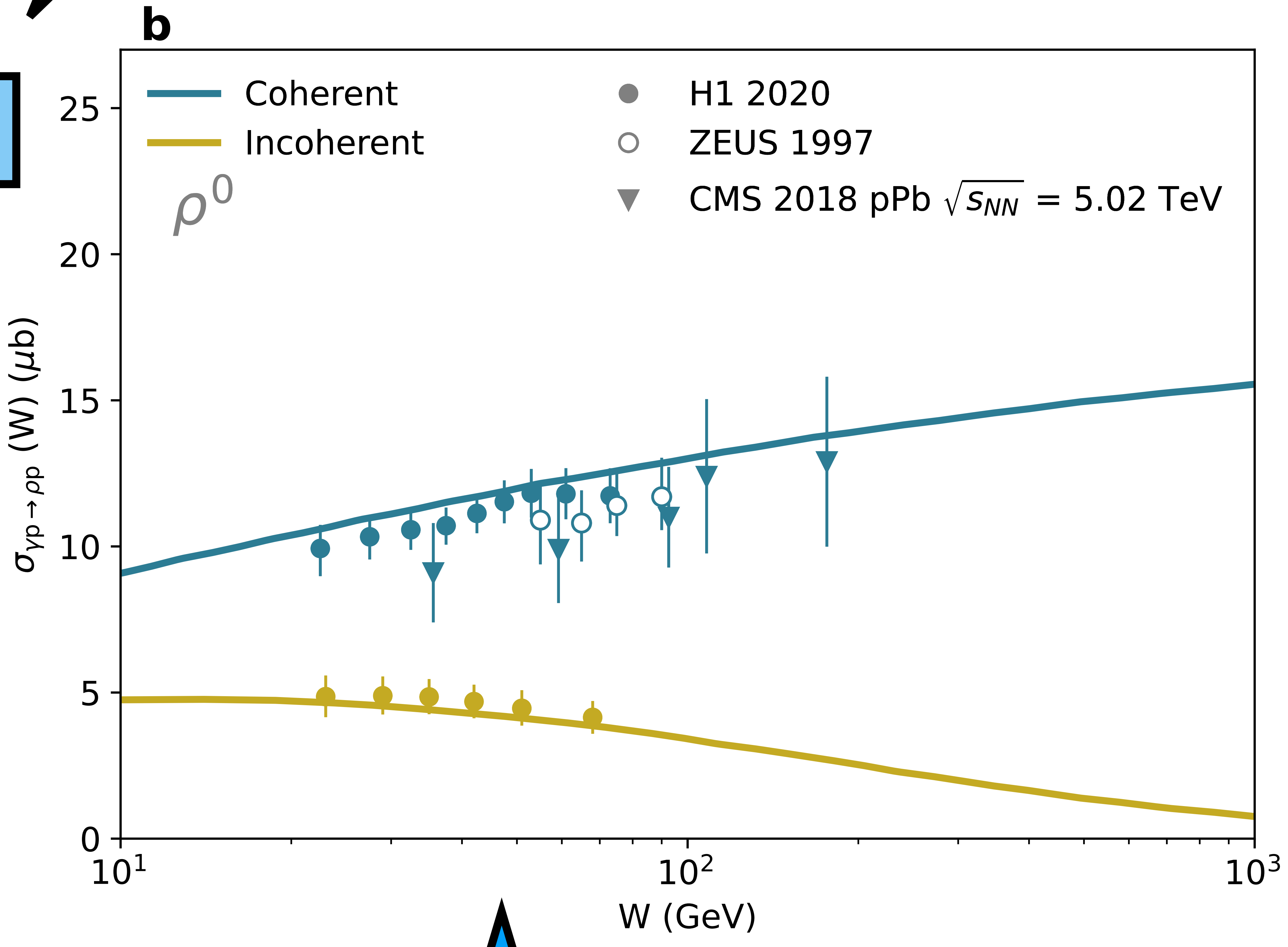

The incoherent (dissociative) cross section is predicted to reach a maximum and then decrease with increasing energy

The incoherent (dissociative) cross section is decreasing according to HERA data, but there are some caveats

Cepila, JGC, Matas, Ridzikova, PLB 852 (2024) 138613

Energy dependence for γPb collisions

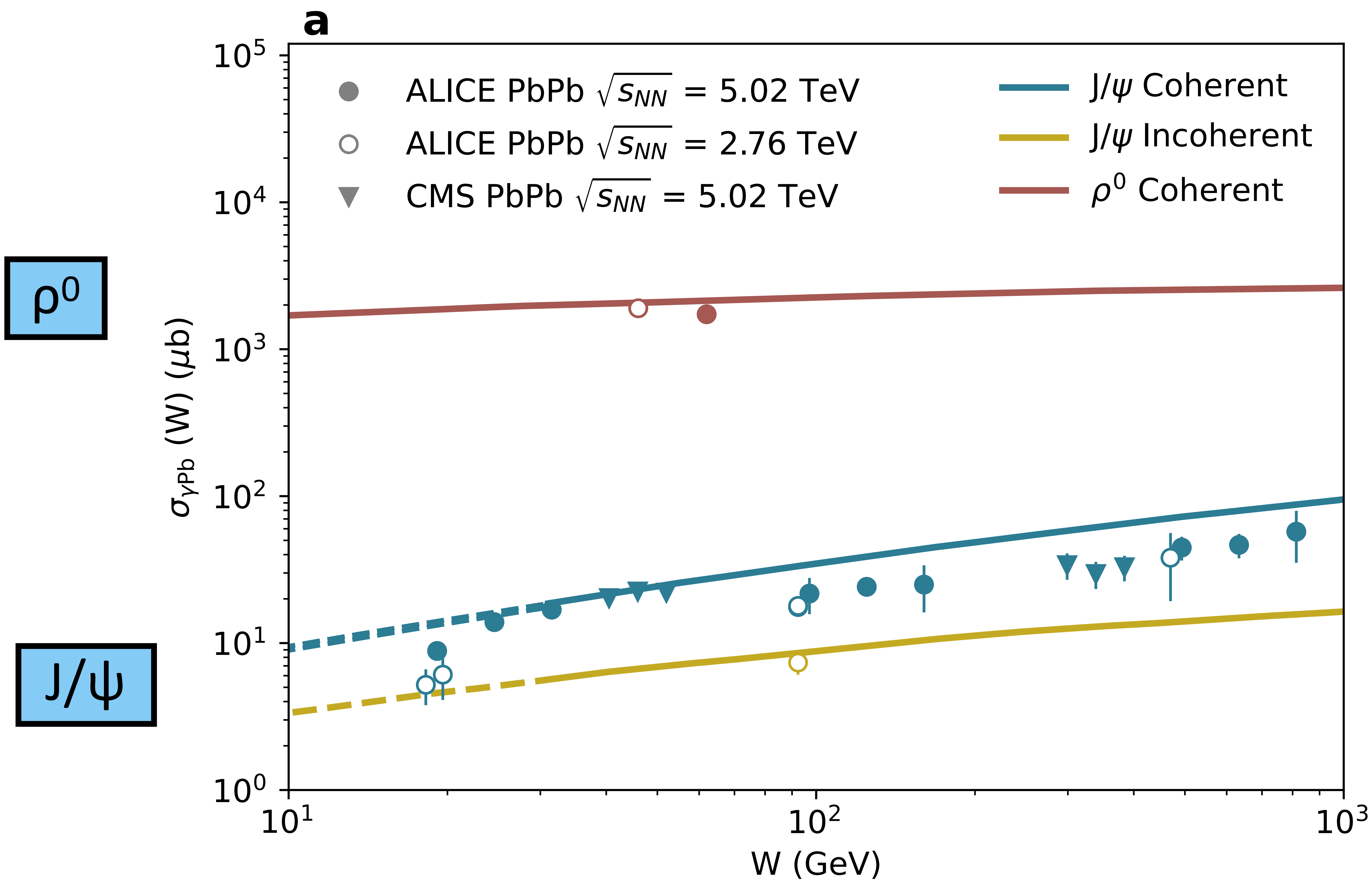

Cepila, JGC, Matas, Ridzikova, PLB 852 (2024) 138613

Energy dependence for γPb collisions

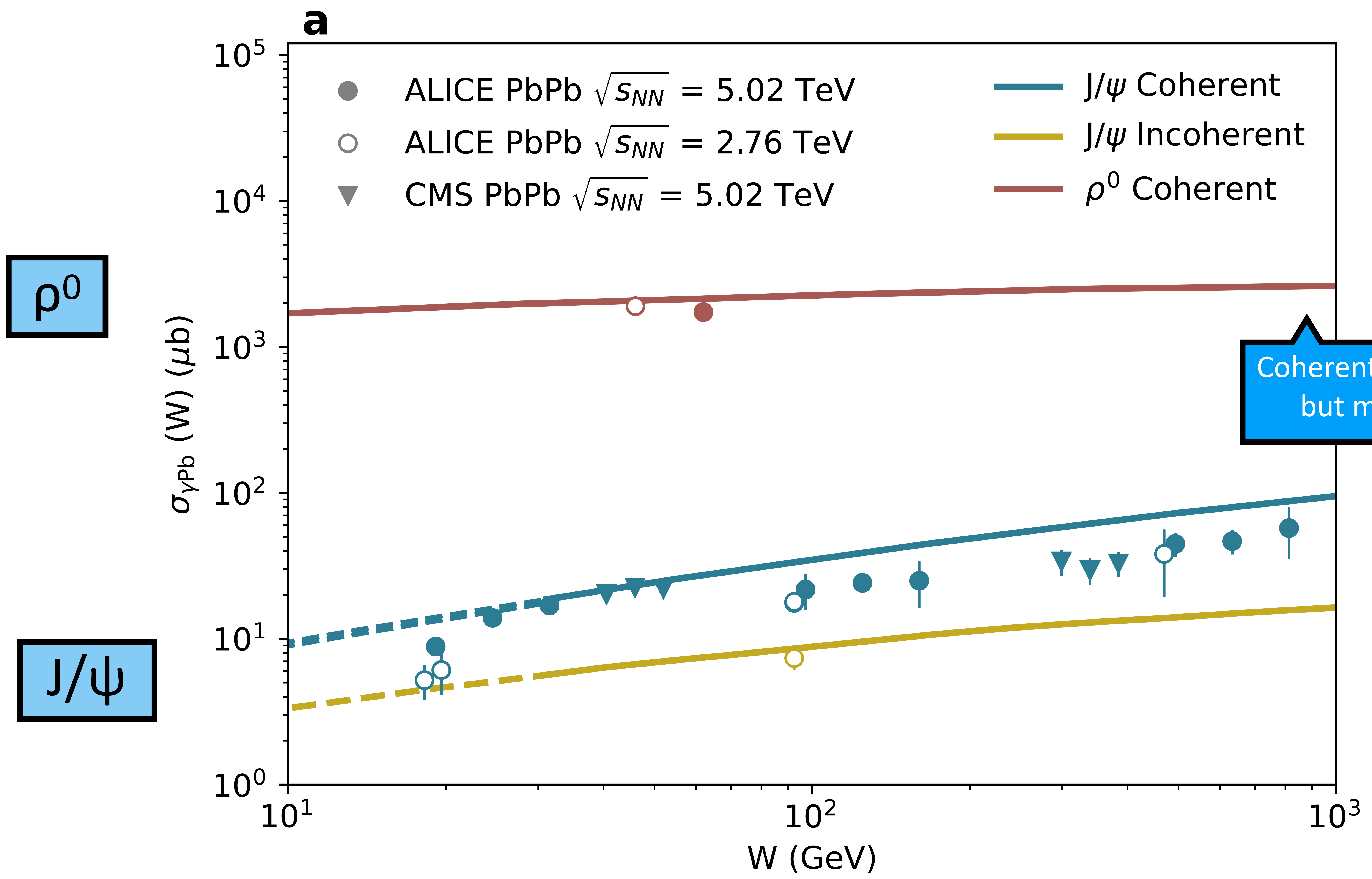

Coherent cross section is quite flat, but mass (ie scale) quite low

Cepila, JGC, Matas, Ridzikova, PLB 852 (2024) 138613

Energy dependence for γPb collisions

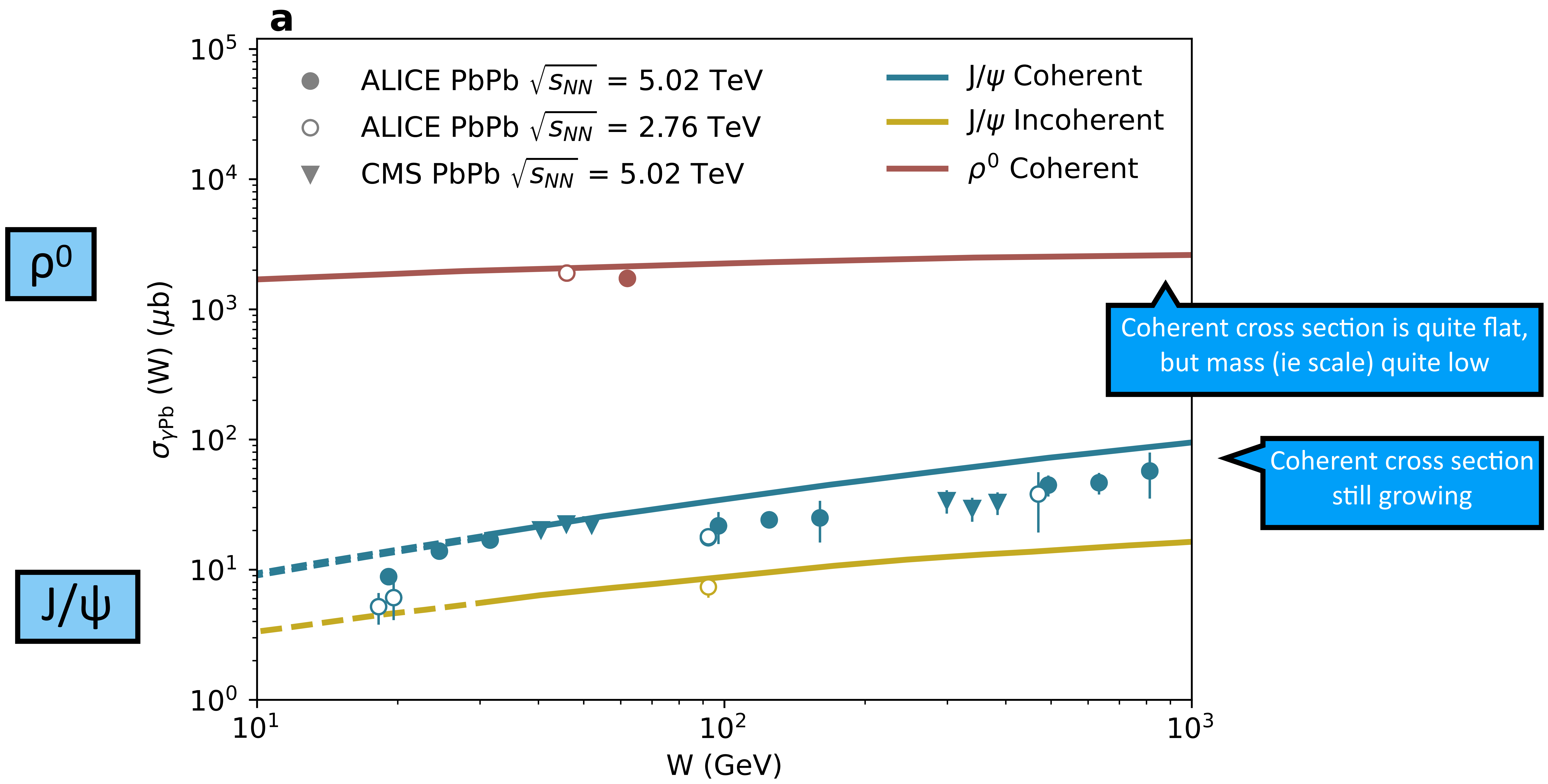

Cepila, JGC, Matas, Ridzikova, PLB 852 (2024) 138613

Energy dependence for γPb collisions

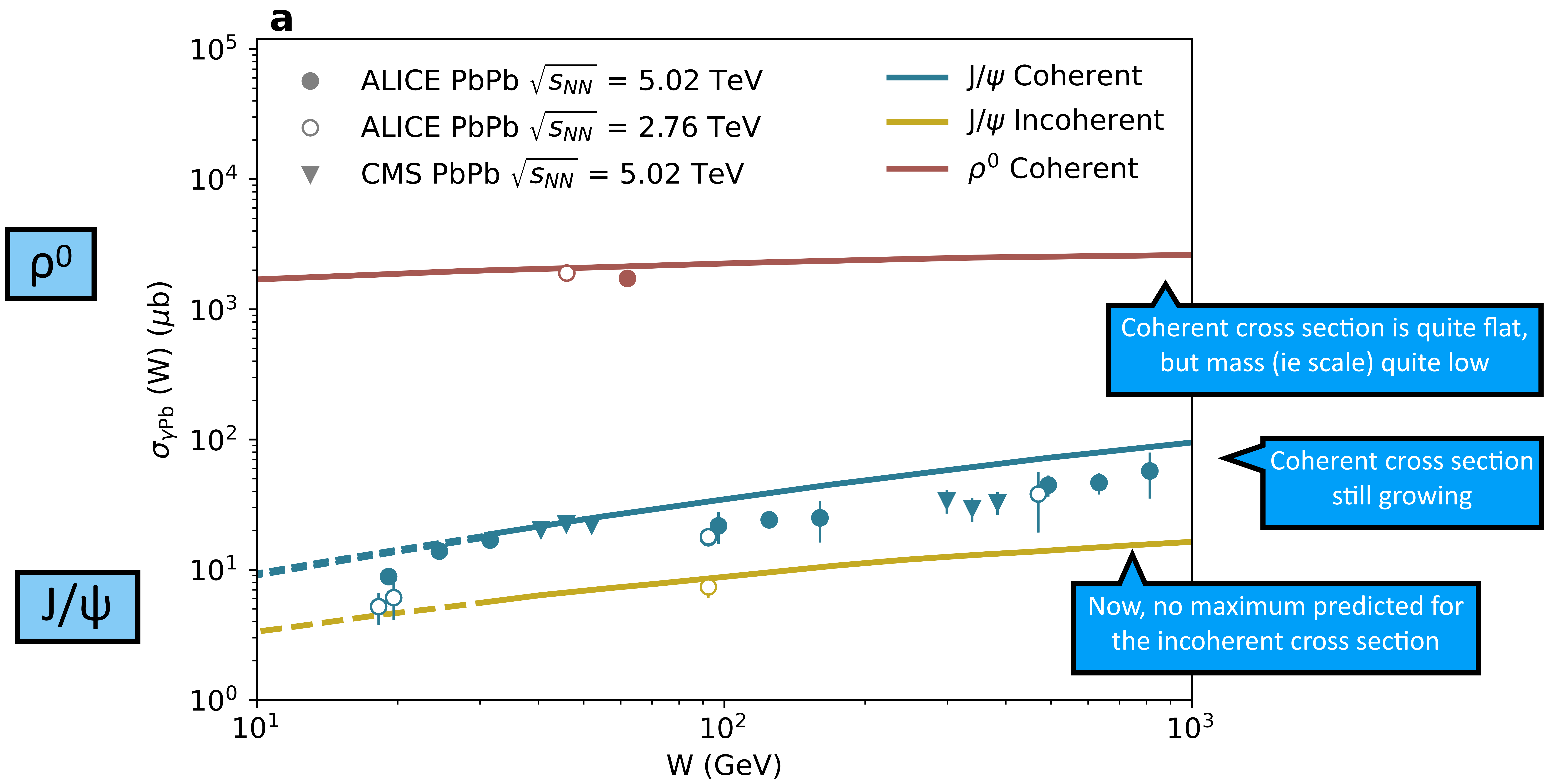

Cepila, JGC, Matas, Ridzikova, PLB 852 (2024) 138613

Predictions: Mandelstam-t dependence

Mandelstam-t and impact parameter

Δ^2=-t

$$\mathscr{A}_{\mathrm{T,L}}(x, Q^2, \overrightarrow{\Delta}) = i \int \mathrm{d}\vec{r} \int_0^1 \frac{\mathrm{d}z}{4\pi} \int \mathrm{d}\vec{b}\, |\Psi_\gamma^* \Psi_{\mathrm{V}}|_{\mathrm{T,L}} \exp\left[-i\left(\vec{b} - (\frac{1}{2} - z)\vec{r}\right)\overrightarrow{\Delta}\right] \frac{\mathrm{d}\sigma_{\mathrm{H}}^{\mathrm{dip}}}{\mathrm{d}\vec{b}}$$

Mandelstam-t and impact parameter

$\Delta^2 = -t$

$$\mathcal{A}_{\mathrm{T,L}}(x, Q^2, \overrightarrow{\Delta}) = i \int \mathrm{d}\vec{r} \int_0^1 \frac{\mathrm{d}z}{4\pi} \int \mathrm{d}\vec{b}\, |\Psi_\gamma^* \Psi_\mathrm{V}|_{\mathrm{T,L}} \exp\left[-i\left(\vec{b} - (\frac{1}{2} - z)\vec{r}\right)\overrightarrow{\Delta}\right] \frac{\mathrm{d}\sigma_\mathrm{H}^{\mathrm{dip}}}{\mathrm{d}\vec{b}}$$

Impact parameter is Fourier conjugate to the momentum transferred at the hadron vertex
→
different ranges in Mandelstam-t are sensitive to different size scales in the impact-parameter plane

Mandelstam-t dependence for γPb collisions

J/ψ

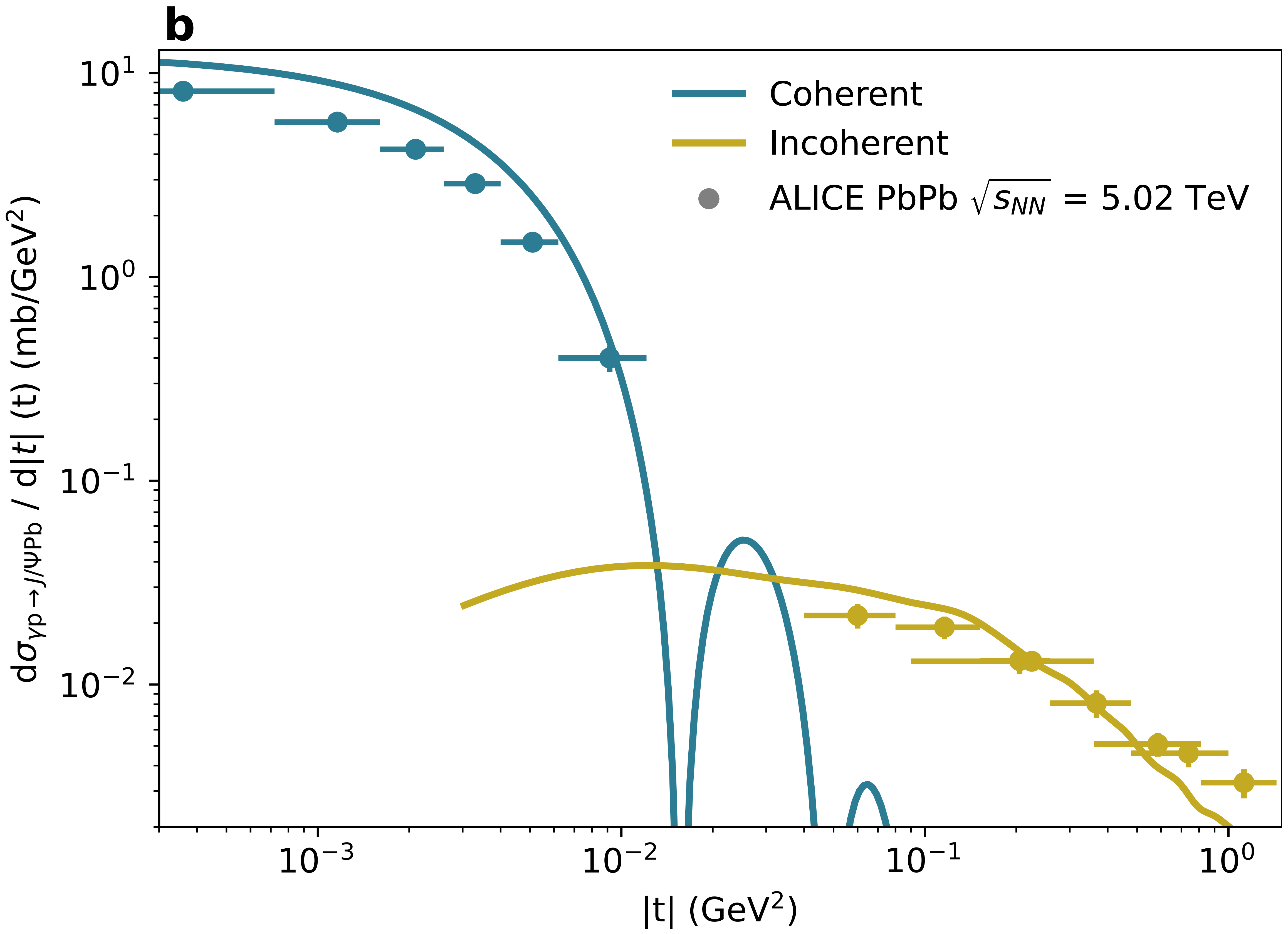

Cepila, JGC, Matas, Ridzikova, PLB 852 (2024) 138613

Mandelstam-t dependence for γPb collisions

J/ψ

Measurements at fixed Bjorken-x, around 0.001

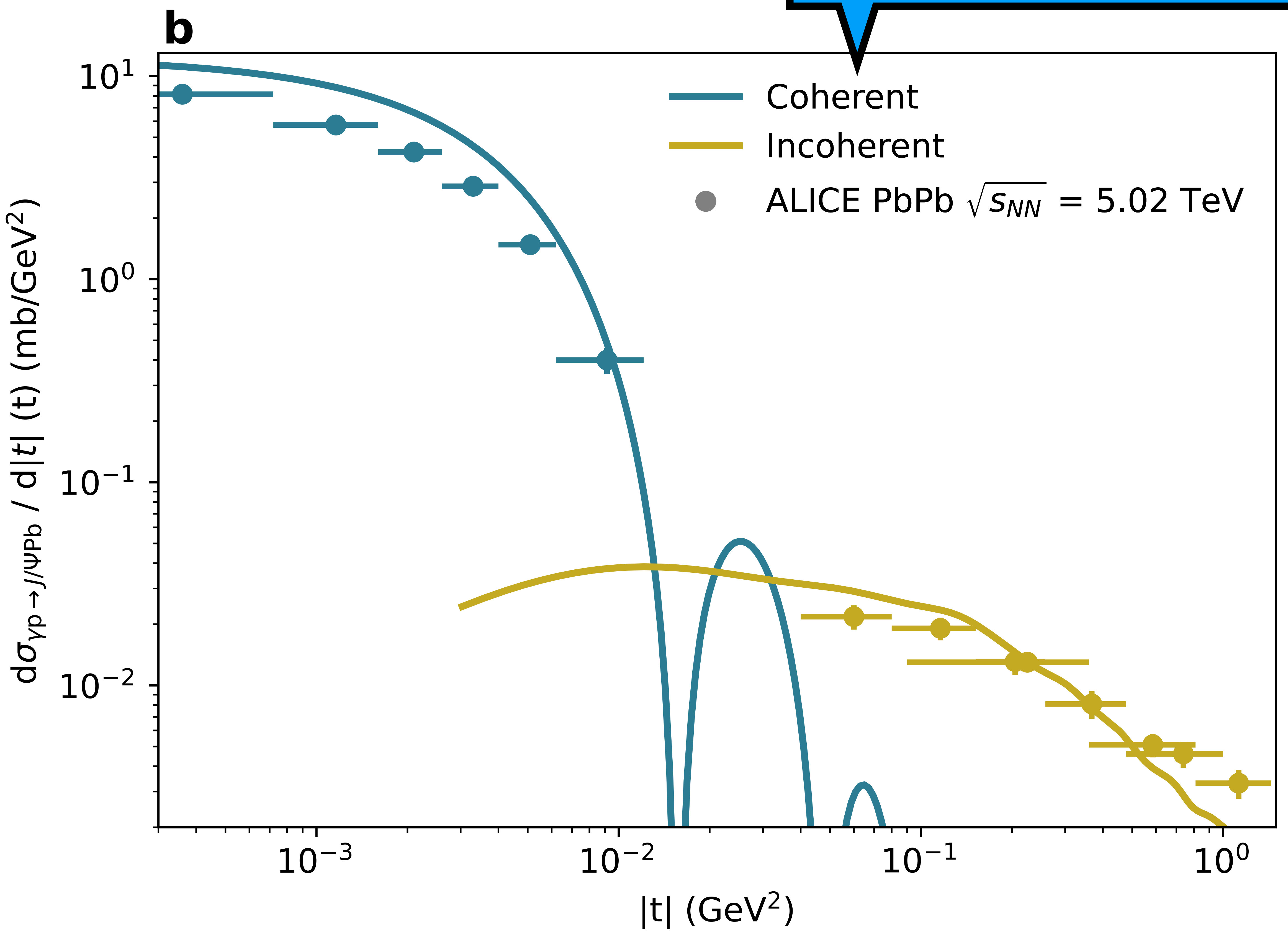

Cepila, JGC, Matas, Ridzikova, PLB 852 (2024) 138613

Mandelstam-t dependence for γPb collisions

J/ψ

Measurements at fixed Bjorken-x, around 0.001

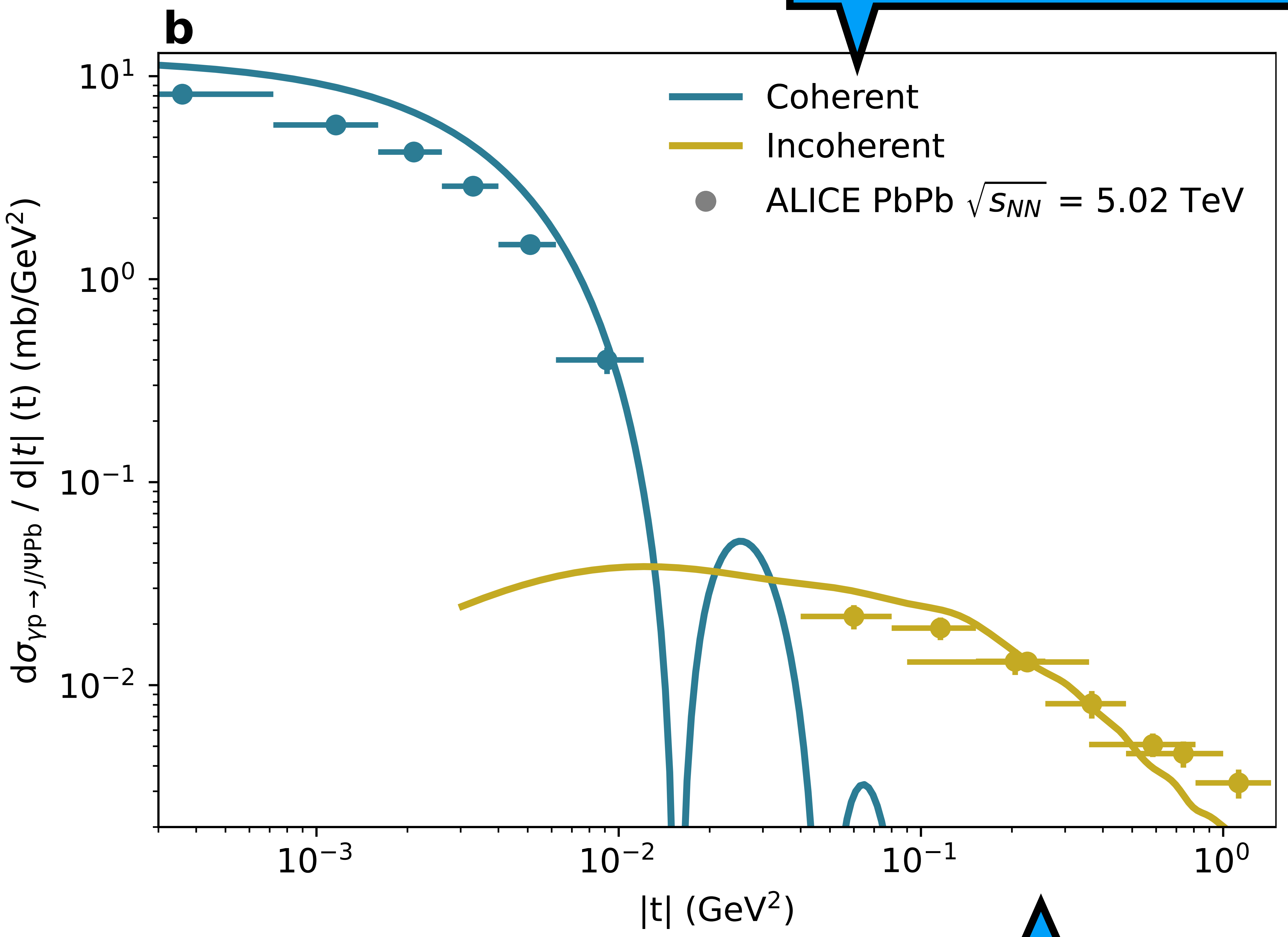

LHC data covers three orders of magnitude in Mandelstam-t

Saturation signature at high |t|

Guillermo Contreras, CTU in Prague

Scanning size scales in the impact-parameter plane

J/ψ

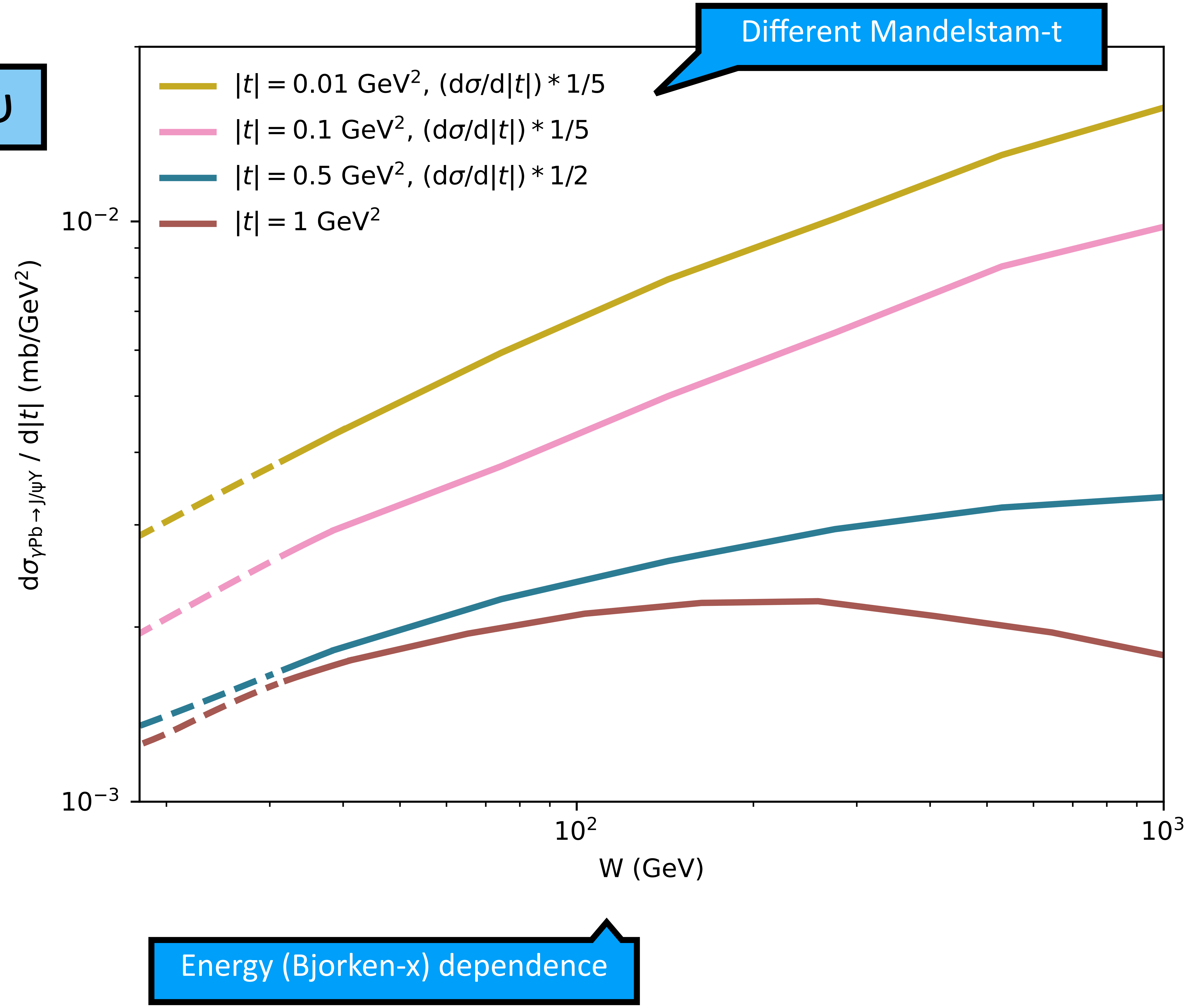

Cepila, JGC, Matas, Ridzikova, PLB 852 (2024) 138613

Scanning size scales in the impact-parameter plane

J/ψ

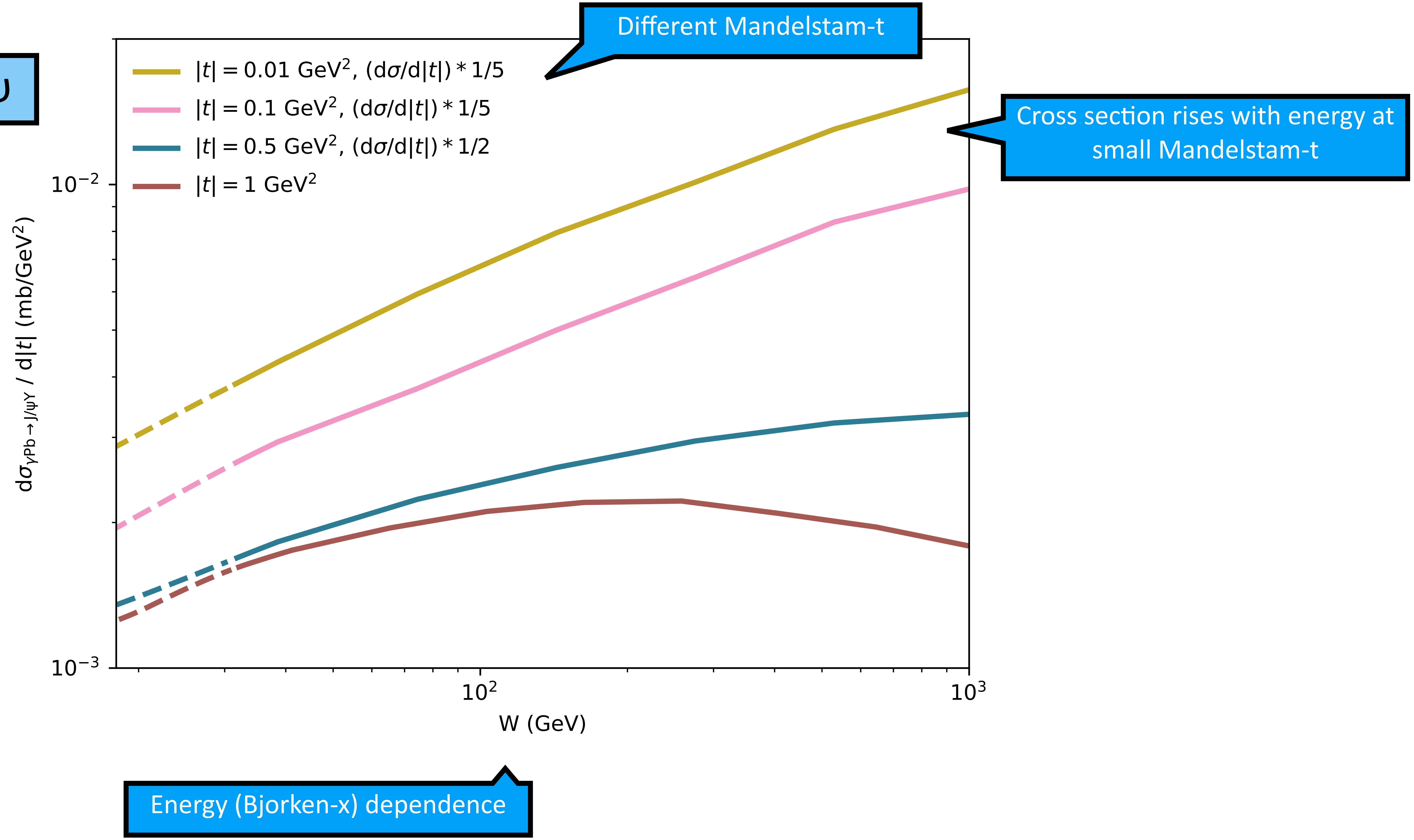

Cepila, JGC, Matas, Ridzikova, PLB 852 (2024) 138613

Scanning size scales in the impact-parameter plane

J/ψ

Different Mandelstam-t

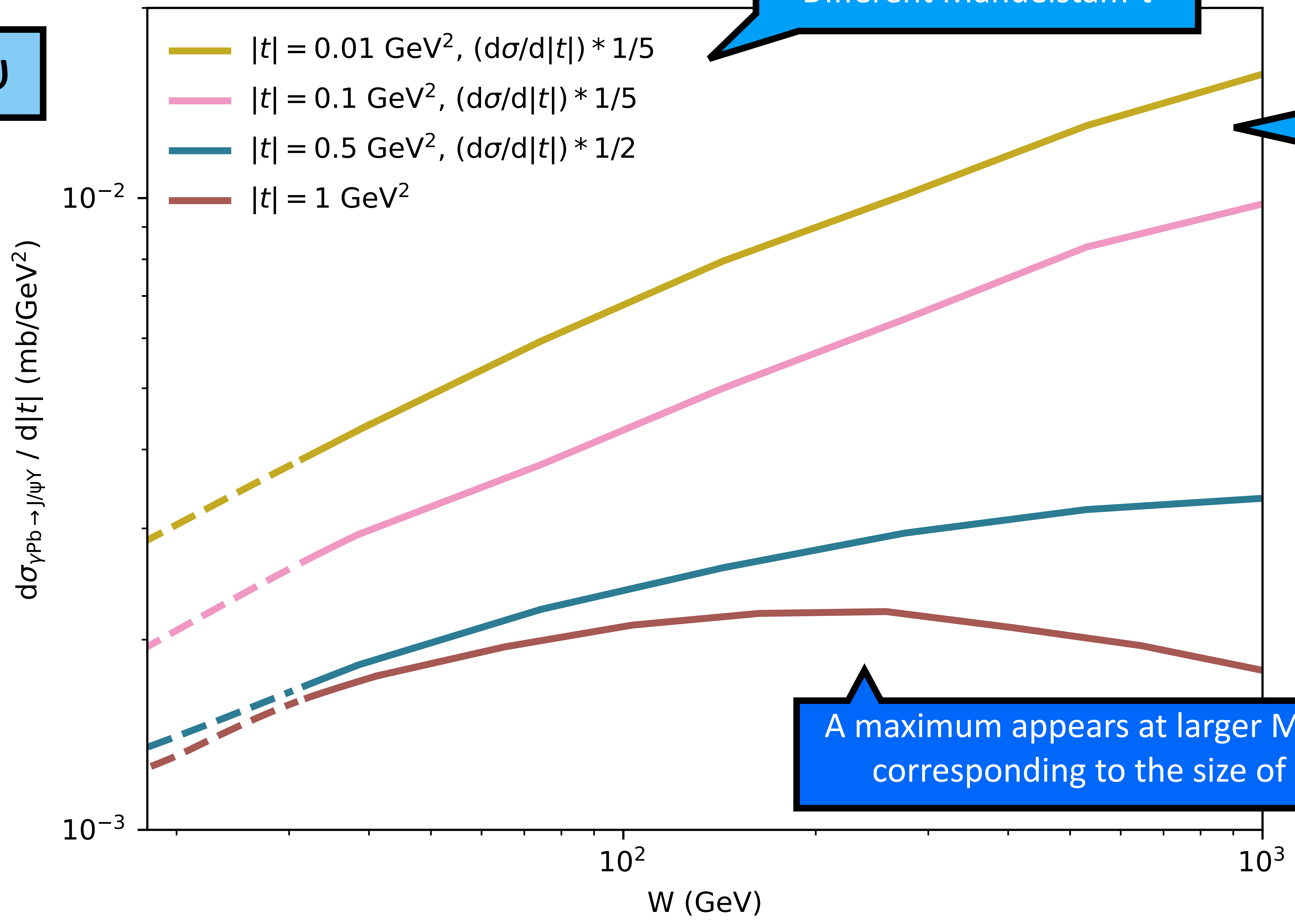

Cross section rises with energy at small Mandelstam-t

A maximum appears at larger Mandelstam-t corresponding to the size of hot spots

Energy (Bjorken-x) dependence

Cepila, JGC, Matas, Ridzikova, PLB 852 (2024) 138613

Scanning size scales in the impact-parameter plane

J/ψ

Different Mandelstam-t

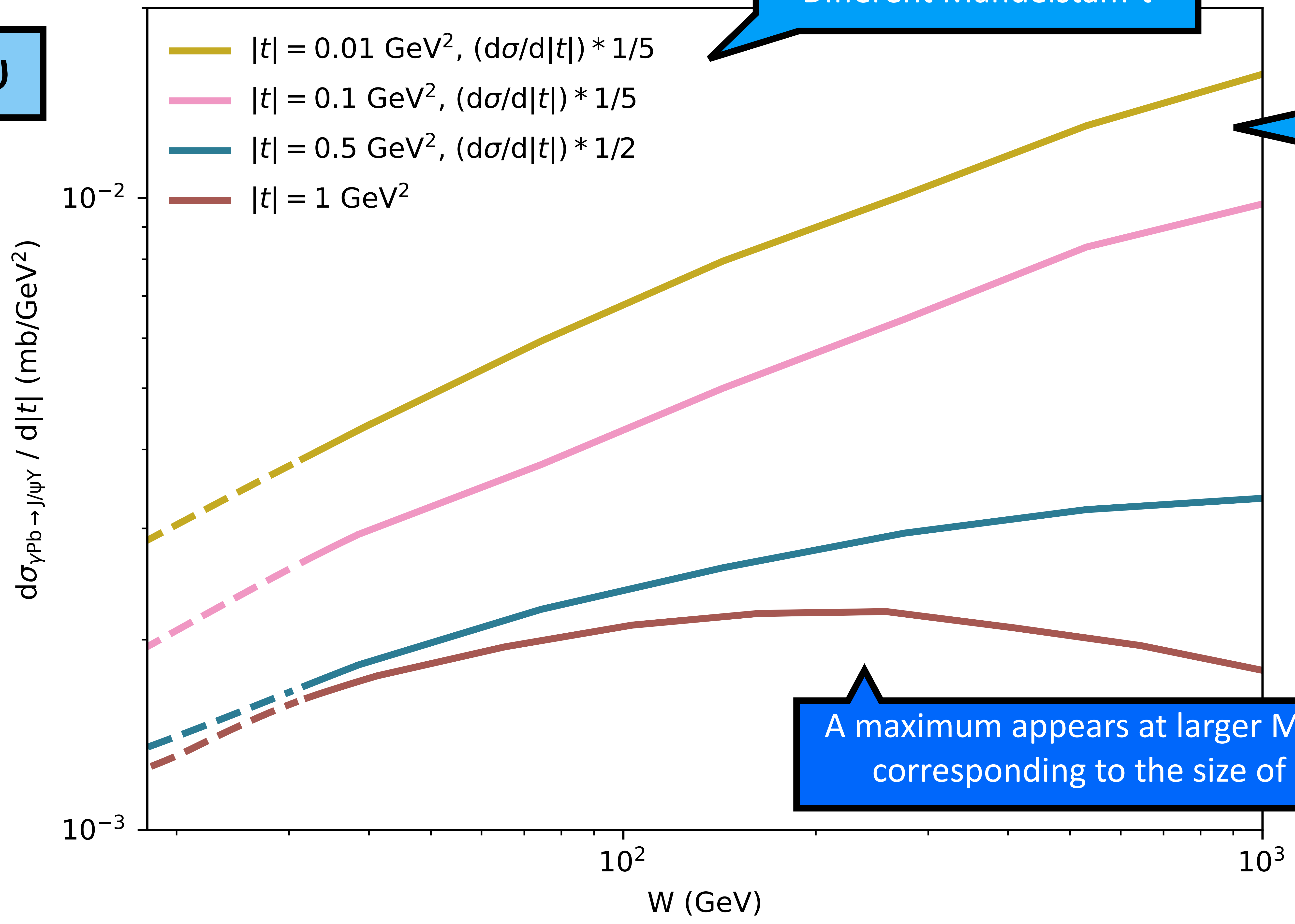

Cross section rises with energy at small Mandelstam-t

A maximum appears at larger Mandelstam-t corresponding to the size of hot spots

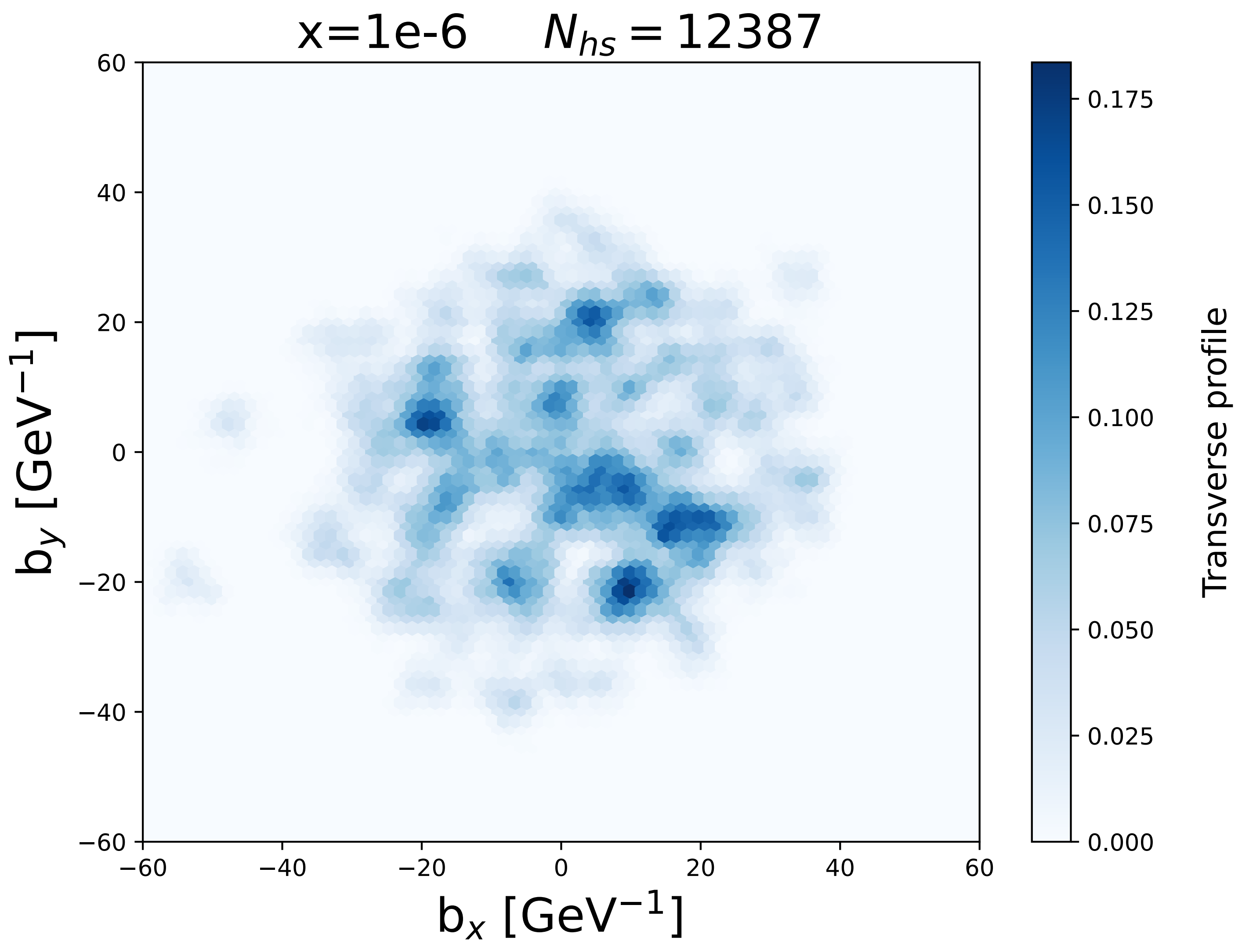

Energy (Bjorken-x) dependence

Cepila, JGC, Matas, Ridzikova, PLB 852 (2024) 138613

Scanning size scales in the impact-parameter plane

J/ψ

Different Mandelstam-t

Cross section rises with energy at small Mandelstam-t

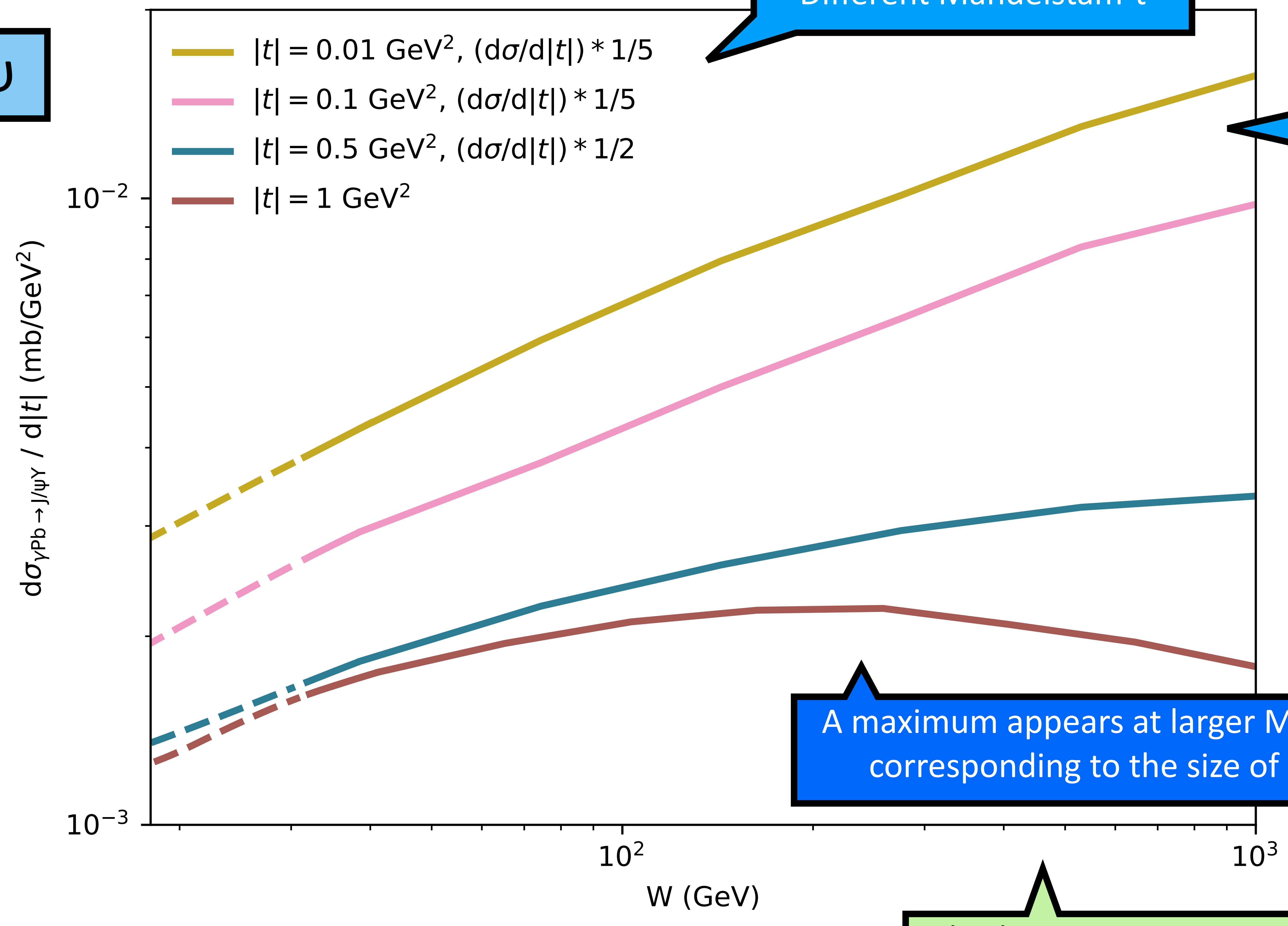

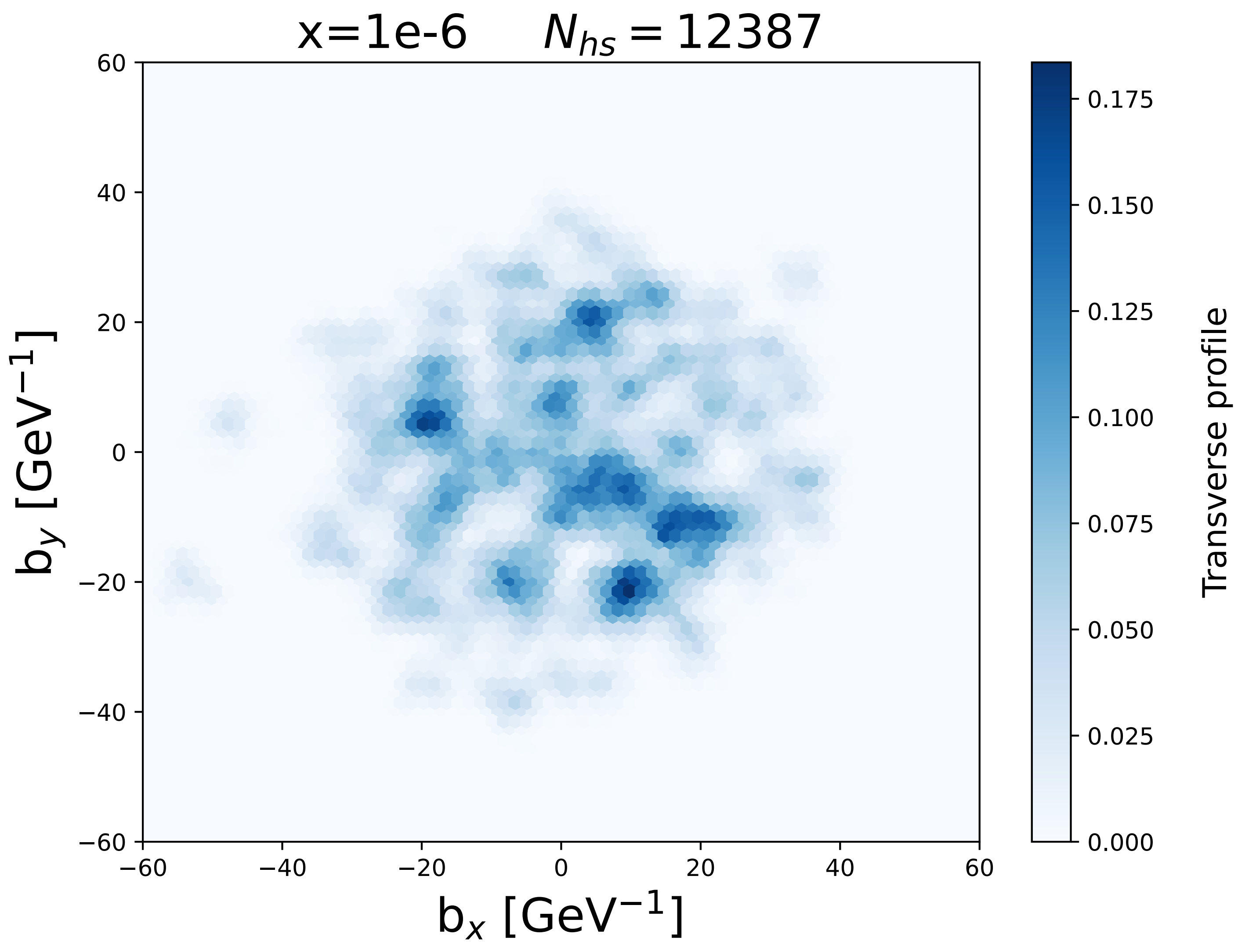

A maximum appears at larger Mandelstam-t corresponding to the size of hot spots

This kinematic region is accessible at the LHC

Energy (Bjorken-x) dependence

Cepila, JGC, Matas, Ridzikova, PLB 852 (2024) 138613

Summary

Deep-inelastic scattering

The structure function of the proton grows rapidly at small Bjorken x

Summary

Deep-inelastic scattering

The structure function of the proton grows rapidly at small Bjorken x

Saturation

This behaviour is modified at some small Bjorken-x when saturation sets in

Summary

Deep-inelastic scattering

The structure function of the proton grows rapidly at small Bjorken x

Saturation

This behaviour is modified at some small Bjorken-x when saturation sets in

Hot spots

In the energy dependent hot-spot model, the incoherent contribution decreases when saturation is reached

Summary

Deep-inelastic scattering

The structure function of the proton grows rapidly at small Bjorken x

Saturation

This behaviour is modified at some small Bjorken-x when saturation sets in

Hot spots

In the energy dependent hot-spot model, the incoherent contribution decreases when saturation is reached

LHC

We propose to use incoherent J/ψ at large Mandelstam-t to search for the onset of saturation at the LHC